UNIVERSITA' DEGLI STUDI DI PARMA

Dottorato di ricerca in
Biologia e Patologia Molecolare

Ciclo XXVII

Targeted therapy in lung and breast cancer: a big deal.

Coordinatore:
Chiar.ma Prof.ssa Valeria Dall'Asta

Tutor:
Chiar.mo Prof. Pier Giorgio Petronini

Dottoranda: Cristina Caffarra

GENERAL INTRODUCTION

1. LUNG AND BREAST CANCER: AN OVERVIEW.

1.1 Lung cancer.

Lung cancer is the leading cause of cancer-related mortality for both men and women with more than 1.6 million deaths worldwide[1,2]. Cigarette smoking is definitely the most important risk factor of lung cancer[3]. Exposure to radon gas (radon is produced by the natural breakdown of uranium in soil, rock and water) is estimated to be the second leading cause of lung cancer in Europe and North America. Other substances that increase the risk of having lung cancer include exposure to secondhand smoke, asbestos, arsenic, diesel exhaust and some forms of silica and chromium[4]. Genetic susceptibility plays a contributing role in the development of lung cancer, especially cancers occurring at a young age. The use of image techniques, such as chest X-ray, computed-tomography (CT scan), magnetic resonance imaging (MRI), and positron emission scan (PET), is pivotal to find, evaluate and stage lung cancer, although the images obtained have to be confirmed with a sample of tumor. The histological or cytological diagnosis of lung cancer is usually obtained by bronchoscopic examination or fine needle aspiration, and fatigue, weight loss and dyspnea are the most common symptoms at onset.

According to histological type there are two major types of lung cancer: non small cell lung cancer (NSCLC) and small cell lung cancer (SCLC). NSCLC represents the 85% of lung cancers. NSCLC arises generally from the epithelial cells of the lung of the central bronchi to terminal alveoli. There are 3 main subtypes of NSCLCs: 1) adenocarcinoma (40%), the most common form of lung cancer among both men and women; 2) squamous cell carcinoma (25%), linked more than the others with smoking; and 3) large carcinomas (10%). There are additional subtypes that occur with low frequency: e.g. adenosquamous carcinoma and sarcomatoid carcinoma[5]. SCLC accounts for approximately 15% of bronchogenic carcinomas. Recent publications have suggested the use of the Tumor-Node-Metastasis (TNM) classification in both NSCLC and SCLC. Lung cancer classification and staging assess the anatomical extension of the tumor which is critical in the choice of a therapy and provide information on prognosis. The T staging is determined by the size of primary tumor in long axis or direct extent of the tumor into adjacent structures. The N classification describes the degrees of spread to regional lymph nodes. The M staging defines the presence of metastases beyond regional lymph nodes[6]. Using the TNM classification system, NSCLC is divided into four stages: from I to IV. The higher the stage the

more extensive is the spread of the disease. Stage 0 is used for some cancers to indicate *in situ* disease. The prognosis for both SCLC and NSCLC remains poor. One of the main reasons is that most lung cancers are not found until they start to cause symptoms. Deciding on the appropriate treatment for NSCLC is a complex multistep process. Treatment options depend on the stage of disease, on the histological type and on the performance status of the patient. SCLC is more responsive to chemotherapy and radiation therapy than other types of lung cancer; however it is difficult to treat because it has a greater tendency to be widely disseminated by the time of diagnosis. Surgery is rarely applied in this type of lung cancer. For early stage NSCLC surgery is the most important curative modality. Unfortunately, as previously mentioned, only approximately 20-30% of patients are diagnosed at resectable stage (stage I-II). For advanced NSCLC patients with good performance status, platinum-based chemotherapy represents the standard treatment and partial responses can be achieved in 30-40% of the cases while complete responses are very rare. Combinations with cisplatin or carboplatin, and third generation cytotoxic drugs, such as gemcitabine, paclitaxel, docetaxel, etoposide or vinorelbine, are used. Moreover, both chemo- and radiotherapy can be used in neo-adjuvant setting to shrink the tumor before surgery or as adjuvant therapy to improve outcome after resection. The use of both neo-adjuvant and adjuvant chemotherapy has been shown to improve patient survival. Despite advances in these combined treatment modalities for lung cancer, prognosis remains poor and severe side effects are often observed[7,8]. Therefore, more effective and less toxic treatments are needed and, as a result, a variety of molecular targeted therapies have been recently introduced for the treatment of advanced NSCLC.

a

Relevant histological subtypes	Description	Pathway	Potentially relevant therapies
Adenocarcinoma	EGFR sensitizing mutations	EGFR	TKIs & chemotherapy
Adenocarcinoma	EGFR resistance mutations including T790M	EGFR	Dual EGFR/HER2 TKI, c-MET inhibitors +/− 1st or 2nd generation EGFR TKIs, Hsp90 inhibitors, dual MET/VEGFR2 inhibitors, Chk1 inhibitors
Adenocarcinoma	VeriStrat proteomic signature	EGFR	TKIs & bevacizumab
Adenocarcinoma	K-ras mutations	K-ras	Dual MAPK & AKT/PI3K inhibitors, Hsp90 inhibitors
Adenocarcinoma	EML4-ALK	EML4-ALK	ALK inhibitors, Hsp90 inhibitors

b

Relevant histological subtypes	Description	Pathway	Potentially relevant therapies
Adenocarcinoma, small cell carcinoma, squamous	c-MET overexpression	c-MET	c-MET inhibitors, Dual Met/VEGFR2 inhibitors, ALK/MET inhibitors, c-MET monoclonal antibodies
Adenocarcinoma, squamous, large cell, small cell carcinoma	c-MET mutations	c-MET	c-MET inhibitors, dual Met/VEGFR2 inhibitors, ALK/MET inhibitors, c-MET monoclonal antibodies
Adenocarcinoma	PI3KCA amplification, mutations	AKT/PI3K	PI3K, AKT, mTOR inhibitors
Adenocarcinoma	PTEN deletions/methylation	AKT/PI3K	PI3K, AKT, mTOR inhibitors
Small cell carcinoma	VEGFR overexpression	VEGFR	VEGFR inhibitors
Small cell carcinoma	Bcl-2 overexpression	P53/BCL	BCL-2 Inhibitors
Adenocarcinoma (1.5%)	ROS1 translocation	ROS-1	ROS1 inhibitors
-	Epigenetic alterations		HDAC inhibitors, epigenetic inhibitors with cytotoxic agents
Adenocarcinoma, Squamous, SCLC	IGF alterations	IGF	IGF1R monoclonal antibodies, IGF1R TKIs

Figura 1. **Principle (a) and secondary (b) lung cancer molecular subtypes.** *(West L et al., PLoS ONE 7(2): e31906, 2012)*

1.2 Breast cancer.

Breast cancer (BC) is the second most common cancer worldwide after lung cancer, the fifth most common cause of cancer death, and the leading cause of cancer death in women, carries a lifetime risk of ~10% in western populations and an estimated 2% risk of death in US women. 61% of breast cancers are diagnosed at localized stage[9]. The global burden of BC exceeds all other cancers and the incidence rates of breast cancer are increasing[10]. BC is a heterogeneous group of neoplasms originating from the epithelial cells lining the milk ducts. Breast tumor heterogeneity has been noted in histology and clinical outcome for a long time, and these differences have served as the basis for disease classification. Based on comprehensive gene

expression profiling, breast tumors are classified into at least three major subtypes: luminal, human epidermal growth factor receptor 2-positive (HER2-positive), and triple negative breast cancer (TNBC)[11]. Each of these subtypes has different risk factors for incidence, response to treatment, risk of disease progression, and preferential organ sites of metastases[12]. Overall, there are common risk factors associated with higher probability to develop BC: age (the risk of developing breast cancer increases with age), genetic factors (about 5-10% of breast cancer demonstrate an autosomal dominant inheritance), dense breast tissue and certain benign breast conditions (proliferative breast disease is associated with an increased risk of breast cancer), and environmental factors[13,14]. Imaging techniques (mammogram, MRI, breast ultrasound) help to find out the presence, the stage, and the spreading of breast cancer. The assessment of cancer must be validated with a biopsy[15].

BC is a complex disease characterized by many morphological, clinical and molecular features. Traditionally, it has been classified according to TNM staging system. Additionally, nowadays, clinical criteria, including immunohistochemical markers, are routinely used in diagnostic laboratories to provide a classification of breast cancer, helping determine the optimal approach for treatment. The presence of specific markers in breast cancer has long been recognized to both define subtypes with differential overall prognosis and to identify tumors susceptible to targeted treatments[16]. Accordingly with these statements, BC can be divided into molecular classes on the basis of the receptor status of the breast cancer cells. Estrogen-receptor (ER)-positive tumors (estrogen dependent) include luminal types A and B (luminal tumors are positive for estrogen and progesterone receptors (PR) and the majority respond well to hormonal interventions); ER-negative (HER2)-positive tumors (estrogen independent) have amplification and overexpression of the HER2 (ErbB2) oncogene and can be effectively controlled with a diverse array of anti-HER2 therapies; and TNBC that is negative for ER, PR and HER2[17]. These phenotypes are responsible for directing the selection of the optimal therapeutic approaches to treatment. Most BCs are estrogen-dependent: approximately 60% in premenopausal women and 75% in postmenopausal women[15]. Therapeutic decisions are formulated in part according to staging categories but primarily according to lymph node status, estrogen- and progesterone-receptor levels in the tumor tissue, menopausal status, and the general health of the patient. Usually a multidisciplinary treatment planning approach is used for management of BC. The elective

treatment is surgery followed by chemotherapy or radiotherapy. Notwithstanding, the probability to have a relapse is high, indicating the need to develop other strategies of treatment. Patients with ER-positive tumors are treated with adjuvant hormonal therapy with tamoxifen in early stages of breast cancer or with an aromatase inhibitor in postmenopausal women. In the last decade the identification of driven mutations that define new molecular subsets of cancer led to the development of targeted drugs, such as trastuzumab and lapatinib in order to defeat breast cancer[18].

Table 1. Clinical and molecular criteria based on molecular subtypes for breast cancer

	Molecular subtypes				
Clinical criteria	Luminal A	Luminal B	HER2-positive	Basal-like (or TNBC)	Claudin-low (or TNBC)
Histologic grade	Low	High	High	High	High
IHC markers	ER+; PR+; HER2–	ER+; PR+/–; HER2+/–	ER–; PR–; HER2+	ER–; PR–; HER2–	ER–; PR–; HER2–
Molecular criteria					
Frequency	50–60%	10–20%	15–20%	10–20%	12–14%
Prognosis	Good	Intermediate/poor	Poor	Poor	Poor
Genetic profile	ER-related genes and low proliferation genes	High proliferation genes	HER2-related genes and high proliferation genes	CKs, P-cadherin, CAV1/2, CD44, KIT	Low cell–cell junction genes and high immune response genes
Treatment	SERMs (tamoxifen) and AIs		HER2 target therapy	–	–
New treatment targets on clinical trials	PI3K/AKT/mTOR pathway inhibitors, CDK4/6 inhibitors, histone deacetylase inhibitors		PI3K/AKT/mTOR pathway inhibitors, neratinib, HSP90	PARP-1 inhibitors, EGFR inhibitor, PI3K/AKT/mTOR pathway inhibitors,	–

AI, hormonal aromatase inhibitor; CK, cytokines; EGFR, epidermal growth factor receptor; ER, estrogen receptor; HER2, human epidermal growth factor receptor 2; IHC, immunohistochemistry; PARP-1, poly [ADP-ribose] polymerase 1; PR, progesterone receptor; SERMs, selective estrogen receptor modulators; TNBC, triple negative breast cancer; VEGF, vascular endothelial growth factor.

Figure 2. Clinical and molecular criteria based on molecular subtypes for breast cancer. *(F.B. Abreu et al, Clin Genet 86:62-67, 2014)*

2. TARGETED THERAPY.

2.1 Targeted therapy at a glance.

In order to battle cancer the World Health Organization (WHO) has developed three strategies: prevention (especially in people habits), early screening (detecting tumors at an early stage) and a comprehensive treatment strategy (improving survival and quality of life of patients with advanced cancer)[19]. Based on type, stage of cancer, and patient conditions, treatments include: surgery, chemotherapy, radiation therapy and targeted therapy. Surgery, when it can be done, is the elective treatment and it provides the best chance to cure cancer. For decades, the hallmark of medical treatment for cancer has been intravenous cytotoxic chemotherapy; chemotherapeutic drugs target rapidly dividing cells, without distinction between cancer cells and certain normal tissues, thus producing a number of side effects such as alopecia, gastrointestinal symptoms, and myelosuppression. In the last ten years, however, a dramatic shift has been gained in the cancer therapy. Identification of different driver mutations that define new molecular subsets of cancer has been critical in defining novel targeted therapeutic approaches. Targeted therapy lays the basis onto the concept that some cancers for their survival and proliferation depend on a single oncogene activated by somatic mutation, identified as a "driver oncogenic mutation"; usually such mutations are mutually exclusive in different cancer subtypes[20].

Targeted cancer therapies are based on the use of drugs that block the growth and spread of cancer by interfering with specific molecules involved in tumor growth and progression. Indeed, targeted therapies focus on proteins involved in cell signaling pathways which form a complex communication system that drives pivotal cellular functions and activities, such as cell division, cell movement, cell metabolism, cell responses to external stimuli and cell death. Tyrosine kinases (TKs) are an especially important target because they play an important role in the modulation of growth factor signaling[21]. A molecular target can be located outside the cell as well as inside the cell; thereby there are two principal approaches: monoclonal antibodies acting against extracellular targets and small-molecule (less than 800 Da) drugs that are able to diffuse into the cell and act against intracellular targets[22]. Although traditional cytotoxic chemotherapy still remains the treatment of choice for many malignancies, targeted therapies are now a component of treatment for many types of cancer, including lung, breast, colorectal and pancreatic cancers, as well as lymphoma, leukemia, and multiple myeloma[23]. Progress in

understanding cancer biology and mechanisms of oncogenesis has allowed the development of treatment against specific molecular targets such as epidermal growth factor receptor (EGFR) in NSCLC. This gene is activated by single amino acid substitution mutations or in-frame amino acid deletion mutations in 10-20% of lung adenocarcinoma cases in the USA and in 30–40% of cases in East Asia. The most frequently targeted pathways in NSCLC have involved EGFR and vascular endothelial growth factor (VEGF) and its receptor VEGFR[24]. Regarding breast carcinoma the targeted therapy focuses on the retrovirus-associated DNA sequences (RAS)/v-raf murine leukemia viral oncogene homolog (RAF)/mitogen-activated protein kinase kinase (MEK)/mitogen activated protein kinase (MAPK) pathway, the phosphoinositide-3-kinase (PI3K)/protein kinase B (AKT) pathway, Janus tyrosine kinase (JAK)/signal transducers and activators of transcription (STAT)signaling pathway, and the VEGF pathway, that are often abnormally activated in this type of cancer[25].

2.2 MAP kinases pathway.

MAP kinases comprise a family of protein-serine/threonine kinases, which are highly conserved in protein structures from unicellular eukaryotic organisms to multicellular organisms, including mammals. These kinases (including extracellular signal-regulated kinases (ERKs), JNKs and p38s) are regulated by a phosphorylation cascade, with a prototype of three protein kinases that sequentially phosphorylate one another[26]. MAPK signaling pathway (also known as RAS/RAF/MEK/ERK signaling pathway) is activated in response to various extracellular stimuli that mediate signal transduction from the cell surface to the nucleus. MAPK signaling pathway transduces extracellular signals into a variety of cellular processes, such as cell division, growth, proliferation, survival, death, differentiation and migration. Consistent with their essential cellular functions, MAPKs have been shown to play critical roles in embryonic development, adult tissue homeostasis and various pathologies[27,28]. The deregulation of this pathway is a common event in many types of cancer. MAPKs signaling pathway (in combination with other pathways) activates several proteins including transcription factors, cytoskeletal proteins and kinases that influence gene expression[30]. Moreover, RAS/RAF/ERK pathway is able to influence cell metabolism through different ways: RAS enhances GLUT-1 expression on cellular membranes and activates MYC that promotes mitochondrial gene expression and mitochondrial biogenesis; it enhances also HIF1 that induces GLUT-1 and GLUT-3 expression,

hexokinase II (HKII) as well glyolytic enzymes. The activation of MAPKs pathway begins when a ligand binds to a receptor tyrosine kinase (RTK), as EGFR or PDGFR. The cascade of activation starts with RAS, that binds to RAF, leading to the phosphorylation and activation of MEK1 and MEK2 kinases that add a phosphate group and activate ERK1 and ERK2, respectively. ERK1 and ERK2 migrate to the nucleus and upregulate some transcription factors such as Fos, Jun, c-Myc and CREB that in turn induce the expression of growth factors, cyclins and regulatory proteins which control growth, proliferation, differentiation, apoptosis (eg. Bim, Bax, Bcl-2) and inflammation[26,30].

2.3 PI3K/AKT/mTOR pathway.

The PI3K/AKT/mTOR pathway is a major cellular signaling pivot in the cellular response to extracellular stimuli, e.g. insulin, insulin-like growth factor-1 (IGF-1), EGF and fibroblast growth factor (FGF). The PI3K/AKT/mTOR pathway plays an essential role in a wide range of biological functions, including metabolism, macromolecular synthesis, cell growth, proliferation and survival; its deregulation is involved in many human cancers, including NSCLC and BC[31].

Growth factor stimuli activate PI3K, a heterodimeric protein composed by two subunits, an 85kDa subunit, and a 110kDa catalytic subunit. PI3K (the catalytic subunit) then converts phosphatidylinositol-4,5-bisphosphate (PIP2) into phosphatidylinositol-3,4,5-trisphosphate (PIP3). PIP3 recruits AKT (also known as protein kinase B, PKB) to the membrane, where AKT is phosphorylated by the enzyme PDK1 at Thr^{308} and by rictor-bound mTOR complex 2 (mTORC2) at Ser^{473}, for full AKT activation[32]. Conversely, phosphorylated AKT (p-AKT) can be dephosphorylated by protein phosphatase 2A (PP2A) and the pleckstrin homology domain leucine-rich repeat protein phosphatase (PHLPP). Activated AKT further activates mTORC1 by two mechanisms. One is through inhibitory phosphorylation of tuberous sclerosis complex 2 (TSC2). Inhibited TSC2 blocks the complex of TSC1/TSC2, converting Rheb-GTP to Rheb-GDP, thus resulting in the activation of mTORC1 by Rheb-GTP. The other mechanism is through AKT inhibition of proline-rich AKT substrate 40 (PRAS40), which inhibits mTORC1. The activated mTORC1, in turn, mediates phosphorylation of 4E-BP1 and p70S6K (S6K) that are involved in the regulation of translation. PI3K/AKT/mTOR pathway is negatively regulated by the tumor suppressor gene PTEN (phosphatase and tensin homologue); in particular PTEN

antagonizes the PI3K/AKT signaling pathway dephosphorylating PIP3. Loss or inactivating mutations of PTEN result in the hyperactivation of PI3K signaling.

As mentioned before, AKT1 is an important constituent of PI3K pathway, whose numerous regulatory functions include the modulation of energy metabolism. AKT1 increases the expression of glucose transporters (GLUT-1), facilitating their transport to the membranes, and phosphorylates important glycolytic enzymes (such as HKII and phosphofructokinase II (PFKII) that, through glucose phosphorylation, facilitate more glucose entry into cells along its concentration gradient; in this way AKT1 stimulates glycolysis[33]. Furthermore, it inhibits forkhead box subfamily O (FOXO) transcription factors increasing the glycolytic activity, it actives ectonucleoside triphosphate diphosphohydrolase 5 (ENTPD5), an enzyme that glicosylates the proteins of endoplasmic reticulum and creates an ATP hydrolysis cycle. AKT activates mTOR kinase, phosphorylating and inhibiting its negative regulator tuberous sclerosis 2 (TSC2, tuberin). Once active, mTOR increases lipid and protein biosynthesis, stimulates mRNA translation and ribosome biogenesis and actives HIF 1 even in the presence of oxygen[34].

The serine/threonine kinase mTOR takes part in PI3K/AKT signaling. It exists in two diverse multiprotein signaling complexes: mTORC1 and mTORC2. mTOR complex1 is sensitive to Rapamycin and includes mTOR, regulatory-associated protein of mTOR (Raptor), mammalian lethal with SEC13 protein 8 (MLST8) and the partners PRAS40 and DEPTOR. This complex is a nutrient-energy-redox sensor and regulates protein synthesis. mTORC2 is insensitive to rapamycin and is composed by mTOR, rapamycin-insensitive companion (RICTOR), GβL, and mammalian stress-activated protein kinase interacting protein 1 (mSIN1). mTORC2 plays an essential role in cell survival and cytoskeleton dynamics and activates AKT increasing AKT/mTOR signaling[35].

2.4 Jak-STAT.

Jak proteins belong to the family of Janus kinases. Jaks and Stats are critical components of many cytokine receptor systems, regulating growth, survival and differentiation. In response to external stimuli (e.g. activation of EGFR), Jaks proteins are phosphorylated on their tyrosine domains that serve as docking sites for the SH2-containing Stats (a family of cytoplasmatic transcription factors), such as STAT3, and for SH2-containing proteins and adaptors that link the receptor to

MAP kinase, PI3K/Akt, and other cellular pathways. Once activated STAT proteins dimerize, translocate to the nucleus and induce the expression of specific target genes. It has been shown a constitutive activation of STAT proteins in a variety of human malignancies[36,37].

2.5 Src

Src family of protein tyrosine kinases (SFKs) is the largest family of non-receptor kinases that plays key roles in regulating signal transduction by a diverse set of cell surface receptors in the context of multiple cellular environments. Src is the prototypical member of SFKs[38]. The SFK family has nine members (Blk, Fgr, Fyn, Hck, Lck, Lyn, Src, Yes, and Yrk) that are implicated in several signal transduction pathways regulating cell division, motility, migration (Src is involved in the downregulation of E-Cadherin), adhesion, angiogenesis and survival. All SFK members share a similar structure: four Src homology (SH1 to SH4) domains and a unique amino-terminal domain. The activation of Src requires a switch from an inactive to an active conformation into the cytoplasm. This corresponds to a phosphorylation switch from a tyrosine residue located in the regulatory C-terminal tail (Y530), which is characteristic of the inactive state, to a tyrosine residue located in the catalytic SH1 domain (Y419). The transition from the off-conformation to the on-conformation occurs upon stimulation by numerous extracellular and intracellular signals. Constitutively activated variants of Src family kinases, including the viral oncoproteins v-Src and v-Yes, are capable of inducing malignant transformation of a variety of cell types[38,39].

2.6 Targeted therapy in NSCLC.

Currently, platinum-based doublet chemotherapy (in the first-line therapy) is the standard of care for the treatment of NSCLC despite its toxicity. Chemotherapy has reached a plateau and the introduction of a third chemotherapeutic agent may increase toxicity without improving efficacy. However, the therapeutic landscape for advanced NSCLC is changing from chemotherapy to targeted therapy for patients whose tumors express specific biomarkers. According to the National Institute of Health (NIH) a biomarker is defined as a characteristic that is objectively measured and evaluated as an indicator of normal biologic processes, pathogenic processes, or pharmacologic responses to a therapeutic intervention. In NSCLC, the biomarkers of current value in targeting therapy are EGFR, ErbB2 and kirsten rat sarcoma viral oncogene homolog (*K*RAS) mutational status; anaplastic lymphoma kinase (ALK) rearrangements; and c-MET

protein expression[2]. In recent years, it has been shown that molecular-targeted therapy is very successful in treating patients with this type of cancer. In particular, extensive preclinical and clinical studies have proven the marked treatment responses and survival advantages over conventional chemotherapies provided by target specific inhibitors to EGFR-activating mutations or ALK fusions[40]. Currently, the available targeted therapies are elotinib, gefitinib and afatinib for EGFR mutations or copy number gain; crizotinib and ceritinib for ALK fusions; crizotinib for MET copy number gain and crizotinib for proto-oncogene tyrosine-protein kinase1 (ROS1) fusions too[41].

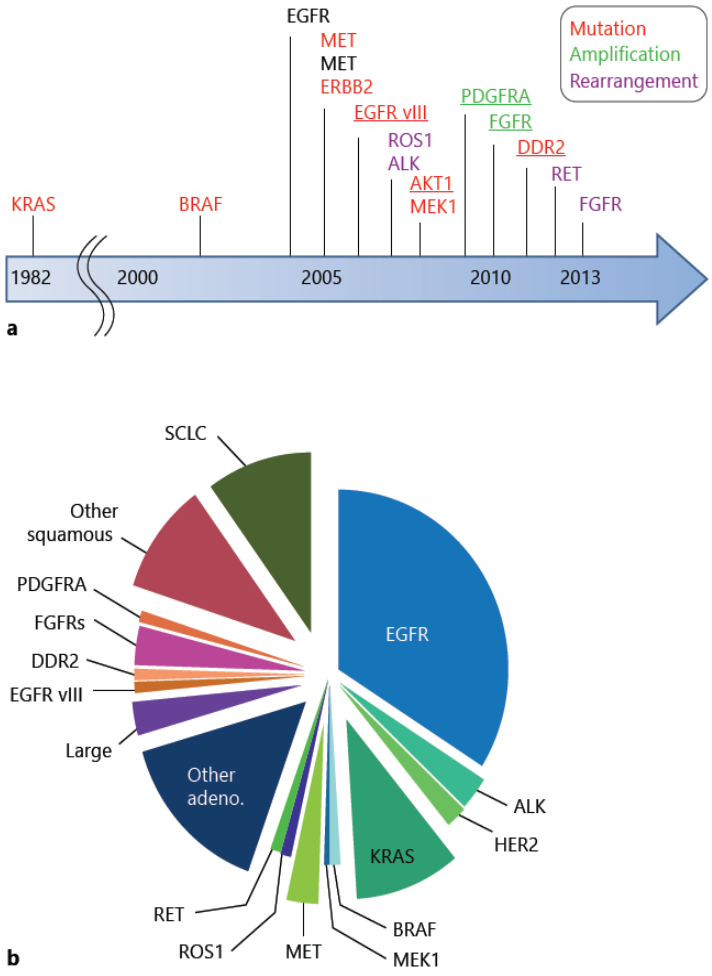

Figure 2. Identified and potential driver oncogenic mutations in lung cancers. (a)Time course (reported year) of discovery of driver oncogenic mutations is shown. Underlined driver oncogenic mutations indicate a higher prevalence in squamous cell carcinomas, while others do so in adenocarcinomas. (b) Prevalence of identified and potential driver oncogenic mutations in lung cancers. *(Peters S. et al, Prog. tumor research. Basel, Karger, vol 41: 62-77, 2014)*

2.6.1 Targeting EGFR

One of the most well-known examples of driven mutations is EGFR, a cell-surface receptor that is activated in more than half of NSCLC patients having a pivotal role in the pathogenesis and progression of lung cancer. The human epidermal growth factor receptor family (HER) (also called erythroblastic leukemia viral oncogene homolog (ErbB), family) comprises four tyrosine kinase receptors: HER-1 (EGFR), HER-2/neu (ErbB2), HER-3 (ErbB3), and HER-4 (ErbB4). EGFR is a multiple domain glycoprotein (170 kDa) that consists of an extracellular ligand-binding domain and an intracellular tyrosine kinase domain separated by a single transmembrane region[5]. Following ligand-binding, EGFR receptors homo- and hetero-dimerize and promote autophosphorylation of the intracellular tyrosine kinase domain that stimulates an intracellular signal transduction cascade through several downstream pathways, including the RAS/RAF/MEK/MAPK pathway, PI3K/AKT pathway, and JAK/signal transducers and activators of transcription (STAT) pathway, which regulate cell proliferation, cell survival, and apoptosis[42].

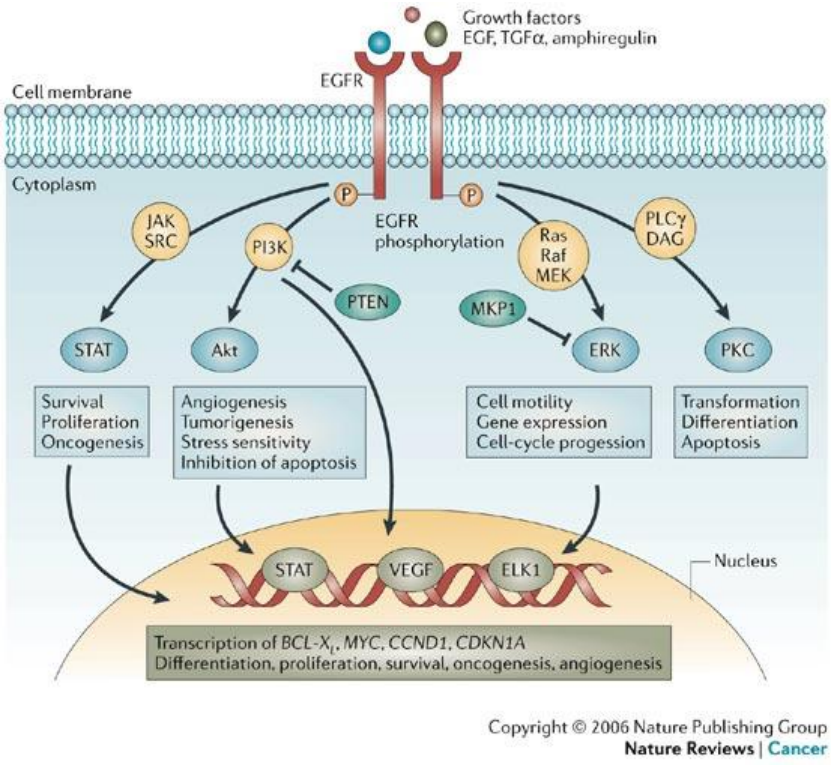

Figure 3. Pathways activated by EGFR. *(Mukesh K. et al, Nature Cancer Reviews, 6: 876-885, 2006)*

The constitutive activation of EGFR signaling pathway, caused by gene mutations or by gene amplification or both, has been demonstrated to have close connection with initiation, progression and poor prognosis of NSCLC. EGFR activating mutations, mainly located in the tyrosine kinase domains and in the form of a base-pair deletion at exon 19 (delE746_A750, account for about 54%), point mutations at exon 21 (L858R, account for about 43% and L861Q) or point mutations at exon 18 (G719A/C), occur in about 20% of NSCLC patients, with significantly increased proportions in the subgroup of adenocarcinoma histology (40%), female sex (42%), Asian ethnicity (30%), and never-smoker status (51%). Three defined regions (exons 18–21) in the EGFR gene are commonly mutated and predict sensitivity to EGFR TKI. These mutations enable EGFR to activate, without ligand binding, the downstream molecules. In order to block EGFR activation, a number of drugs have been developed against its tyrosine kinase domain: small-molecule receptor tyrosin kinase inhibitors (TKIs) bind to the intracellular catalytic domain of the tyrosine kinase and inhibit receptor autophosphorylation and activation of downstream signaling pathways by competing with adenosine triphosphate (ATP). At present there are three generations of TKIs. The so-called ‘‘first generation’’ drugs, such as erlotinib and gefitinib, compete reversibly with ATP for binding to the intracellular catalytic domain of EGFR tyrosine kinase and thus inhibit EGFR autophosphotylation and downstream signaling. The “second generation” TKIs, such as afatinib, dacomitinib and neratinib, also target multiple ErbB-family members (in particular HER2 and some also inhibit HER4), and form an irreversible covalent bind to the ATP-binding site competing with ATP. The second generation TKIs may overcome the acquired resistance observed with erlotinib and gefitinib. Finally, there are “third generation” EGFR-TKIs targeting activating EGFR mutations and resistance (T790M) mutations but sparing wild-type EGFR. They are used when the second generation drugs don’t work. Examples of the third generation drugs are the oral, irreversible, selective inhibitors WZ4002 (it was the first third generation drug conceived but it has not progressed to clinical trials), CO-1686 (it is currently in early phase II clinical trials) and HM61713 (it is in early phase I trials), finally the novel AZD9291 (a mono anilino–pyrimidine compound that is structurally and pharmacologically distinct from all other TKIs)[43].

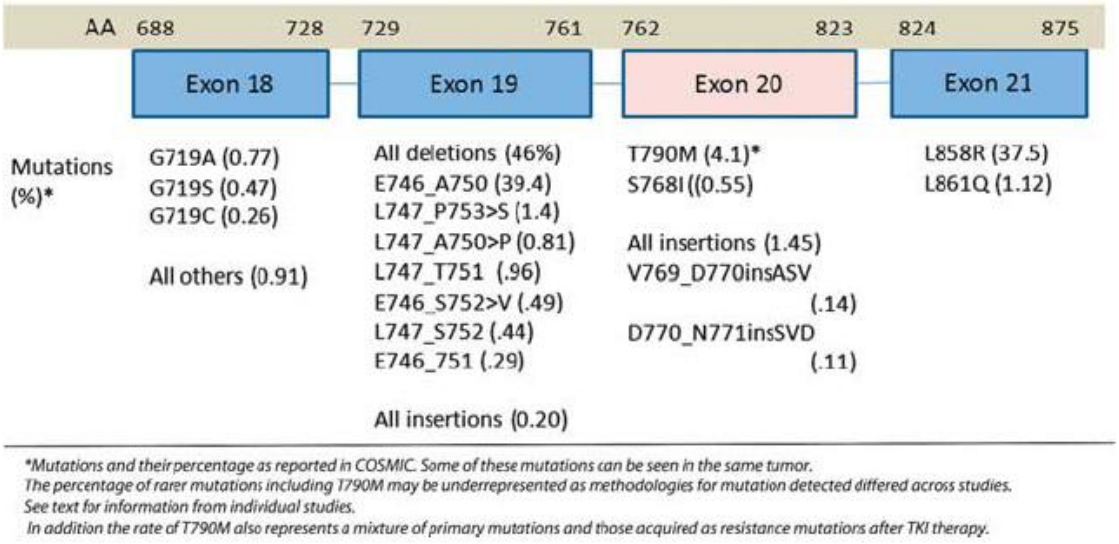

Figure 4. EGFR mutations and their frequency based on COSMIC annotations. The amino-acid location based upon the exon structure of EGFR is highlighted to show areas of mutation that alter amino-acid sequence. The common mutation are noted to encompass alterations reported in COSMIC (Catalogue of Somatic Mutations in Cancer). Because many data entries in COSMIC reflect studies focused on exons 21 and 19, the frequency of rarer mutations may be underestimated *(Siegelin M.D. et al, Laboratory Investigation, 94: 129-137, 2014).*

2.6.2 Erlotinib (Tarceva) and gefitinib (Iressa)

Erlotinib and gefitinib are two oral, reversible and highly specific inhibitors of EGFR tyrosine kinase domain, especially effective in tumors with activating EGFR mutations. In 90% of cases these mutations are exon 19 deletions or exon 21 substitutions.

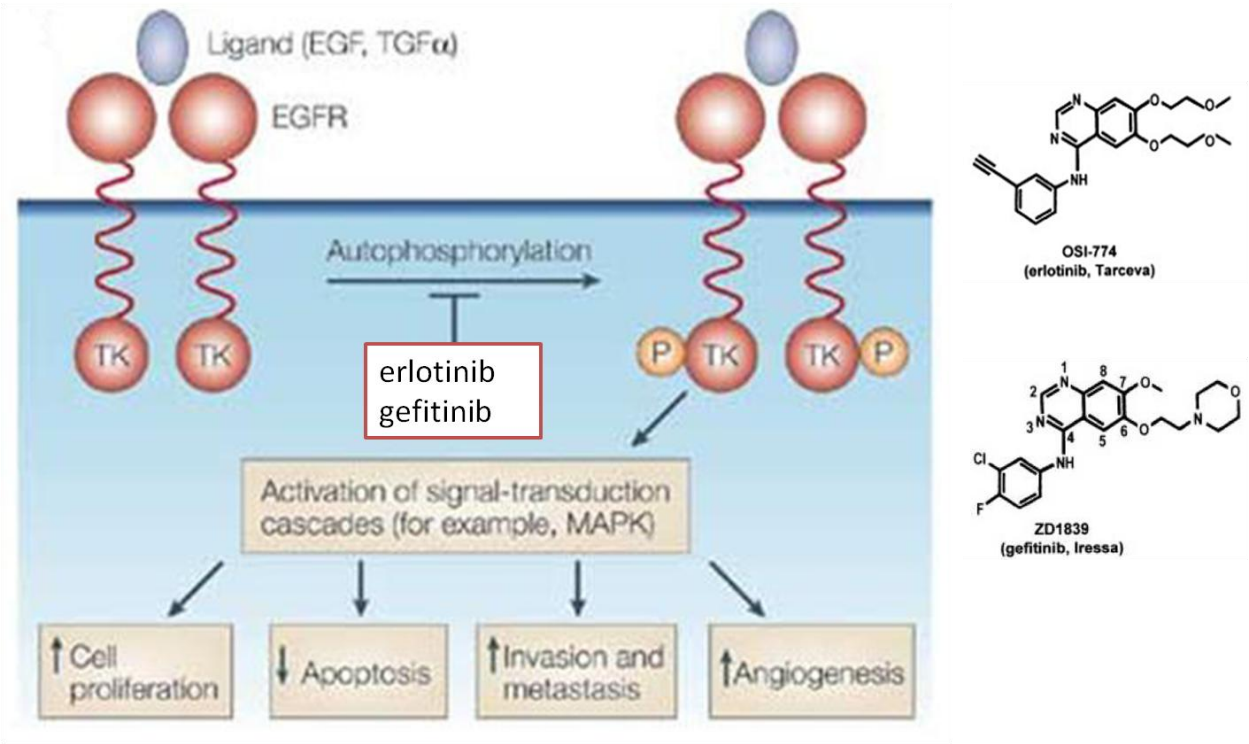

Figure 5. Erlotinib and gefitinib inhibit EGFR autophosphorylation.

In 2013, erlotinib was approved in the first, second and third line treatment of metastatic and advanced NSCLC and as a maintenance therapy in patients carrying in-frame deletions in exon 19 and point mutations within exon 21 (L858R). In 2009, the European Commission granted marketing authorization for IRESSA for use in all lines of treatment for NSCLC patients harboring EGFR mutations, but it is not currently approved by the Food Drug Administration (FDA). In patients with mutated EGFR in the first-line setting, five clinical trials that compared EGFR TKI treatment with chemotherapy revealed a prolongation of progression-free survival (PFS) of 9.6–13.7 months for TKIs versus 4.6–6.6 months for platinum-doublet chemotherapy, with hazard ratios (HRs) ranging from 0.16 to 0.58. The median overall survival of those patients ranged from 19.3 to 38.8 months, which is far longer than that observed in the ECOG 1594 trial, in which four platinum-doublet regimens were compared and where a median overall survival of 7.4-7.9 months was seen[44].

Study	N	RR (%)	PFS (mo)	OS (mo)
IPASS	261	71.2 *vs.* 47.3 $p < 0.001$	9.5 *vs.* 6.3 HR 0.48, $p < 0.001$	21.6 *vs.* 21.9 HR 1, $p = 0.99$
First-SIGNAL	42	84.6 *vs.* 37.5 $p = 0.002$	8.0 *vs.* 6.3 HR 0.54, $p = 0.086$	27.2 *vs.* 25.6 HR 1.043
WJTOG 3405	177	62.1 *vs.* 32.2 $p < 0.001$	9.2 *vs.* 6.3 HR 0.48, $p < 0.001$	35.5 *vs.* 38.8 HR 1.185
NEJGSG 002	228	73.7 *vs.* 30.7 $p < 0.001$	10.8 *vs.* 5.4 HR 0.30, $p < 0.001$	27.7 *vs.* 26.6 HR 0.887, $p = 0.483$
OPTIMAL	154	83 *vs.* 36 $p < 0.001$	13.7 *vs.* 4.6 HR 0.16, $p < 0.001$	22.6 *vs.* 28.8 HR 1.065, $p = 0.685$
EURTAC	173	58 *vs.* 15 $p < 0.001$	9.7 *vs.* 5.2 HR 0.37, $p < 0.001$	19.3 *vs.* 19.5 HR 1.04, $p = 0.87$
LUX-Lung	345	56 *vs.* 23 $p = 0.001$	11.1 *vs.* 6.9 HR 0.58, $p = 0.001$	HR 1.12, $p = 0.60$
LUX-Lung6	364	67 *vs.* 23 $p < 0.0001$	11 *vs.* 5.6 HR 0.28, $p < 0.0001$	22.1 *vs.* 22.2 HR 0.95, $p = 0.76$

Figure 6. Randomized phase III trials comparing first-line reversible/irreversible EGFR TKI with platinum-based chemotherapy in advanced NSCLC harbouring EGFR activating mutation. *(Remon J et al, Cancer Treatment Reviews, 40: 723-729, 2014)*

Regarding gefitinib, the landmark Iressa Pan-Asia Study (IPASS) showed that this drug could significantly prolong PFS compared with carboplatin/paclitaxel in the subgroup of patients with EGFR mutation-positive tumors, together with much improved qualification of life (QoL) and delayed deterioration of symptoms. Similar benefits of EGFR-TKIs in EGFR mutation-positive NSCLC patients were shown in several other large-scale studies, such as WJTOG3405 comparing gefitinib with cisplatin/docetaxel as first-line treatment in Asian patients. Similar results were observed in other two studies: OPTIMAL study comparing erlotinib with chemotherapy as first-line treatment in Asian patients and EURTAC study, the counterpart in European patients **(Figure 6)**. This evidence is widely recognized and promotes practices of detecting EGFR mutation status and applying the EGFR-TKIs to the subset of EGFR mutant

patients. However, problems arose that almost all the patients with initial responses to gefitinib or erlotinib ultimately underwent tumor progression and inevitably became resistant to them mostly within 6-12 months (acquired resistance)[45]. Thus, the necessity to develop new drugs/strategies in order to overcome or to delay the resistance.

2.7 Targeted therapy in breast cancer

Breast cancer is a heterogeneous disease with different molecular alterations driving its growth, survival and response to therapy. As mentioned before, breast cancer is divided in three major subtypes based on the pattern of expression of hormone receptors and HER2: luminal tumors, *HER2* amplified tumors, and TNBCs. Differently from NSCLC, there is no a unique standard of care for the treatment of breast cancer. In terms of therapy, an increasingly rational drug development effort has resulted in agents against new molecular targets that are active against only those tumors with the targeted molecular alteration or phenotype. These agents include receptor and non-receptor tyrosine kinase inhibitors (HER1, HER2, HER3, insulin-like growth factor receptor, c-Met, fibroblast growth factor receptor and heat shock protein-90 (HSP-90) inhibitors), intracellular signaling pathways (PI3K, AKT, mTOR) and angiogenesis inhibitors, agents that interfere with DNA repair (poly-adenosine diphosphate-ribose polymerase (PARP)-inhibitors)[25]. Currently, the biomarkers valuated in targeting therapy are ER, PR and HER2, which are evaluated at diagnosis and characterize the three main immunophenotypes of BC. ERα-positive expression is considered one of the most important biomarkers in breast cancer and represents the principal mark for endocrine therapy. Endocrine therapy is divided in two classes of drugs: selective estrogen receptor modulators (SERMs), such as tamoxifen, raloxifene, and toremifene, and aromatase inhibitors (AIs), that are divided in non-steroidal, such as letrozole and anastrozole, and steroidal, such as exemestane. HER2 is another important biomarker in breast cancer: its activation, which occurs through gene amplification leading to receptor protein overexpression, is identified in 15–20% of all breast cancers and is associated with a more aggressive phenotype. Currently, *HER2* gene amplification is used as a pharmacogenomic test to identify breast cancer patients who may benefit from treatment with HER2-targeted agents. Currently, the agents used against HER2 are trastuzumab (or herceptin), lapatinib, pertuzumab, and trastuzumab emtansine (T-DM1). Regarding TNBC, which represents about 15% of all cases of breast cancer, unfortunately, there is no approved targeted therapy. Thanks to genomic and

transcriptomic technologies novel biomarkers have been discovered which are involved in multiple signaling pathways and could be conveniently targeted. Several clinical trials in TNBC are in progress investigating the effect of PI3K/AKT/mTOR inhibitors, CDK4/6 inhibitors, histone deacetylases (HDACs) inhibitors, and PARPs inhibitors, involved in cell proliferation, metabolism, motility, angiogenesis, apoptosis or DNA damage repair[46].

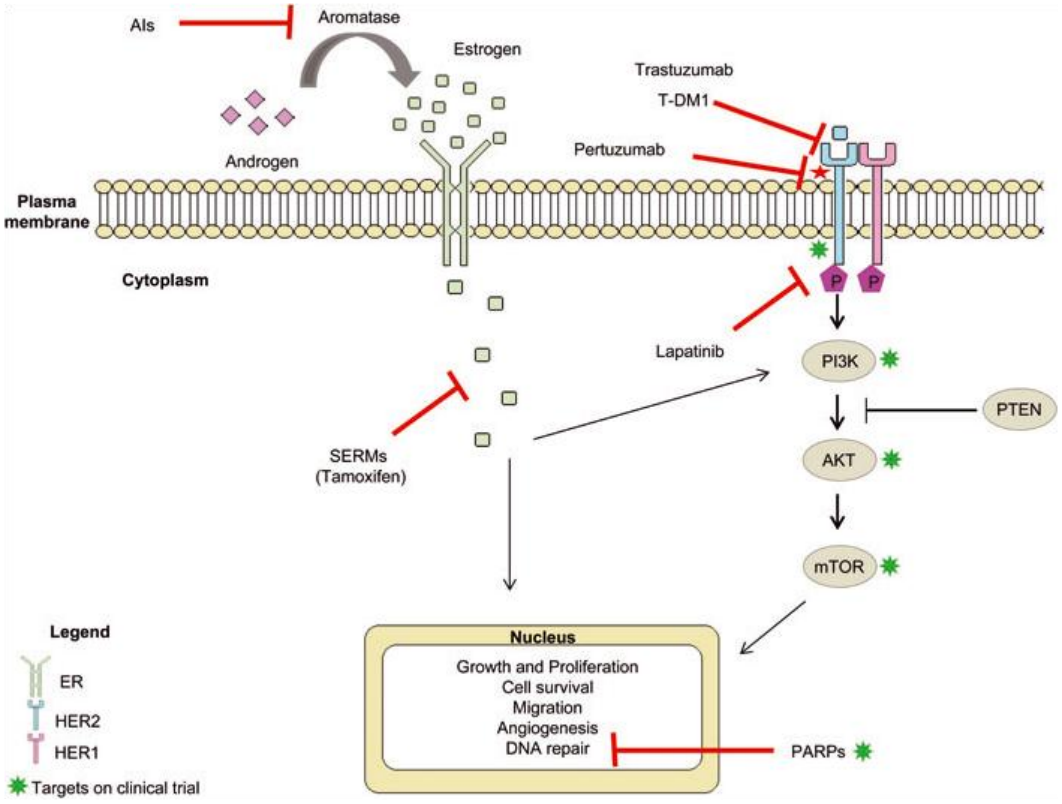

Figure 7. Therapies targeting ER-positive and HER2-positive breast cancer. *(De Abreu F.B. et al, Clin Genet 86: 62–67, 2014)*

2.7.1 Sorafenib

Sorafenib (Nexavar, BAY 43-9006) is an oral multikinase inhibitor with anti-proliferative and antiangiogenic activity approved by the FDA for the treatment of patients with advanced renal carcinoma (RCC) and those with unresectable hepatocellular carcinoma (HCC) [47,48]; it has also shown efficacy against a wide variety of tumors in preclinical studies.

Sorafenib blocks tumor cell proliferation and angiogenesis by inhibiting serine/threonine kinases c-RAF, and mutant and wild-type BRAF, as well as VEGFR2 and VEGFR3, PDGFR, FLT3, Ret, and c-KIT[49,50]. Moreover, sorafenib inhibits mTORC1 and induces apoptosis in several tumor cell lines (e.g. in ERα-positive BC and HCC cell lines) through inhibition of translation and down-regulation of the anti-apoptotic myeloid cell leukemia-1 protein (Mcl-1, a Bcl-2 family member), and consequent activation of the mitochondrial pathway, associated with mitochondrial membrane depolarization (MMD) [51,52]. Moreover, emerging evidence suggests that sorafenib may have a more specific effect on mitochondria; indeed, it has been shown to inhibit oxidative phosphorylation (OXPHOS) in HCC and to directly target mitochondrial electron transport chain complex I in neuroblastoma cells, impairing mitochondrial energy production[53,54]. Currently, sorafenib is under evaluation in a variety of solid tumors (e.g. colon cancer and NSCLC) and phase II/III clinical trials are ongoing in advanced/metastatic breast cancer in combination with conventional chemotherapy or endocrine therapy. Recent results demonstrated a significant PFS benefit with the addition of sorafenib to first- or second-line capecitabine in metastatic HER2-negative breast cancer. A significant PFS benefit was also obtained by combining sorafenib with gemcitabine or capecitabine[55,56]. Recently, addition of sorafenib to paclitaxel was shown to improve disease control, although without significantly increasing PFS[57]. Finally, addition of sorafenib to anastrozole was associated with an increase in clinical benefit rate[58].

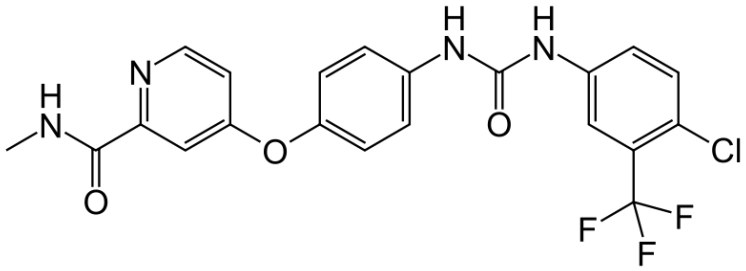

Figure 8. Sorafenib *(www.lclabs.com)*

AIM OF THE THESIS

Great strides have been done in treating cancer. For decades, the hallmark of medical treatment for cancer has been intravenous cytotoxic chemotherapy which targets all dividing cells. In the last ten years the identification of different driver oncogenic mutations has allowed the development of targeted drugs. Targeted cancer therapies are based on the use of drugs that block the growth and spread of cancer by interfering with specific molecules involved in tumor growth and progression. The aim of my work was outlining the importance of targeted therapy in treating cancer, especially NSCLC and breast cancer. We focused our attention on these two tumors because of their deep impact in the society; lung cancer is the leading cause of cancer-related mortality for both men and women with more than 1.6 million deaths worldwide[1,2], and breast cancer is the second most common cancer worldwide after lung cancer, the fifth most common cause of cancer death, and the leading cause of cancer death in women[8].

In particular, here I studied the molecular mechanisms underneath three targeted drugs: erlotinib and gefitinib in NSCLC, and sorafenib in BC. The research performed during my PhD course was divided in three parts.

In the first part, I worked in collaboration with the Oncology Unit of University Hospital of Parma. The aim of the work was to demonstrate the utility of FDG-PET to identify early resistant patients (after 2 days of erlotinib treatment) and to predict the clinical outcome in an unselected population with pretreated advanced NSCLC. In particular, in order to mimic the assessment of tumor glucose utilization, we evaluated, *in vitro*, the uptake of radio-labeled deoxy-D-Glucose 2-[1,2-3H(N)] (2DG) in a panel of NSCLC cell lines treated with or without erlotinib. In accordance with the clinical data, our preclinical results suggest that conditions where erlotinib treatment increase or fails to reduce glucose uptake can be associated with resistance, whereas a decrease of glucose uptake does not necessarily indicate drug sensitivity. Moreover, the inhibition of AKT signaling pathways seems to play a role in erlotinib-mediated down-regulation of glucose transport activity. Therefore FDG-PET assessment, after 2 days of erlotinib treatment, could be clinically useful to identify early resistant patients and to predict clinical outcome in unselected population with pretreated advanced NSCLC.

In the second part of my research, I focused the attention exploring the possible benefits of maintaining gefitinib in a NSCLC cell line become resistant to TKIs. Here, I studied the retained antitumor activity of gefitinib in resistant HCC827 GR5 carrying *MET* amplification (leading to ERBB3-mediated activation of PI3K/AKT signaling) in order to establish the possible benefits of

maintaining gefitinib in patients developing an acquired resistance. In particular, our data demonstrated that despite tumor progression after treatment with gefitinib, NSCLCs with *MET* amplification are still dependent on EGFR signaling. In these tumors EGFR plays an important role in cell motility and invasiveness and prompts the EMT process possibly via Src signaling. In addition, our preliminary data demonstrated that maintaining gefitinib after acquired resistance in HCC827 GR5 cell line could sensitize cells to chemotherapy increasing cell death after 48 and 72h of treatment.

In the last part of my work I investigated the effects and the molecular mechanisms of the multi-kinase inhibitor sorafenib in a panel of BC cell lines of different subtypes with particular attention on the effects on intracellular signaling pathways that control either cell proliferation/survival or energy metabolism. We demonstrated that sorafenib inhibited cell proliferation and induced apoptosis through the mitochondrial pathway. Sorafenib promoted an early perturbation of mitochondrial function, inducing a deep depolarization of mitochondrial membrane, associated with drop of intracellular ATP levels and increase of ROS generation. As a response to this stress condition, the energy sensor AMPK was activated and this activation persisted all along sorafenib treatment. As an early response, in MCF-7 and SKBR3 cells AMPK stimulated glucose metabolism, enhancing glycolysis, and lactate production, and increasing glucose uptake by GLUT-1 upregulation. However, persistence of energy stress during sorafenib treatment in MCF-7 and SKBR3 cells as well as in the highly-glycolytic model MDA-MB-231 resulted in the inhibition of mTORC1 pathway and the consequent decrease of glucose utilization. Our results suggest that sorafenib, being effective in all the BC cell subtypes, may be proposed as a valid support to the current established therapy for ERα-positive or HER-positive BC. Regarding TNBC the use of sorafenib in clinical practice warrants further validations.

In conclusion, targeted therapy (here we give three examples of targeted drugs in NSCLC and breast cancer) could be a promising strategy in order to defeat cancer. Genomic and proteomic technologies have generated an enormous amount of information critical to expanding our understanding of cancer biology. New research on the differences between normal and malignant cell biology has paved the way for the development of drugs targeted to specific biological molecules, potentially increasing antitumor efficacy while minimizing the toxicity to the patient that is seen with conventional therapeutics. Thus collaboration among researchers, clinicians, and

pharmaceutical companies is vital to conducting clinical trials to translate laboratory findings into clinically applicable therapeutics (Translation Medicine) and then helping to choose “the right therapy for the right patient”.

MATERIALS AND METHODS

Cell culture

Human NSCLC cell lines H322, H292, Calu-3, A549, SKMES-1, H460, H1299, Calu-1 were purchased from American Type Culture Collection (ATCC) (Manassas, VA). Human PC9, HCC827 and HCC827 GR5 NSCLC cell lines were kindly provided by Dr P. Jänne (Dana-Farber Cancer Institute, Boston MA). HCC827 GR5 cell line was obtained from gefitinib-sensitive EGFR exon 19 mutant HCC827 cell line by exposing HCC827 cells to increasing concentration of gefitinib for 6 months. HCC827 GR5 cells were cultured in the presence of gefitinib 1μM.

Human BC cell lines MCF-7, T47D, BT474 (ERα-positive), MDA-MB-231, MDA-MB-468 (triple negative), and SKBR3 (ERα-negative/HER2-positive) were obtained from ATCC.

All the cells were cultured as recommended: H322, H292, SKMES-1, HCC827, A549, H460, H1299, Calu-1, MCF-7, T47D, BT474, MDA-MB-231, MDA-MB-468, and SKBR3 were cultured in RPMI-1640 growth medium; Calu-3 cells were cultured in DMEM (high glucose) growth medium and SKMES-1 cells were cultured in MEM growth medium supplemented with 10% fetal bovine serum (FBS), 2mM glutamine (GLN), 1% antibiotics (penicillin 100UI/ml, streptomycin 100μg/ml). All the cell lines were maintained under standard cell culture conditions at 37 ºC in a water-saturated atmosphere of 5% CO_2 in air.

Chemicals and reagents

Erlotinib, cisplatin and pemetrexed were from inpatient pharmacy. Gefitinib (ZD1839/Iressa®) was provided by AstraZeneca (Milan, Italy). NVP-BEZ235 was provided by Novartis Institutes for BioMedical Research (Basel, Switzerland). Dasatinib was from LC Laboratories (Woburn, MA). U0126, SU11274, Oligomycin, 2-Deoxy-glucose (2DG) and z-VAD-fmk (MP) were from Sigma-Aldrich (St. Louis, MO). Sorafenib was from Bayer HealthCare LLC (Tarrytown, NY), diphenyleneiodonium chloride (DPI) and fasentin were from Merck-Millipore (Darmstadt, Germany). Drugs were dissolved in dimethyl sulfoxide (DMSO) (Sigma-Aldrich) and diluted in fresh medium before use. Final DMSO concentration in medium never exceeded 0.1% (v/v) and equal amounts of the solvent were added to control cells. 2DG was dissolved in bi-distilled water; fasentin was dissolved in 50% DMSO in water and N-Acetyl-L-cysteine (NAC, Sigma-Aldrich) was directly dissolved into the medium before the experiments. Media and FBS were from Gibco.

Antibodies against p-EGFR^{Tyr1068}, EGFR, MET, p-Src^{Tyr416}, p-Src^{Tyr527}, Src, p-Akt^{Ser473}, Akt, p-p70S6K^{Thr389}, p70S6K, phospho-mTOR^{Ser2448}, mTOR, p-ERK1/2$^{Thr202/Tyr204}$, ERK1/2, p-p38 MAPK, p38 MAPK; p-STAT5^{Tyr694}, STAT5, p4E-BP1^{Ser65}, PARP-1, caspase-7, caspase-9, p-STAT3, Mcl-1, and p-AMPKα1^{Thr172}, E-cadherin, N-cadherin, vimentin, SNAIL, SLUG were from Cell Signaling Technology (Beverly, MA). Anti-GLUT-1 and anti-AMPKα1 antibodies were from Abcam (Cambridge, UK). Anti-actin antibody was from Sigma-Aldrich. Antibody against GAPDH was from Ambion (Austin, TX). Horseradish peroxidase (HRP) conjugated secondary antibodies were from Pierce (Rockford, IL) and chemoluminescence system (Immobilion TM Western Chemiluminescent HRP Substrate) was from Merck-Millipore. Reagents for electrophoresis and blotting analysis were from Bio-Rad (Hercules, CA).

MTT assay

Cell viability was detected by tetrazolium dye [3-(4,5-dimethylthiazol-2-yl)-2,5-diphenyltetrazolium bromide] (MTT) assay. The assay is based on the reduction of the yellow tetrazole MTT, to its insoluble formazan, giving a purple colour. MTT reduction is dependent on NAD(P)H-dependent oxidoreductase enzymes expressed in the cell. Therefore, reduction of MTT increases with cellular metabolic activity due to elevated NAD(P)H flux.

3-5x10^3 cells were seeded into 96-well plates in quadruplicate and were exposed to various treatments. After 72h, 100µl of MTT solution (1 mg/ml, Sigma-Aldrich) was added to each well and incubated. After 1h, crystalline formation was dissolved with DMSO and the absorbance at 570nm was measured using a microplate-reader (Bio-Rad). Data are expressed as percent inhibition of cell proliferation versus control cells.

Crystal violet (CV) assay

Crystal violet (triphenylmethane dye {4-[(4-dimethylaminophenyl)-phenyl-methyl]-N,N-dimethyl-aniline}) assay is a colorimetric assay for measuring cell vitality. Crystal violet dye stains nuclei. Upon solubilization, the amount of dye taken-up by the monolayer and the intensity of the colour produced are proportional to cell number.

5x10^3 cells were seeded into 96-well plates in quadruplicate and were exposed to various treatments. After 72h, medium was removed and the cells washed twice with cold phosphate

buffered saline (PBS), fixed with ice-cold methanol for 10min and stained with 0.5% crystal violet in PBS. The unbound dye was removed by washing carefully with water. Bound crystal violet was solubilized with 0.2% TritonX-100 in PBS. Light excitation which increases linearly with the cell number was analyzed at 570nm using a microplate-reader (Bio-Rad).

Analysis of cell death

Cell death was assessed by morphology on stained (Hoechst 33342, propidium iodide (PI) or unstained cells using light-phasecontrast-and fluorescence-microscopy. Hoechst and PI were used to differentiate between apoptotic and necrotic cells.

Analysis of cell cycle

Distribution of the cells in the cell cycle was determined by PI staining and flow cytometry analysis. Briefly, 5×10^5 cells were incubated overnight at 4°C in 1ml of hypotonic fluorochrome solution (50µg/ml PI, 0.1% Triton X-100 in PBS). Analysis was performed with Coulter EPICS XL-MCL cytometer (Coulter Co., Miami, FL, USA). Cell-cycle-phase distributions were analyzed by MultiCycle DNA Content and Cell Cycle Analysis Software (Phoenix Flow Systems, Inc., San Diego, CA, USA).

Wound healing assay

A wound-healing assay was performed with the CytoSelect24-well Wound Healing Assay Kit (Biolabs, San Diego, CA). Wound healing inserts were put into 24-well cell culture plates and cell suspension ($1.5x10^5$ cells in 250µl) was added to either side of the insert and incubated overnight to form a monolayer. The inserts were then removed to allow the cells to migrate. After 24h cells were fixed with 100% methanol, stained with hematoxylin. Images of wound healing were captured by microscope equipped with digital camera at a magnification of $\times$40 at zero time point and after 24h. Cell migration was quantified by measuring the migration distances. Percent closure was calculated as wound area 24h/wound area zero time point x 100.

Cell migration and invasion

The migration and invasion assays were carried out using Transwell chamber with 6.5-mm diameter polycarbonate filters (8µm pore size, BD Biosciences, Erembodegem, Belgium) uncoated or coated with MatrigelTM. Cells were trypsinized and $2x10^5$ cells suspended in serum free RPMI-1640 medium and loaded in the upper wells. FBS (10%) was used as a chemoattractant in the lower chambers. After incubation for 16h all of the non-migrated (or non-invaded) cells were removed with a cotton swab, and cells that had migrated (or invaded) through the membranes were fixed with 100% methanol, stained with hematoxylin and counted under a Phase contrast microscope.

Gelatin zymography

The gelatin zymography was performed to determine the activity of matrix metalloproteinases (MMP). Equal number of cells were seeded and incubated with serum-free RPMI-1640 for 24h. Medium was collected and centrifuged at 300g for 5min to remove cell debris. Equal amounts of media were mixed with SDS-PAGE sample buffer 3X in the absence of reducing agent and electrophoresed in 10% polyacrylamide gel containing 1mg/ml gelatin. After running, the gel was incubated in the Renaturating Buffer (50mM Tris-HCl pH 7, 6.5mM $CaCl_2$, 1µM $ZnCl_2$, 2.5% Triton X-100) twice for 15min at room temperature. The gel was washed with Washing Buffer (50mM Tris-HCl pH 7, 6.5mM $CaCl_2$, 1µM $ZnCl_2$) and then incubated in Developing Buffer (50 mM Tris-HCl pH 7, 6.5 mM $CaCl_2$, 1µM $ZnCl_2$, 1% Triton X-100, 0.02% NaN_3) overnight at 37º C. The gel was stained with 0.25%. Coomassie Brilliant Blue R-250 solution containing 45% methanol and 10% glacial acetic acid for 3h and then washed with a solution containing 10% glacial acetic acid, 45% methanol for 1h. Areas of protease activity appeared as clear bands. The activity of MMPs was determined by densitometric scanning of the bands and analysis by Quantity One 1-D Analysis Software (Bio-Rad).

RNA interference assay

Lung cancer cells were transfected with Invitrogen StealthTM siRNA (Invitrogen, Carlsbad, CA) against: EGFR (mixture of HSS103114, HSS103116 and HSS176346) with a final concentration of 60nM; Src (mixture of HSS186080, HSS186081 and HSS186082) with a final concentration

of 60nM; p38α (mixture of HSS102352, HSS102353 and HSS175313) with a final concentration of 60nM; STAT5a/b (mixture of HSS186133, HSS186134, HSS186135, HSS110287, HSS110288 and HSS110289) with a final concentration of 90nM. Negative controls (medium GC content and low GC content) were from Invitrogen.

BC cells were transfetced with siRNA against AMPKα1 (Ambion Silencer_Select si RNA 4392420, mixture of s100, s101, s102 antisense sequences) or Silencer_Select negative control siRNA with a final concentration of 60nM. Negative controls (medium GC content and low GC content) were from Invitrogen. The transfection was carried out according to the Invitrogen forward transfection protocol for LipofectamineTM RNAiMAX transfection reagent. After 48h of transfection, the medium was replaced with fresh medium for subsequent analysis.

Quantitative Real-Time PCR

Total RNA was isolated using the TRI REAGENT LS (Invitrogen). One μg RNA was retro-transcribed using the DyNAmo cDNA Synthesis Kit (Thermo Scientific, Vantaa, Finland), according to the manufacturers' instructions. Primers and probes to specifically amplify vimentin were obtained from Applied Biosystems Assay-on-Demand Gene expression products (Hs00185584_m1). Quantitative real-time PCR was performed in a 25μl reaction volume containing TaqMan Universal master mix (Applied Biosystems, Forster City, CA). All reactions were performed in triplicate using the ABI PRISM 7500 sequence detection system instrument (Applied Biosystems). Samples were amplified using the following thermal profile: 50ºC for 2 min, 95ºC for 10mins, 40 cycles of denaturation at 95ºC for 15sec followed by annealing and extension at 60ºC for 1min. Amplifications were normalized to GAPDH (Hs02758991_g1). The fold change was calculated by the ΔΔCT method and results were plotted as 2 -ΔΔCT.

Western Blot analysis

Cells were washed twice with ice-cold PBS, scraped in lysis buffer solution (150 mM NaCl, 5mM MgCl2, 50mM Tris-HCl pH 7.4, 0.1% sodium dodecyl solfate (SDS), 1% Triton-X-100, 10g/ml 4-amido-phenyl-methane-sulfonyl fluoride (APMSF), 0.5g/ml leupeptine, 0.7g/ml pepstatine, 0.5mM ethylenediaminetetraacetic acid (EDTA), 1mM sodium ortovanadate, 50mM NaF, 5mM sodium pyrophosphate, 10mM sodium glycerol phosphate, 0.5% sodium

deoxycholate), sonicated and collected by centrifugation. For GLUT-1 detection, cells were lysed in GLUT-1 lysis buffer (1% Triton X-100, 0.1% SDS, protease inhibitors) for 1h on ice, and precleared by centrifugation for 10min at 4ºC. Protein concentration was determined by the dye-binding method (Bio-Rad) with bovine serum albumin (BSA) as standard. 30-40µg of proteins for each sample were denaturated in sample buffer for 30min, separated on 7.5-15% acrylamide gels by SDS–PAGE and electrophoretically transferred to a polyvinyldene difluoride (PVDF) membrane. Membranes were blocked with blocking solution (5% non-fat-powdered milk or 5% BSA in tris buffered saline 1% tween 20, TTBS) for 1h. The membranes were incubated with primary antibody overnight at 4°C on a shaker platform, and then they were incubated for 1h with HRP-anti-mouse or HRP-anti-rabbit secondary antibodies at room temperature. Immunoreactivity was visualized with enhanced chemiluminescence.

Determination of pattern of proteins phosphorylation

Relative levels of phosphorylation of 46 kinase phosphorylation sites (38 selected proteins) were obtained by using Proteome Profiler Human Phospho-kinase Array (Kit ARY003B from R&D System, Minneapolis, MN) according to the manufacturer's guidelines. A total of 300µg of proteins was used for each array. The resulting spots were quantified using Quantity One 1-D Analysis Software (Bio-Rad).

Immunofluorescent staining

Cells were grown on poly-L-lysine‑coated glass slides for 24h. For E-cadherin staining, cells were fixed with 4% formaldehyde in PBS for 20min and unspecific epitopes were blocked with 3% BSA in PBS. Then, cells were incubated for 3h at RT with the anti-E-cadherin antibody (Cell Signaling Technology). For vimentin staining, cells were fixed in 4% paraformaldehyde in PBS for 15min, washed with PBS, permeabilized with 0.2% Triton X-100 at RT for 30min and blocked with 3% BSA. Then, cells were incubated overnight at 4°C with anti-vimentin antibody (Cell Signaling Technology). For E-cadherin and vimentin staining FITC-conjugated donkey anti-rabbit secondary antibodies (Jackson Immunoresearch, West Grove, PA) were used. Nuclei were stained with Draq5 (Cell Signaling Technology). Samples were observed using a confocal

system (LSM 510 Meta scan head integrated with the Axiovert 200M inverted microscope; Carl Zeiss, Jena, Germany) with X63 oil objective. Image acquisition was carried out in multitrack mode, namely through consecutive and independent optical pathways.

ATP, mitochondrial membrane depolarization (MMD) and reactive oxygen species (ROS) measurements

Cellular ATP changes were determined by a luminescence assay (ATPLite-1step, PerkinElmer). MMD was measured as reduced staining with the potentiometric fluorescent dye tetramethylrhodamine–methylester (TMRM, Molecular Probes). Intracellular hydrogen peroxide H_2O_2 and superoxide anion O_2^- were assessed by oxidation of the cell permeable fluorescent probes 5-(and-6)-chloromethyl-20,70-dichlorodihydrofluorescein diacetate, acetyl ester (CM-H2DCFDA, Molecular Probes), and dihydroethidium (DHE, Merck-Millipore), respectively. $3x10^5$ cells, seeded into 6-well plates, were incubated in different conditions depending on the experiment. During the last 30min of treatment, the cells, loaded with TMRM 0.01µM, CM-H2DCFDA 0.2µM, or DHE 5µM, were left in the dark at 37ºC, and then trypsinized and analyzed on a Beckman-Coulter EPICS XL flow cytometer.

Cellular glucose uptake

10^5 cells were seeded into 12-well plates in complete growth medium. 48h later the medium was replaced with fresh drug-containing or-free RPMI-1640 and the cells were cultured for additional 6h or 24h depending on the experiment. For glucose uptake measurements, Kreb's Ringer HEPES (KRH) buffer containing 2µCi/ml Deoxy-D-Glucose 2-[1,2-^{3}H(N)] (2DG, 1mCi/mmol, Perkin-Elmer, Waltham, MA,USA) was used (uptake buffer). The cells were quickly rinsed with KRH and incubated in uptake buffer at 37°C for 5min. The incubation was stopped by removal of the uptake buffer and the cells were quickly rinsed three times in fresh cold KRH solution containing 0.1mM phloretin (Sigma-Aldrich). Ice-cold trichloroacetic acid (TCA, 5%, w/v) was added to denature the cells and after 15min at 4°C the radioactivity in samples of the acid extracts was measured by liquid-scintillation counting in 3 independent determinations. Cell proteins, precipitated by TCA, were dissolved in 0.5N NaOH and their concentration was determined by a dye-fixation method (Bio-Rad) using BSA as standard.

Measurement of glycolytic flux

Glycolytic flux was determined by analyzing the conversion of [5-^{3}H]glucose to ^3H_2O. Cells were incubated as described for cellular glucose uptake. After 6h or 24h, depending on the experiment, the cells were washed in PBS once and resuspended in drug-containing or-free KRH buffer for 30min. For glycolytic flux measurements, KRH buffer containing 10 µCi/ml D-Glucose [5-^{3}H(N)] (1mCi/mmol, Perkin-Elmer) and unlabelled D-glucose to a final concentration of 10 mM (glycolysis buffer) was used. Cells were incubated with 0.5ml drug-containing or-free glycolysis buffer for 1h at 37°C. To stop the reaction, HCl was added at a final concentration of 0.04M. After 15min at 4°C, 0.2 ml of the reaction mixture was transferred to a small open tube that was placed in a scintillation vial containing 0.5ml water. The scintillation vial was then sealed to allow ^3H_2O to evaporate from the tube and condense in the 0.5ml water in the bottom of the scintillation vial. After at least 24h, ^{3}H in water and [5-^{3}H]glucose in the cell lysate were measured by liquid-scintillation counting to determine the glycolytic flux. Cell proteins, precipitated by HCl, were dissolved in 0.5N NaOH and their concentration determined by a dye-fixation method. Glucose utilization rates were calculated as pmol of glucose utilized/mg of protein/1h from the formula:

$$\text{Glucose utilized (pmol)} = \frac{\text{[3H]water formed (d.p.m.)}}{\text{sp radioactivity of [5-3H]glucose } \left(\frac{\text{d.p.m.}}{\text{pmol}}\right)}$$

Lactate production

Cells were incubated as indicated for glycolytic flux. After 6h media was collected and lactate was measured in accordance with the manufacturer's instructions by a colorimetric assay kit (Biochemical Enterprise).

Statistical analysis

Statistical analysis were carried out using GraphPad Prism version 5.00 software (GraphPad Software, San Diego, CA). IC_{50} values, expressed as means ± standard deviations (SD) of three

independent experiments, were calculated by fitting the experimental data with a hyperbolic function and constraining Y_{max} to 100. Results are expressed as mean values ± SD for the indicated number of independent measurements. Differences between the mean values recorded for different experimental conditions were evaluated by two tailed Student's t-test. Differences were considered significant at ***P<0.001, **P<0.01 and *P<0.05.

CHANGES IN GLUCOSE UPTAKE AFTER ERLOTINIB TREATMENT IN NSCLC CELL LINES.

PREDECTIVE AND PROGNOSTIC VALUE OF EARLY RESPONSE ASSESSMENT USING 18FDG-PET IN ADVANCED NON-SMALL CELL LUNG CANCER PATIENTS TREATED WITH ERLOTINIB (Tiseo M, Ippolito M, Scarlattei M, Spadaro P, Cosentino S, Latteri F, Ruffini L, Bartolotti M, Bortesi B, Fumarola C, Caffarra C, Cavazzoni A, Alfieri R. R., Petronini P.G., Bordonaro R, Bruzzi P, Ardizzoni A, Soto Parra H. J.; *Predictive and prognostic value of early response assessment using 18FDG-PET in advanced non-small cell lung cancer patients treated with erlotinib*; Cancer Chemother Pharmacol (2014) 73:299–307)**.**

Background

As mentioned before, great strides have been done in treating NSCLC. Thanks to the progression in understanding the mechanisms of cancer development, nowadays, there are much more specific treatments to defeat NSCLC. In particular, the presence of EGFR gene activating mutations is a strong predictive factor of response to EGFR TKIs (such as erlotinib and gefitinib). Unfortunately for many NSCLC patients *EGFR* status remains unknown, since only small tumor samples, not adequate for molecular analysis, are available[59]. Recently, EGFR TKIs (in particular erlotinib) demonstrated to be effective also in a small percentage of patients not harboring *EGFR* mutations. Nevertheless, at present there is no predictive factor available to identify the minority of patients with EGFR wild type NSCLC who may derive some benefits from EGFR TKIs, in particular from erlotinib[60,61]. As a consequence, the use of erlotinib in *EGFR* wild-type patients is widely empirical. It is very important and useful find non invasive, simple and efficacy techniques that identify patients that could benefit from treatments with EGFR TKIs in order to avoid side effects and costs of inactive treatment. At the same time there is also the necessity to understand better the molecular mechanisms underneath the action of these drugs in order to use "the right drug onto the right patient".

In clinic, PET and CT imaging have become essential diagnostic tools physicians use to reveal the presence and severity of cancers: malignant cells need much more glucose than normal cells showing as an increase in glucose uptake. Before a PET/CT scan, the patient receives an intravenous injection of radioactive glucose, then cancer cells rapidly accumulate the radioactive

glucose. Information regarding the location of abnormal levels of radioactive glucose obtained from the whole-body PET/CT scan helps physicians effectively pinpoint the source of cancer and detect whether cancer is isolated to one specific area or has spread to other organs. This phenomenon is due to the issue that, as well known, cancer cell metabolism is unequivocally altered[62]. Compared to normal cells, malignant cells show an increased glucose uptake, a higher rate of glycolysis associated with reduced pyruvate oxidation and increased lactic acid production; normal tissues exhibit the Pasteur effect (inhibition of lactate production in the presence of oxygen) while tumor tissues maintain lactate production regardless of oxygen tension[63]. Moreover, cancer cells present an increased glutaminolytic activity, penthose phosphate pathway activation and modified amino acid metabolism[64]. Warburg effect is established through many mechanisms as the overexpression of glucose transporters (GLUTs; GLUT proteins catalize the facilitative bidirectional transfer of their substrate across membranes. GLUT-1 and GLUT-3 are overexpressed in several cancer cell lines), the upregulation/deregulation of gycolitic enzymes (such as, HK, and PFK) and pyruvate kinase 2 (PK2), the pyruvate crossroad, krebs cycle, oxidative phosphorylation defects and glutamine metabolism[62].

In order to evaluate the response to chemotherapy and to target agents (such as erlotinib) the Response Evaluation Criteria in Solid Tumors (RECIST) based on CT scan is currently used. Nevertheless, conventional imaging techniques have some limitations in the assessment of response to biological agents, considering their prevalent cytostatic activity. For example an increasing number of drugs in development inhibit cell growth (cytostatic) and thus do not shrink the tumor like conventional chemotherapy drugs, which kill cells (cytotoxic); as a consequence, you have some benefits from the treatment but you are not able to see the improvement[65]. PET, and recently PET/CT, with fluorodeoxyglucose (FDG) has been evaluated as a method to predict tumor response in various tumor types including NSCLC and its superiority to conventional imaging was shown in several studies. FDG-PET is a valuable tool for predicting tumor response to both chemotherapy and TKIs therapy. In particular, FDG-PET is attractive for monitoring treatment with TKIs, because many signaling pathways targeted by protein kinase inhibitors have a demonstrated role also in regulating tumor glucose metabolism[66]. Moreover PET is a non invasive, simple and safe technique.

In the first part of my work I performed *in vitro* experiments in support of clinical data that demonstrated the utility of FDG-PET to identify early resistant patients, after two days of erlotinib treatment, and to predict clinical outcome in unselected population with pretreated advanced NSCLC. In particular, we evaluated the uptake of radio-labeled deoxy-D-Glucose 2-[1,2-3H(N)] (2DG) in a panel of NSCLC cells treated with or without erlotinib in order to mimic the assessment of tumor glucose utilization; in addition, we studied the molecular mechanisms of erlotinib action related to the effects on cell glucose metabolism.

Clinical results

The aim of this study was to evaluate the predictive value of PET response after two days of erlotinib in unselected pretreated patients with stage IV NSCLC. FDG-PET/CT scans were conducted at baseline and after 2 days of erlotinib treatment, with a CT evaluation performed at baseline and after 45–60 days of therapy. PET responses were evaluated by quantitative changes on Standardized Uptake Value **(***SUV)max* tumor/non-tumor ratio and classified according to European Organization for Research and Treatment of Cancer (EORTC) criteria. PET responses were compared with RECIST responses and related to PFS and overall survival (OS). Fifty-three patients were enrolled in the clinical study. At 2 days of erlotinib treatment, 20 (38 %) patients showed partial metabolic response (PMR), 25 (47 %) had stable metabolic disease (SMD) and 8 (15 %) had progressive metabolic disease (PMD). All patients with PMD had confirmed RECIST progression at 45–60 days. Patients with early PMR and SMD had significantly longer PFS ($p < 0.001$ and $p = 0.001$, respectively) and OS ($p = 0.001$ for both) than PMD patients.

Preclinical results

Effects of erlotinib on cell proliferation and basal level of 2DG uptake in a panel of NSCLC cell lines.

EGFR expressing NSCLC cell lines were treated with increasing concentrations of erlotinib (0.01μM, 0.1μM, 0.5μM, 1μM, 2.5μM, 5μM and 10μM) and were submitted to MTT assay. Erlotinib inhibited cell proliferation in a dose-dependent manner, with IC_{50} values ranging from <0.02μM for HCC827 cells to >20μM for Calu-1 cells **(Figure 10)**. An IC_{50} value of 1μM was chosen as a cut-off to distinguish *sensitive* (H322, H292 and Calu-3) from *resistant* (A459, SKMES, H1299, H460, and Calu-1) cell lines. The HCC827 cell line, harboring a delE746-A750 activating EGFR mutation, was selected as a model for highly erlotinib-*sensitive* cells, in contrast with its derivative HCC827 GR5 cell clone, that is highly erlotinib-*resistant* due to *MET* amplification.

Cell line	**Erlotinib IC_{50} (μM)**
HCC827	< 0.02
H322	0.258 ± 0.01
H292	0.468 ± 0.01
Calu3	0.497 ± 0.02
A549	2.834 ± 0.3
SKMES	3.723 ± 0.2
H1299	4.578 ± 0.5
H460	5.868 ± 0.4
HCC827GR5	> 10
Calu-1	> 10

Figure 10. Effects of erlotinib on cell proliferation. 3-5x10^3 cells were seeded in 96-multiwell plates and 24h later were treated with or without increasing concentrations of erlotinib (0.0.1-10μM). After 72h cell survival/proliferation was assessed using MTT assay. The IC_{50} values, expressed as mean ± SD of three independent experiments, were calculated by fitting the experimental data with a hyperbolic function and constraining Ymax to 100 (GraphPad Prism 4.00).

Radio labeled 2DG uptake by cells was used as an assay to measure glucose transport activity, thus mimicking the assessment of tumor glucose utilization by PET in tumor. Cells were incubated in RPMI-1640 medium for 16h and the basal level of 2DG uptake for a period of 5min

was then measured; as shown in **Figure 11,** there is no correlation between basal level of 2DG uptake and sensitivity to erlotinib treatment.

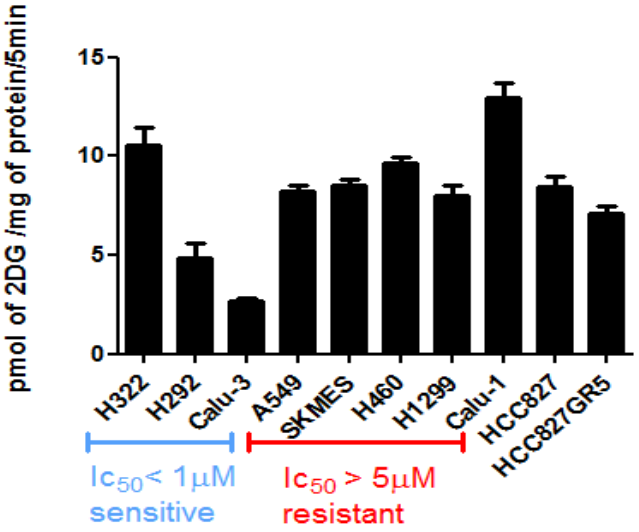

Figure 11. Basal level of 2DG uptake. Cells were incubated in RPMI-1640 medium for 16h and the basal level of radiolabelled 2DG uptake for a period of 5min was then measured. Radioactivity in TCA extracts was measured by liquid-scintillation. Data are expressed as pmol of 2DG/mg protein/5 min. Columns, mean of twelve measurements performed in three independent experiments, bars, SD.

Effects of erlotinib treatment on glucose uptake.

A panel of NSCLC cells was incubated with or without erlotinib 1µM for 16h, and then 2DG uptake was measured. As shown in **Figure 12a**, a 16h treatment with erlotinib 1µM significantly reduced 2DG uptake in the *sensitive* cell lines, while producing no effect in *resistant* H460, H1299 and Calu-1 cells. Erlotinib induced a smaller but significant decrease in 2DG uptake levels also in two *resistant* cell lines (A549 and SKMES). Interestingly, the highly erlotinib sensitive HCC827 cells showed a 50% decrease in 2DG uptake after erlotinib treatment, in contrast with their resistant counterpart HCC827 GR5 cells **(Figure 12b)**.

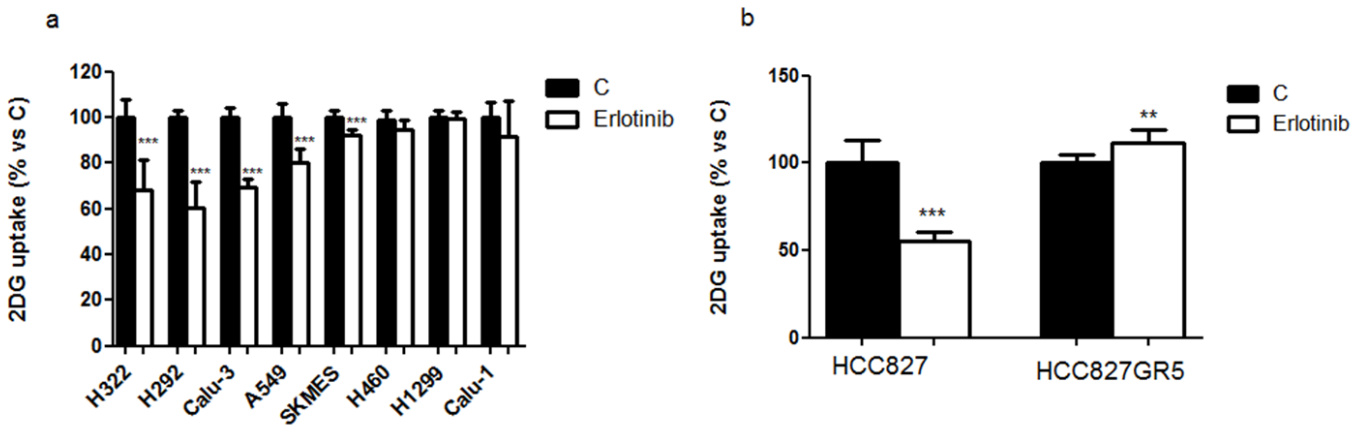

Figure 12. Effects of erlotinib on glucose uptake. (a) A panel of *resistant* and *sensitive* NSCLC cell lines was incubated with or without erlotinib 1μM for 16h and then the level of 2DG uptake for a period of 5min was measured. (b) HCC827 cell line and its derivative HCC827 GR5 cell clone were respectively treated with or without 0.05μM or 1μM erlotinib and then incubated as described above. Data are expressed as percent versus control cells. Columns, means of twelve measurements performed in three independent experiments, bars, SD. *Statistical significance versus C. **P<0.01, ***P<0.001.

In order to assess whether the decrease in 2DG uptake was due to the inhibition of cell proliferation or reflects a direct effect of erlotinib treatment on glucose transport, H292 *sensitive* cells were incubated with or without erlotinib 1μM for 2, 4, 8 and 16h and the level of 2DG uptake was measured **(Figure 13a)**: erlotinib 1μM significantly reduced 2DG uptake just after 4h of treatment. In addition, H460 *resistant* cells and H292 *sensitive* cells were incubated with or without erlotinib 1μM or the DNA-damaging agent cisplatin 2.5μM for 16h and then the level of 2DG uptake was measured **(Figure 13b)**: erlotinib significantly reduced 2DG only in the *sensitive* cell line H292, while 2.5μM cisplatin produced no effects either in the *sensitive* H292 cells or in the *resistant* H460 cells. Finally, H292 cells were incubated with or without erlotinib 1μM or cisplatin 2.5μM for 8h and then cell cycle distributions were analyzed by flow cytometry: as shown in **Figure 13c,** erlotinib had no effect on cell cycle distribution while cisplatin produced a significant block of the cell cycle at S phase.

Taken together these results show that in H292 *sensitive* cells erlotinib-mediated decrease in 2DG uptake occurred at early time points, when the effects on cell proliferation and cell cycle distribution were not yet detectable.

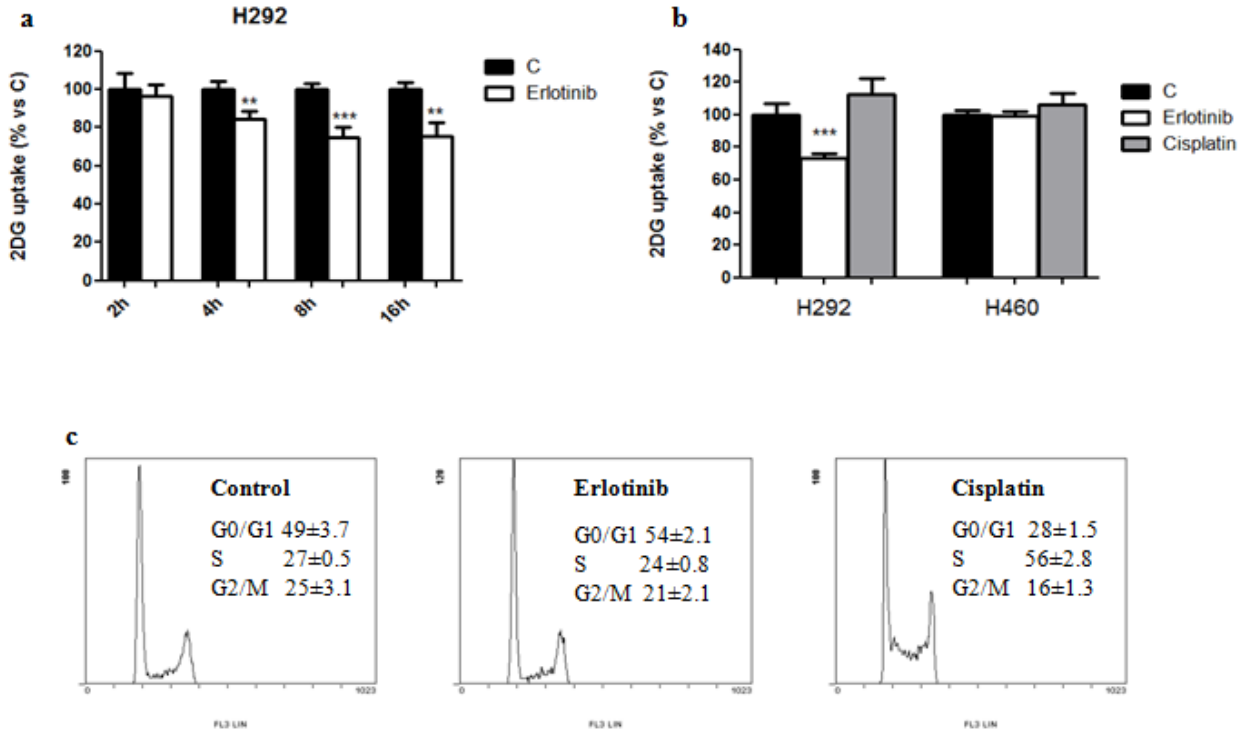

Figure 13. Effects of erlotinib and cisplatin on glucose uptake and cell cycle distribution. (a) H292 cells were incubated with or without erlotinib 1μM and the level of 2DG uptake for a period of 5min was measured at the indicated time intervals; (b) H292 and H460 cells were incubated with or without erlotinib 1μM or cisplatin 2.5μM and the level of 2DG uptake for a period of 5min was measured after 16h; (c) H292 cells were incubated as described in (b) and cell cycle distributions were analyzed by flow cytometry after 8h. (a,b) Data are expressed as percent versus control cells. Columns, means of twelve measurements performed in three independent experiments, bars, SD. *Statistical significance versus C. **P<0.01, ***P<0.001.

Effects of erlotinib treatment on GLUT-1 expression, PI3K/AKT/mTOR and MAPK pathways.

In order to understand the mechanism underlying the decrease of 2DG uptake after erlotinib treatment we analyzed the effects of erlotinib on the expression of the glucose transporter GLUT-1, the predominant glucose transporter in many types of cancer cells. As shown in **Figure 14,** GLUT-1 total expression appeared to be down-regulated in *sensitive* HCC827 cells but not in HCC827 GR5 cells after 16h of erlotinib treatment. Moreover, only in HCC827 cells erlotinib caused the de-phosphorylation/inactivation of the relevant components of MAPK (p-ERK1/2) and AKT (p-AKT, p-mTOR, p-p70S6K) signaling pathways.

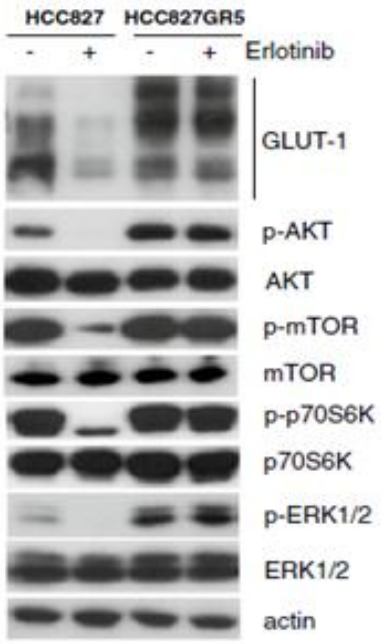

Figure 14. Effects of erlotinib on GLUT-1 expression, PI3K/AKT/mTOR and MAPK pathways. HCC827 and HCC827 GR5 cells were incubated with or without erlotinib (0.05μM and 1μM respectively) for 16h. Then the cells were lysed and protein expression was assessed by Western blot analysis.

To further investigate the role of MAPK and AKT pathways on glucose uptake we treated the *sensitive* cell model H322 with 1μM erlotinib, 0.1μM NVP-BEZ235 (a dual PI3K/mTORC1-C2 inhibitor) or 3μM U0126 (a MEK1/2 inhibitor) and after 16h the level of 2DG uptake for a period of 5min was measured. As shown in **Figure 15**, in H322 *sensitive* cells NVP-BEZ235 caused a reduction of 2DG uptake comparable with that induced by erlotinib, whereas U0126 had no effect.

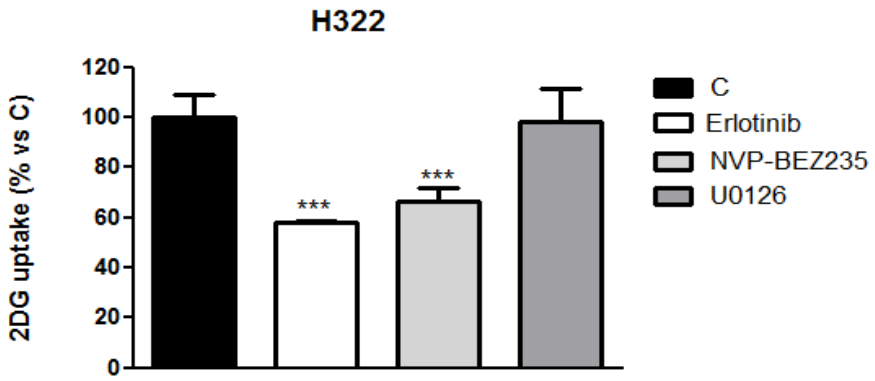

Figure 15. Effects of erlotinib, MAPK and AKT inhibitors on glucose uptake. H322 cells were treated with 1μM erlotinib, 0.1μM NVP-BEZ235 (a dual PI3K/mTORC1-C2 inhibitor) or 3μM U0126 (a MEK1/2 inhibitor) and after 16h the level of 2DG uptake for a period of 5min was measured. Columns, means of twelve measurements performed in three independent experiments, bars, SD. Data are expressed as percent versus control cells. *Statistical significance versus C. *** P<0.001.

Effects of erlotinib treatment on glycolytic flux.

Data from literature showed the active role of AKT in the upregulation of HK and PFK activity, and hence in the regulation of glycolysis[33,34]. Thus, we wanted to evaluate if erlotinib treatment could influence the glycolytic flux. The erlotinib *sensitive* cell line H292 and the erlotinib *resistant* cell line H460 were incubated with or without erlotinib 1μM for 16h and then glycolytic flux was measured with radiolabelled glucose (D-glucose[5-^{3}H(N)]). As shown in **Figure 16** erlotinib impaired the glycolytic flux only in the *sensitive* cell model H292 while it produced no effect in the *resistant* cell line H460.

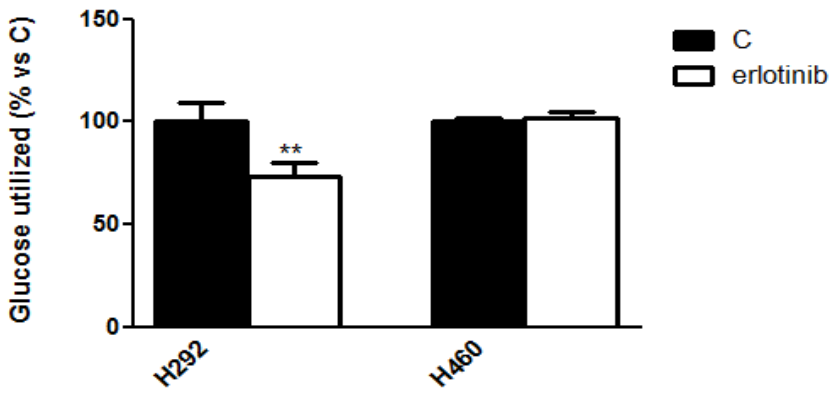

Figura 16. Effects of erlotinib on glycolytic flux. Cells were incubated with or without 1μM erlotinib for 16h. To measure the glycolytic flux, the cells were incubated in the presence of radiolabelled glucose (D-glucose[5-^{3}H(N)]) for 1h. The reaction was stopped by adding HCl. $^{3}H_2O$ was separated from [5-^{3}H]glucose by diffusion in an airtight container for 72h. Radioactivity was measured by liquid-scintillation. Data are expressed as percent versus control. Columns mean of twelve measurements performed in three independent experiments, bars, SD. * Statistical significance versus C. **P<0.01.

Discussion and conclusions

Traditionally, the response to cancer treatment in solid tumors is evaluated by clinical or radiological assessments of target lesions and is defined as a significant decrease in measurable tumor dimensions. However, there are important limitations to the evaluation of tumor response by volume changes: first of all, volume changes are rather late events, thus the first evaluation of objective responses measured by CT are performed not earlier than 2-3 months after the beginning of treatment; in addition, conventional imaging techniques have some limitations in the assessment of response to biological agents, due to their prevalent cytostatic activity[65]. Therefore, patients are often unnecessarily exposed to non useful and/or toxic treatments during a prolonged time. In recent years, metabolic imaging with PET has become increasingly important in cancer management. During the last few years, there was a growing interest in the possible utility of PET as a predictive factor of response to new targeted agents, in particular, in NSCLC[67,68]. Indeed, it has been demonstrated that TKIs have a role also in regulating tumor glucose metabolism.

The clinical study was aimed at evaluating whether FDG-PET performed early, after only two days from the beginning of erlotinib treatment, could predict clinical outcome in unselected NSCLC pretreated patients. The clinical results demonstrated that a metabolic response can be reported after two days of erlotinib treatment; 20 patients showed a metabolic response at early PET, and these patients had an increased probability of not showing radiological progression after two months. Nevertheless, the most interesting result concerns the very strong negative predictive value of early PET: all patients with early metabolic progressive disease experienced progression at CT evaluation. Although a disease progression within two days from starting therapy may seem to be an unlikely event, recent work demonstrates that rapid progression can occur in NSCLC[69]. Hence, it is plausible that an early metabolic progression reflects an aggressive biology, associated with poor survival, consistent with clinical results. In these cases, an early modification of the treatment strategy could be considered to save costs, avoid side effects and anticipate the use of more effective therapies. In support of the clinical data, our preclinical results suggest that conditions where erlotinib treatment fails to reduce or increase glucose uptake can be associated with resistance, whereas a decrease of glucose uptake does not necessarily indicate drug sensitivity. Our data demonstrated that a 16h erlotinib treatment reduced 2DG uptake and glucose consumption in erlotinib *sensitive* cell lines, either EGFR wild-type (H322, H292 and Calu3) or EGFR mutated (HCC827), while producing no effect in *resistant* EGFR wild-type cell lines (H460, H1299 and Calu-1) or even an increase in EGFR mutated cells (HCC827GR5). Unexpectedly a reduction of 2DG uptake was also observed in two *resistant* EGFR wild-type cell lines. Moreover, the inhibition of AKT signaling pathway seems to play a role in erlotinib-mediated down-regulation of glucose transport activity, possibly through down-regulation of GLUT-1 expression, in *sensitive* cells. In these cells, erlotinib was also demonstrated to decrease glucose consumption, an effect that could result either from down-regulation of glucose transport into the cells or from inhibition of AKT-dependent modulation of glycolysis, being AKT also involved in upregulation of HK and PFK activity[33]. Considering this intersection between signaling cascades and cellular metabolism, patients with known tumors harboring *EGFR* gene activating mutations showed early metabolic response. Clinical results demonstrated that early PET could identify EGFR TKI-resistant patients among those with *EGFR* mutational status wild-type or unknown. Moreover, patients who had an early PMR also experienced a prolonged control of the disease and longer survival when compared with patients with

metabolic progression. Survival was found significantly increased also in patients with non-progressive metabolic disease when compared with patients with PMD, confirming that an early metabolic progression is predictive of poor prognosis. In order to confirm the results obtained so far in various studies and ensure the reproducibility, there is a need for standardization of early PET evaluation for further investigations.

Taken together our preclinical and clinical results suggest that FDG-PET assessment after 2 days of erlotinib treatment could be useful to identify early resistant patients and to predict clinical outcome much earlier than conventional CT in unselected population with pretreated advance NSCLC. An early identification of erlotinib activity could be a better strategy of therapy tailoring, providing a solution to low availability of tumor tissue for genotype analyses in NSCLC. Further, randomized trials are needed in order to confirm our data and to evaluate whether an immediate switch to other treatments could improve outcome in erlotinib non-responders.

CONTINUING GEFITINIB TREATMENT IN ACQUIRED RESISTANT NSCLC CELLS INHIBITS INVASION AND EMT.

GEFITINIB INHIBITS INVASIVE PHENOTYPE AND EPITHELIAL-MESENCHYMAL TRANSITION IN DRUG-RESISTANT NSCLC CELLS WITH MET AMPLIFICATION (La Monica S, Caffarra C, Saccani F, Galvani E, Galetti M, Fumarola C, Bonelli M, Cavazzoni A, Cretella D, Sirangelo R, Gatti R, Tiseo M, Ardizzoni A, Giovannetti E, Petronini P.G., Alfieri R. R.; *Gefitinib Inhibits Invasive Phenotype and Epithelial-Mesenchymal Transition in Drug-Resistant NSCLC Cells with MET Amplification;* PLoS One. Oct 22;8(10):e78656, 2013).

Background

The discovery of EGFR activating mutations and the response to TKIs, such as gefitinib and erlotinib, deeply changed the management of advanced NSCLC in the last decade. As mentioned before, the most common EGFR activating mutations are small frame deletions in exon 19 and point mutations within exon 21. These mutations increase the susceptibility to EGFR-TKIs activity. Treatment with either erlotinib or gefitinib is associated with an objective response in 10‑20% of patients with advanced NSCLC[70,71]. Although impressive clinical and radiological responses have been observed in these patients, tumor progression occurs after prolonged administration of gefitinib/erlotinib as acquired resistance develops. Usually the disease progression occurs within 8 to 14 months from the beginning of the therapy. Various mechanisms of resistance have been identified. The two most common resistance mechanisms are a secondary mutation in the *EGFR* gene, T790M (responsible for half of the cases of acquired resistance; the substitution could enhance the ATP affinity to EGFR or could inhibit the binding between TKIs and the ATP task), and the amplification of *MET* proto-oncogene (described in 5 to 15% of cases.) [72,73,74,75]. The other main mechanisms involved in the acquisition of resistance are PIK3CA mutations and transformation to SCLC[76]. Furthermore, recent studies reported that the epithelial-mesenchymal transition (EMT) is also involved in the acquisition of resistance[77,78]. EMT is a process that occurs early in embryonic development (notably during the gastrulation) in which epithelial cells undergo cytoskeletal changes and lose cell-cell contacts to gain mesenchymal traits and become more motile. During carcinoma progression, pathological EMT occurs to promote tumor cell invasion and metastasis. Essential steps in the EMT process are the

loss of E-cadherin, an adherens junction protein that maintains cell-cell adhesion and epithelial tissue integrity, and the acquisition of a mesenchymal fibroblastoid phenotype, both enhancing cell motility and invasion capability. This process is followed by the secretion of lytic enzymes such as metalloproteinases (MMPs). At this point mesenchymal-like tumor cells are able to invade through the basement membrane into the underlying tissue. The association between EMT and local invasion as well as distant metastasis has been demonstrated in numerous *in vivo* and *in vitro* studies. Also, recent studies have shown that EMT confers drug resistance and anti-apoptotic phenotypes to cancer cells[79]. EMT is under tight control of multiple regulatory pathways; first and foremost transforming growth factor-β (TGF-β) signaling activity is enhanced in many physiological and pathological conditions in which EMT is observed, such as tumor invasion. The binding of TGF-β to its receptor activates complex formation of Smad family transcription factors, which translocate to the nucleus and cooperate with transcription factors of the Snail and Twist family. Non-Smad signaling molecules downstream TFG-β and supportive of EMT include activated Rho-like GTPases, PI3K and MAPK[80]. Taken together, these effectors mediate transcriptional repression of genes involved in cell polarity and cell-cell adhesion, such as RhoA and E-cadherin[81]. Other signaling pathways involved in the activation of EMT include hypoxia inducible factor1α (HIF1α)[82].

Normally, TKI-resistant NSCLC patients are treated with chemotherapeutic drugs. However, several clinical indications suggest that EGFR-mutant lung cancers maintain partial sensitivity to TKIs despite development of acquired resistance and tumors can still be sensitive to EGFR-TKIs treatment beyond progression[83,84,85,86] or re-treatment at further progression[87,88,89]. Novel strategies under investigation include the continuation beyond progression of EGFR-TKIs combined with chemotherapy, the re-challenge with TKIs after second-line chemotherapy, the use of irreversible TKIs or the combination with novel agents targeting different molecular pathways. Further preclinical studies to describe molecular mechanisms and potential markers of drug activity are also warranted.

In accordance with this statement, in the second part of my thesis I focused the attention in exploring the retained antitumor activity of gefitinib in resistant HCC827 GR5 carrying MET amplification in order to define the possible benefits of maintenance gefitinib in patients developing an acquired resistance.

Results

All the experiments were performed in the gefitinib-resistant clone HCC827 GR5. The resistant clone was obtained after the exposure of the HCC827 cell line (adenocarcinoma) to increasing concentration of gefitinib, and was routinely maintained in the presence of 1μM gefitinib. As previously reported[74] these cells showed a 1000-fold higher IC_{50} than the parental cell line HCC827 (10μM versus 10nM, respectively) and are characterized by amplification of the *MET* oncogene, leading to ERBB3-mediated activation of PI3K/AKT signaling.

Effect of gefitinib withdrawal on cell proliferation and cell cycle distribution.

HCC827 GR5 cells, grown for ten days in the presence (HCC827 GR5) or in the absence (HCC827 GR5-G) of 1μM gefitinib, were seeded in a 96-multiwell plate. After 24, 48 and 72h cell proliferation was assessed using crystal violet staining. As shown in **Figure 17a**, cells did not modify the proliferation index. In addition, after a 10 days gefitinib removal the HCC827 GR5 cells did not modify either the proliferation index nor the cell cycle distribution as compared to HCC827 GR5 cells grown in the presence of 1μM gefitinib **(Figure 17b)**. Moreover, the absence of gefitinib did not alter HCC827 GR5 resistance to gefitinib for up to 90 days of deprivation. Indeed, as shown in **Figure 17c**, cells deprived of gefitinib for different periods of time and acutely treated with the drug for 72 hours still maintained the resistant phenotype (IC_{50}>7μM). Taken together these results show that gefitinib is not necessary for the maintenance of the resistant phenotype.

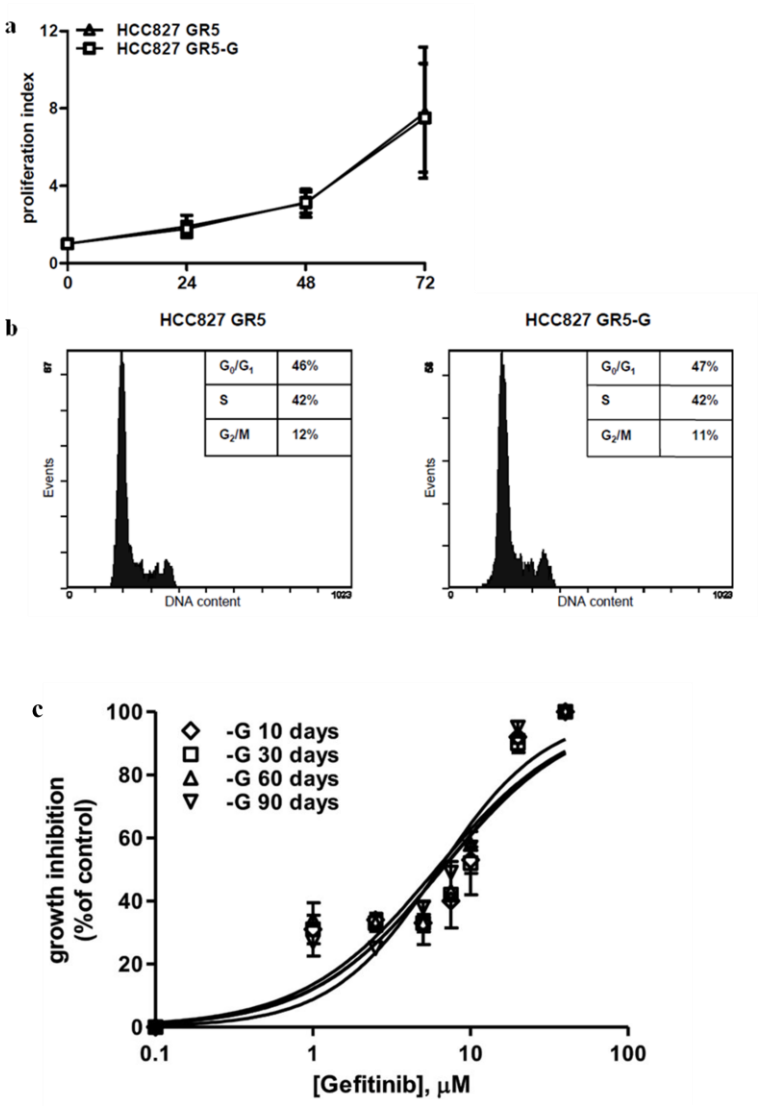

Figure 17. Effect of gefitinib withdrawal on cell proliferation. (a) HCC827 GR5 grown in the presence of 1µM gefitinib and HCC827 GR5-G (maintained in the absence of gefitinib for 10 days) cells were seeded in a 96-multiwell plate. After 24, 48 and 72h cell proliferation was assessed using crystal violet staining; cell proliferation index was calculated as the ratio between the optical density (OD) at each point time and the OD at zero time point. Mean values of three independent measurements (±SD) are shown. (b) 24h from seeding, HCC827 GR5 and HCC827 GR5-G were stained with PI and analyzed by flow cytometry. Cytofluorimetric profiles and percentages of cells residing in each cycle phase are from a representative experiment of three independent experiments. (c) HCC827 GR5 cells gefitinib-deprived for the indicated period of time were exposed for 72h to different concentrations of gefitinib (1 to 40µM) and then cell growth was assessed using MTT assay. Data are expressed as percent inhibition of cell proliferation versus control cells and are means (±SD) of three independent experiments.

Effect of gefitinib on cell migration and invasion in HCC827 GR5 cells.

Then we studied the effects of gefitinib on cell migration and invasion in HCC827 GR5 cells.

To study the effects of gefitinib on cell migration we performed wound-healing and migration assay on HCC827 GR5 cells cultured in the presence or absence of gefitinib for 10 days. As shown in **Figure 18a,** HCC827 GR5-G cells spread into the wound area more efficiently than cells continuously exposed to gefitinib, with wound closure percentages of 48%±4.2 and 37%±3.2 respectively ($P<0.01$).

In addition, HCC827 GR5 cells cultured in the absence of gefitinib for 10 days showed a significant increase in both cell migration and invasion as detected in the Boyden chambers assay, **Figure 18 (b,c)**.

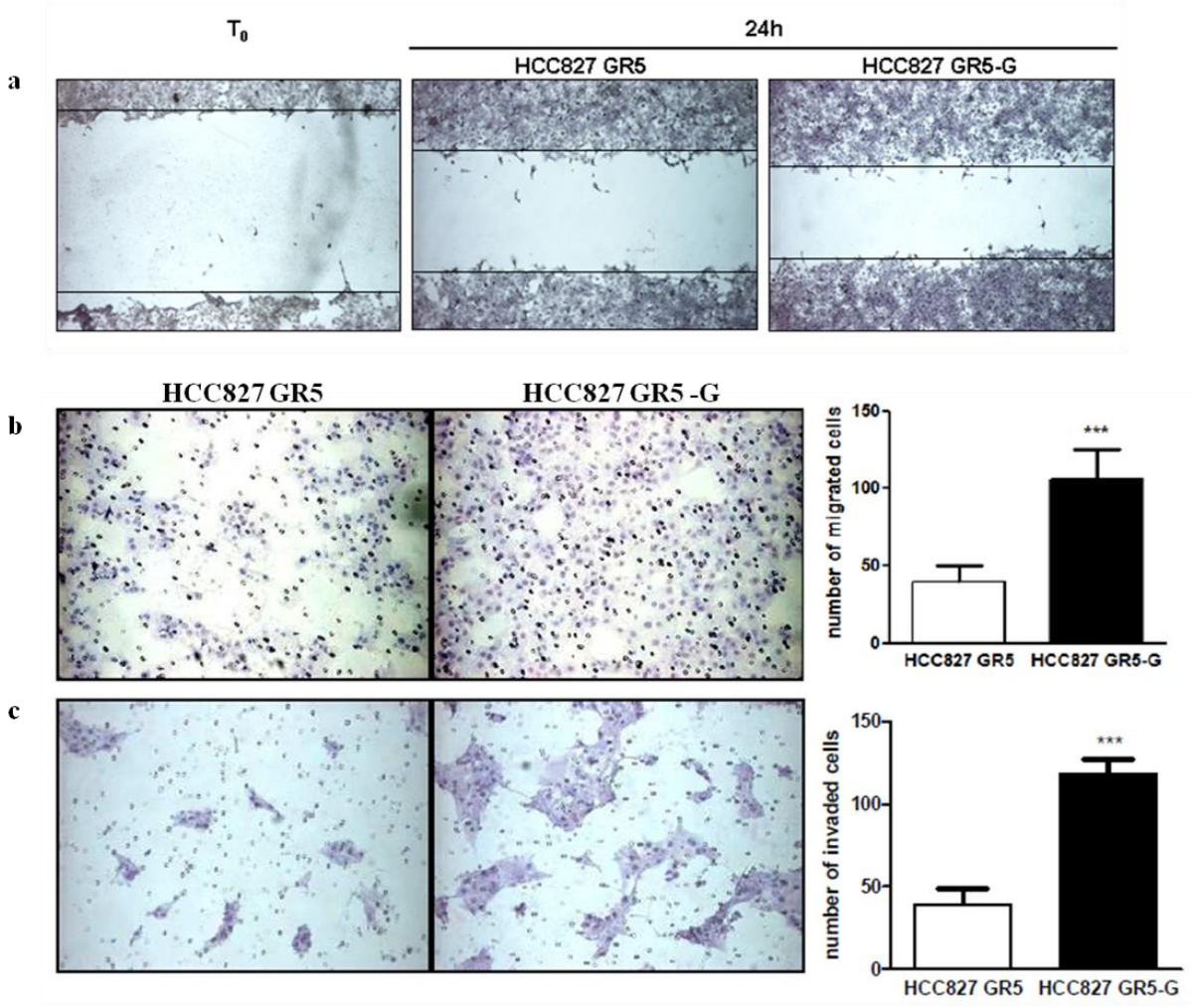

Figure 18. Effect of gefitinib withdrawal on cell migration and invasion. Wound-healing, migration and invasion were performed on HCC827 GR5 cells grown in the presence of 1μM gefitinib and HCC827 GR5-G cells maintained in the absence of gefitinib for 10 days. (a) Representative images of the wound tracks were obtained at time point zero and after 24h (magnification of 40X). Representative fields of migration (b) or invasion

(c) are shown (magnification of 100X). Columns, mean of 10 fields counted; bars, SD. Results are representative of three independent experiments. ***P<0.001.

Moreover, considering the role of MMPs in degrading extracellular matrix components, the effect of gefitinib removal on the proteolytic activity of MMP-2 and MMP-9 was evaluated by using a gelatin zymography assay. As shown in **Figure 19,** there was an approximately 2 fold increase of MMP-2 and MMP-9 activity in cells deprived of gefitinib for 10 days. These results indicate that maintenance of gefitinib inhibits secretion and activation of gelatinolytic MMP-2 and MMP-9.

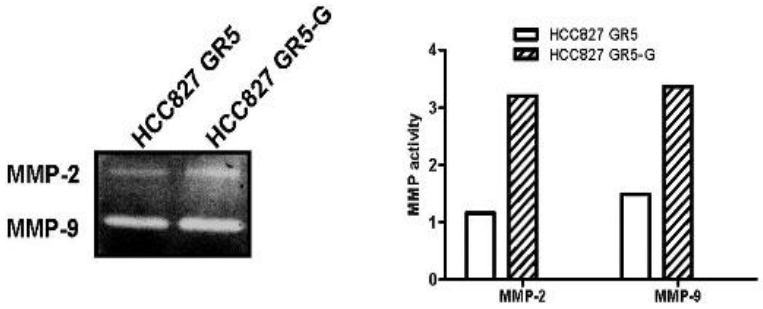

Figure 19. Effect of gefitinib withdrawal on cell invasion. HCC827 GR5 cells were grown in the presence of 1μM gefitinib and HCC827 GR5-G cells were maintained in the absence of gefitinib for 10 days. Gelatin zymography analysis was performed on media from these cells incubated with serum-free medium for 24h.Columns, enzyme activity of MMP-2 and MMP-9, were determined by densitometric analysis. Representative images are shown.

Gefitinib inhibits signal transduction pathways involved in cellular motility and EGFR modulation correlates with gefitinib-related regulation of cell motility.

HCC827 GR5 cells were deprived of gefitinib for different periods of times from 1 up to 30 days. As shown in **Figure 20a**, increased motility was observed in HCC827 GR5 cells after 3 days of gefitinib withdrawal. A plateau of cellular migration was reached after 7 days and this phenomenon correlates with the increase in EGFR, and Src^{Tyr416} phosphorylation **(Figure 20b)**. Moreover, we observed a marked reduction in Src^{Tyr527} phosphorylation (which negatively regulates Src kinase activity) after 7 days since gefitinib removal. No differences were detected for MET, Akt and ERK 1/2 phosphorylation status.

To better investigate the signaling pathways activated after 7 days of gefitinib removal, 43 specific Ser/Thr or Tyr phosphorylation sites of 35 different proteins were analyzed by a human phospho-kinase array kit. As shown in **Figure 20c**, 8 proteins, including p38α, EGFR, Src^{Tyr416}, Lyn, STAT2, STAT6, STAT5a/b and c-Jun, exhibited a significant increase (P<0.05) in their phosphorylation status following gefitinib withdrawal. The increased phosphorylation of p38, STAT5 and Src was validated by Western blotting in cells deprived of gefitinib for 7 days **(Figure 20d)**.

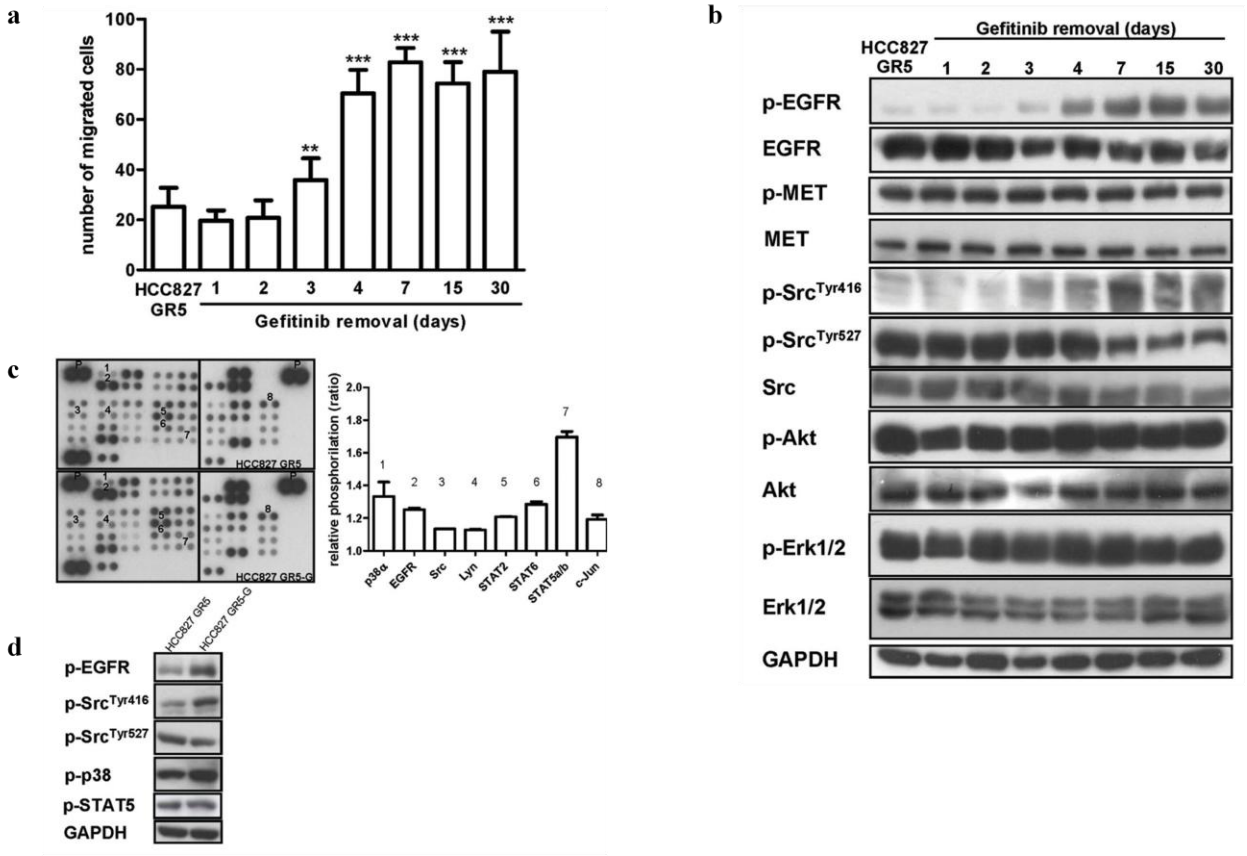

Figure 20. Effect of gefitinib withdrawal on signal transduction pathways. HCC827 GR5 cells were deprived of gefitinib for 1, 2, 3, 4, 7, 15 or 30 days. (a) Migration assay was performed at each time point. Columns, mean of 10 fields counted; bars, SD. * Significance versus HCC827 GR5. ***P<0.001, **P<0.01. (b) Expression of the indicated proteins was analyzed by Western blotting at each time point. Results are representative of three independent experiments. (c) Lysates from HCC827 GR5 grown in the presence of 1μM gefitinib, and HCC827 GR5-G maintained in the absence of gefitinib for 7 days were incubated with human phospho-kinase array membranes and bound phospho-proteins were detected according to kit instructions. Each membrane contains

specific kinases and positive control antibodies (P) spotted in duplicate. Columns, means of relative levels of protein phosphorylation (ratio of phosphorylation of HCC827 GR5-G/ HCC827 GR5 cells) of duplicate spots 1-9 from a single experiment; bars, SD. (d). Lysates were analyzed by Western blotting using the indicated antibodies.

In order to assess the role of EGFR re-activation in the acquisition of migratory capability, HCC827 GR5 cells (maintained for 10 days in the absence of gefitinib) were transfected with EGFR-specific or scramble siRNAs for 48h. EGFR expression was verified by Western blotting 72h post-transfection **(Figure 21a)**. Where indicated, 1μM gefitinib was added for 24 hours. siRNA-EGFR completely inhibited EGFR expression compared to the negative scramble control siRNA. As shown in **Figure 21b**, the inhibitory effect on cell migration obtained by silencing EGFR in HCC827 GR5 cells was similar to that observed in the presence of gefitinib in scramble siRNA-transfected cells. Moreover, the addition of gefitinib to siRNA-EGFR transfected cells did not further decrease the amount of migrating cells. These results demonstrated the dependency of HCC827 GR5 cells motility on EGFR activity and suggested that the observed effect of gefitinib on cell migration is associated with the inhibition of its target.

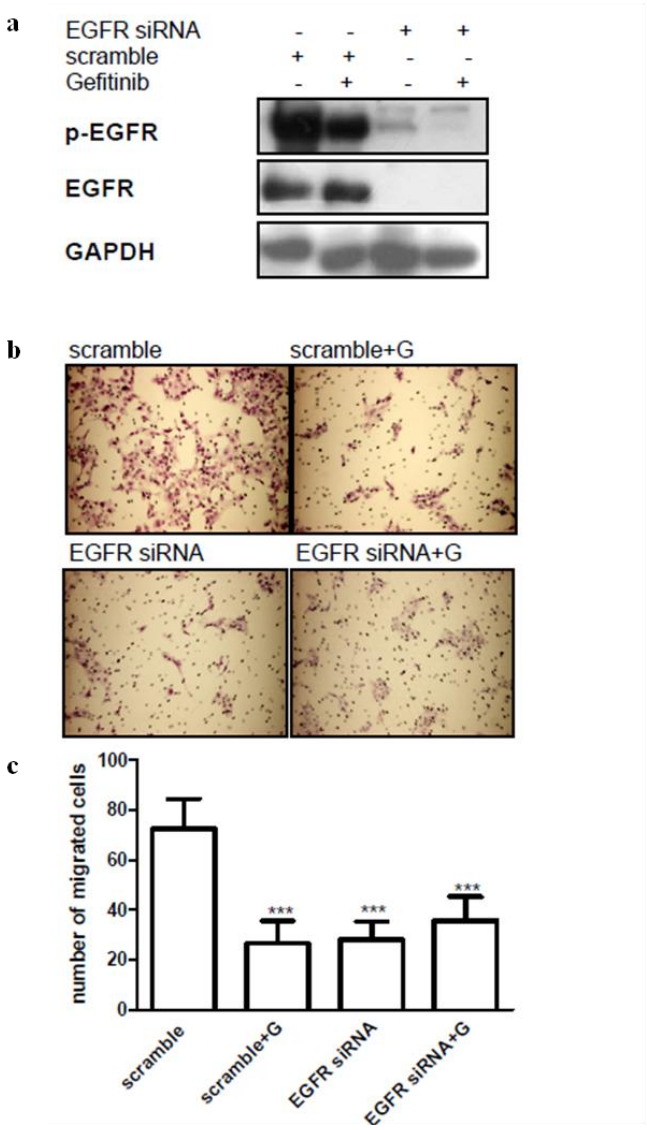

Figure 21. Effect of EGFR silencing on cell migration. HCC827 GR5-G cells (maintained in the absence of gefitinib for 10 days) were transfected with EGFR siRNA or control siRNA (scramble) for 48h. Then the medium was replaced with fresh medium with or without gefitinib 1μM for 24h and the expression of the indicated proteins was analyzed by Western blotting (a), or cells were seeded on culture inserts in the absence or in the presence of 1μM gefitinib for migration assay (b). Representative fields of migration are shown (magnification of 100X). Columns, mean of 10 fields counted; bars, SD. Results are representative of three independent experiments. * Significance versus scramble. ***P<0.001.

EGFR and MET independently control cellular migration via Src signalling.

To assess the contribution of different signaling pathways in the increased migratory capability, dasatinib (Src inhibitor), SU11274 (MET inhibitor), U0126 (ERK1/2 inhibitor), and

NVPBEZ235 (PI3K/mTOR inhibitor) were tested in HCC827 GR5 cells deprived of gefitinib for 7 days by Boyden chambers assay.

At first, HCC827 GR5 cells deprived of gefitinib for 7 days were submitted to Western Blot analysis in order to verify the target specificity of each inhibitor. As shown in **Figure 22,** dasatinib, SU11274, , U0126, and NPV-BEZ235 completely inhibited, respectively, the activation of Src^{Tyr416} (which positively regulates Src kinase activity), MET phosphorylation, Erk1/2, and AKT.

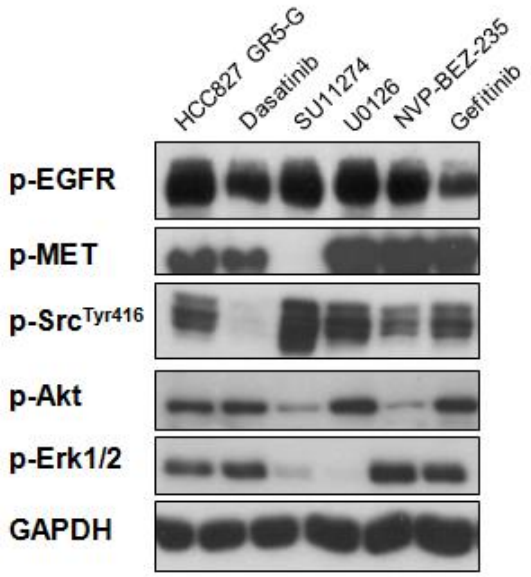

Figure 22. Effect of specific inhibitors on signaling pathways. HCC827 GR5 cells were deprived of gefitinib for 7 days (HCCR GR5-G), then were treated for 24h with dasatinib 0.1µM, SU11274 1µM, U0126 10µM, NVP-BEZ235 0.1µM, or gefitinib 1µM. Expression of the indicated proteins was analyzed by Western blotting. Results are representative of three independent experiments.

As shown in **Figure 23a,** a 24h treatment with U0126 or NVP-BEZ235 did not affect migration of HCC827 GR5-G cells deprived of gefitinib for 7 days. By contrast, SU11274 inhibited cell migration with results similar to those achieved with gefitinib. Moreover, dasatinib and the combination of gefitinib with SU11274 almost completely suppressed migration.

We verified that the drugs, at the dose used, did not affect cell proliferation and cell viability at least until 24h **(Figure 23b)**. Taken together, these findings suggest that cell migration was

controlled by both EGFR and MET through Src activation. In order to further confirm these results and the data shown in **Figure 20c** and **20d** showing the up-regulation of Src, STAT5 and p38 after gefitinib deprivation, HCC827 GR5 cells maintained for 7 days in the absence of gefitinib were transfected with siRNAs targeting Src, STAT5a/b or p38α. We found that knock-down of Src, STAT5a/b or p38α resulted in an almost complete suppression of the corresponding proteins expression **(Figure 23c)**, and significantly inhibited cell migration induced by gefitinib deprivation compared to the negative scramble control siRNA **(Fig. 23d)**.

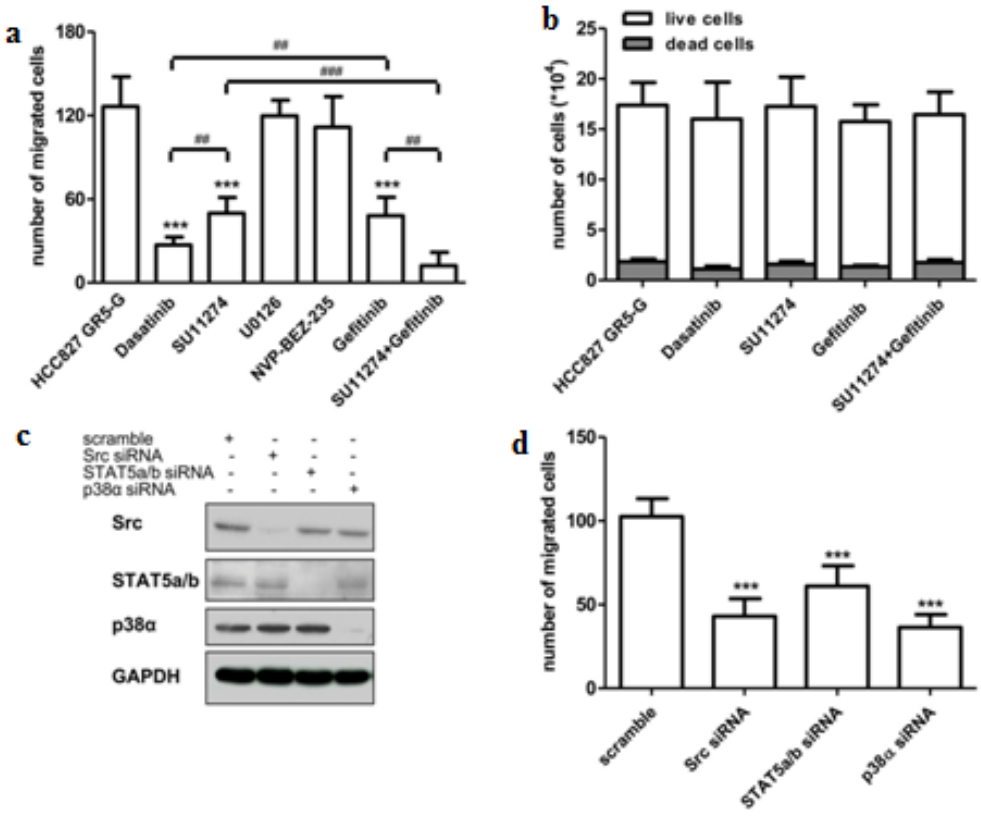

Figure 23. Effect of signal transduction pathways inhibition on cell migration of HCC827 GR5 cells deprived of gefitinib. (a) HCC827 GR5-G cells (maintained in the absence of gefitinib for 7 days) were exposed to dasatinib 0.01μM, SU11271 1μM, U0126 10μM, NVP-BEZ235 0.1μM, gefitinib 1μM or SU11271 1μM + gefitinib 1μM during migration time. Columns, mean of 10 fields counted; bars, SD. Results are representative of three independent experiments. *Significance versus HCC827 GR5-G. ***P<0.001, **P<0.01; ###P<0.001, ##P<0.01. (b) HCC827 GR5-G cells were incubated with dasatinib 0.01μM, SU11271 1μM, gefitinib 1μM or SU11271 1μM + gefitinib 1μM. After 24h the cells were counted and cell death was evaluated by fluorescence microscopy on Hoechst/PI stained cells. Columns, mean of three independent experiments; bars, SD. HCC827 GR5-G were transfected with Src, STAT5a/b, p38 siRNA or control siRNA (scramble) for 48h. Then the medium was replaced with fresh medium for 16h and the expression of the indicated proteins was analyzed by Western blotting (c) or cells were seeded on culture inserts for migration assay (d). Columns, means of 10 fields

counted; bars, SD. Results are representative of three independent experiments. * Significance versus scramble. ***P<0.001.

Gefitinib inhibits epithelial-mesenchymal transition.

In order to assess the involvment of EMT in the enhanced cell migration and invasion after gefitinib removal, mesenchymal associated features were evaluated.

On the molecular level, EMT is defined by down-regulation of E-cadherin and increased expression of N-cadherin and vimentin. Furthermore, E-cadherin expression is regulated by the Wnt/β-catenin-mediated transcription of zinc-finger proteins, such as SLUG and SNAIL. HCC827 GR5 cells were deprived of gefitinib for 1, 7, 14, 21 or 30 days. As reported in **Figure 24a**, gefitinib removal induced a decrease in E-cadherin expression, while the expression level of N-cadherin, vimentin, and the negative regulators β-catenin, SLUG, and SNAIL were increased compared to cells continuously maintained with gefitinib. Moreover, we also observed an increase in the expression of the tight junction protein Claudin-1, recently reported to have a pivotal role in the induction of the EMT program[90]. Unexpectedly, these markers of EMT appeared after 21 days of gefitinib removal, whereas enhanced motility, as previously reported, was observed already after 3 days.

The decrease of E-cadherin expression on the cell membrane and the increased levels of vimentin after 30 days of gefitinib removal were confirmed by immunofluorescence confocal microscopy **(Figure 24b)**. A significant increase of vimentin was also detected at gene expression level by qRT-PCR after 15 days of gefitinib removal as compared to gefitinib maintenance **(Figure 24c)**.

Considering the recent finding of the active role of TGF-β1 in the induction of the EMT phenotype in human lung cancer cells, we analyzed whether gefitinib could inhibit TGF-β1-induced EMT. HCC827 GR5 and Calu-3 cells (a NSCLC cell line with epithelial features) were treated with 2ng/ml TGF-β1 for 72h with or without 1μM gefitinib, and after 3 days protein expression was assessed by Western blotting. As shown in **Figure 24d**, TGF-β1 treatment induced an increase of vimentin expression, which was partially reverted by addition of gefitinib in the culture medium. These results confirm the involvement of TGF-β1 in the transforming process to mesenchymal phenotype, and indicate the potential role of gefitinib in counteracting EMT after tumor progression.

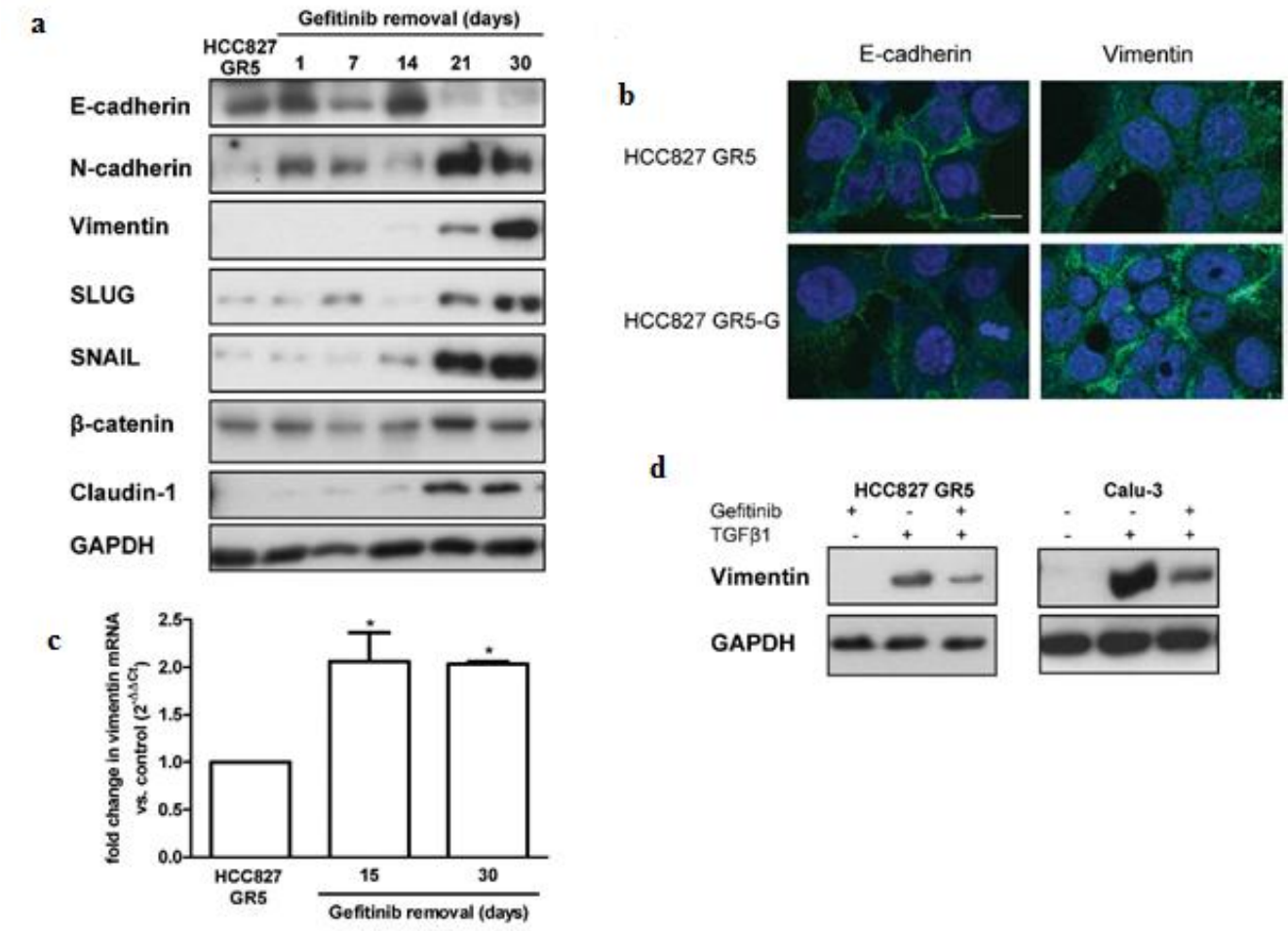

Figure 24. Effect of gefitinib on EMT. (a) HCC827 GR5 cells were deprived of gefitinib for 1, 7, 14, 21 or 30 days. Expression of the indicated proteins was analyzed by Western blotting at each time point. Results are representative of three independent experiments. (b) Confocal immunofluorescence analysis of HCC827 GR5 and HCC827 GR5-G (maintained in the absence of gefitinib for 30 days) with antibody against E-cadherin and vimentin (green fluorescence). The nuclei were stained with Draq5 (blue fluorescence). Scale Bar: 10μm. (c) Comparison of vimentin mRNA by quantitative RT-PCR between HCC827 GR5 gefitinib-maintained cells and gefitinib-deprived cells. The fold change was calculated using the 2−ΔΔCT method relative to gefitinib-maintained cells used as a control. Results are representative of three independent experiments. * Significance versus HCC827 GR5.*P<0.05. (d) HCC827 GR5 cells were incubated with 2ng/ml TGFβ1 in the absence or in the presence of 1μM gefitinib. After 3 days, protein expression was assessed by Western blotting using the indicated antibodies.

Maintaining gefitinib despite the acquired resistance sensitizes NSCLC cells to chemotherapy.

Data from literature showed that continuing erlotinib with chemotherapy improves the response rate with acceptable side effects and it is therefore a reasonable treatment option for patients with *EGFR*-mutant lung cancer with acquired resistance to EGFR TKIs[91,92,93].

Here, we evaluated whether maintaining gefitinib after acquired resistance could sensitize NSCLC cells to chemotherapy. HCC827 GR5 cells and HCC827 GR5-G (deprived of gefitinib for 10 days) were treated with increasing concentrations of cisplatin or pemetrexed (from 0.01μM to 50μM) and were submitted to MTT assay. HCC827 GR5 cells showed lower IC_{50} values as compared with gefitinib-deprived cells for both cisplatin (3μM vs 5.3μM) and pemetrexed (2μM vs 4μM) (**Figure 25**).

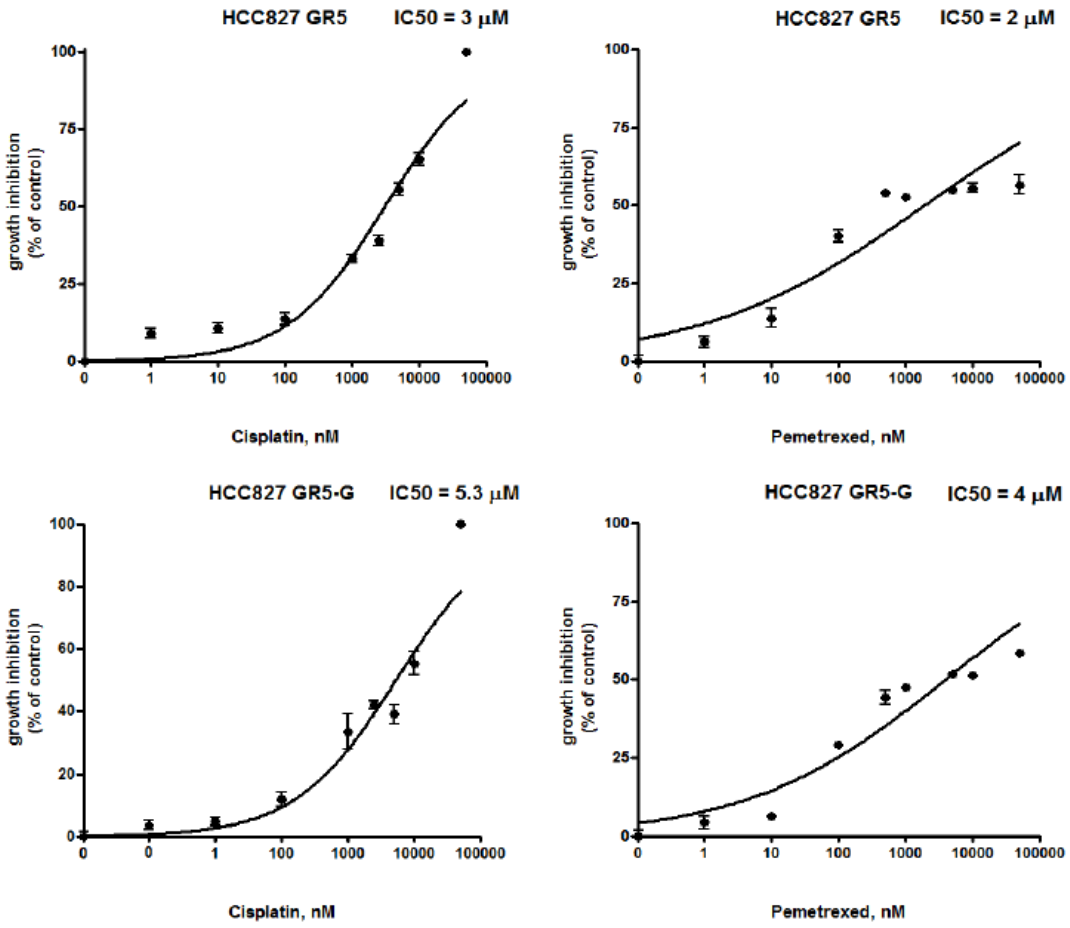

Figure 25. Effects of cisplatin and pemetrexed on cell proliferation. $3\text{-}5x10^3$ cells were seeded in 96-multiwell plates and 24h later were treated with or without increasing concentrations of cisplatin or pemetrexed (0.01-50μM). After 72h cell survival/proliferation was assessed using MTT assay. IC_{50} values, expressed as mean ± SD, of three independent experiments, were calculated by fitting the experimental data with a hyperbolic function and constraining Ymax to 100 (GraphPad Prism 4.00).

HCC827 GR5 and HCC827 GR5-G (deprived of gefitinib for 10 days) cells were treated with 1μM cisplatin/pemetrexed for 24, 48 or 72h and then were counted using fluorescence microscope after staining with Hoechst 33342 and PI. As shown in **Figure 26,** there were no effects on cell death after 24h of treatment; the percentage of death cells increased in both HCC827 GR5 and HCC827 GR5-G cells treated with cisplatin/pemetrexed combination after 48 and 72h. Interestingly, HCC827 GR5 cells were more sensitive to cisplatin/pemetrexed than the counterpart deprived of gefitinib.

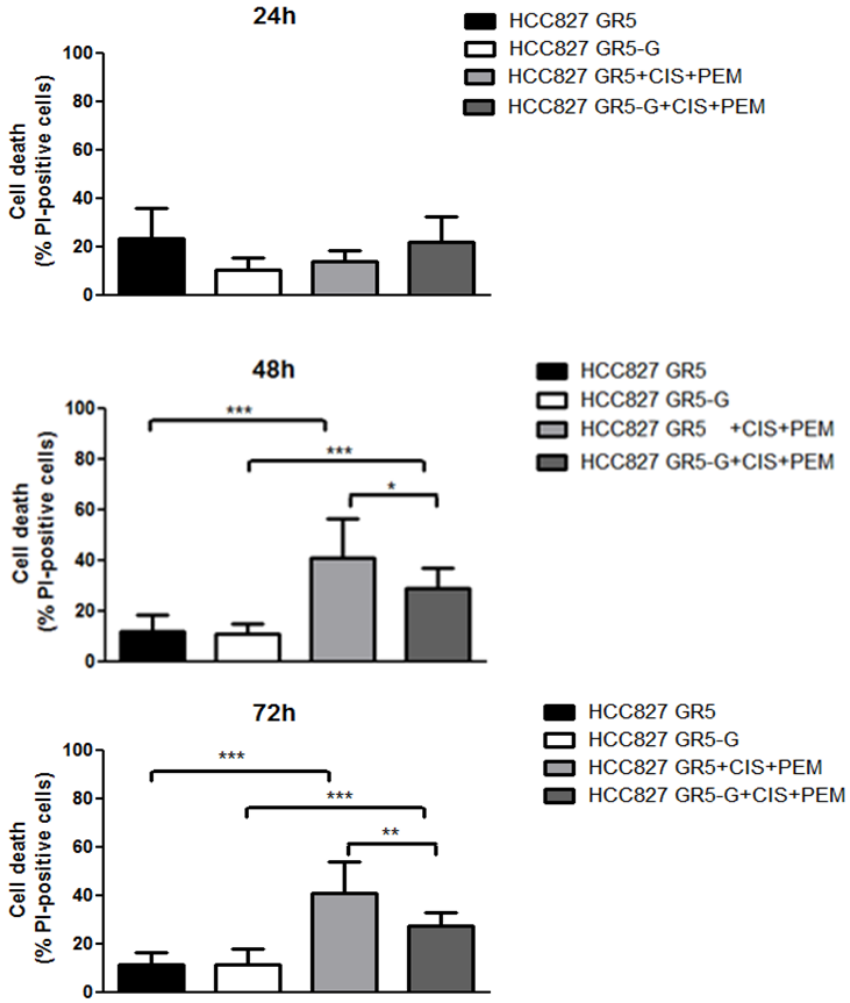

Figure 26. Effects of gefitinib combination with cisplatin/pemetrexed on cell death. 1-2 x 10^5 cells were seeded in 6-multiwell plates and 24h later were treated with or without 1μM cisplatin and pemetrexed. After 24, 48 or 72h cells were detached and counted by fluorescence microscopy after staining with Hoechst and PI. Data are expressed as percentage of PI-positive cells and are from a representative experiment. Bars, SD. Results are representative of two independent experiments. ***P<0.001, **P<0.01, *P<0.05.

Discussion and conclusions

First of all this study confirmed that maintenance of gefitinib, even though it has no effect on cell proliferation and growth, potentially limits the acquisition of a migratory and invasive phenotype in NSCLC cells carrying *MET* amplification-driven resistance. We also demonstrated that gefitinib withdrawal leads to EGFR signaling reactivation, which is involved in the acquisition of a cell aggressive behavior. In particular, despite amplification of *MET*, whose migration/invasion-promoting activity is well established, our results suggest that persistent inhibition of EGFR is sufficient to maintain a low invasive phenotype in HCC827 GR5 gefitinib-resistant cells. These data support the role of EGFR in cell motility and invasiveness and suggest the importance of maintaining EGFR-TKIs treatment after tumor progression. Data from literature showed the active role of the cross-talk between MET and EGFR in cancer growth, migration, and invasion[94,95,96]. Activation of these two receptors initiates similar signal transduction pathways including Src signaling. Published data demonstrated that either EGFR or MET signaling were essential to sustain cell proliferation and viability in HCC827 GR5 cells and that only the combination of gefitinib with a MET-TKI (PHA-665752) inhibited proliferation and induced cell death in HCC827 GR5 cells[74]. Conversely, the Src inhibitor dasatinib alone was able to overcome gefitinib resistance in this cell line. Our data showed that treating HCC827 GR5 cell line with gefitinib or the MET inhibitor SU11274 as single treatments inhibits cell migration with the same efficacy, suggesting their parallel and independent control in cell migration process. Moreover, combined inhibition of EGFR and MET resulted in a further inhibition of cell migration, a similar result was obtained with the Src inhibitor dasatinib. There are some evidences indicating the active role of Src and other members of its family in cell migration and invasion[97]. We detected also some of these pathways in our studies: here we demonstrated the active involvement of eight phosphorylated kinases (EGFR, p38α, Src, Lyn, STAT2, STAT6, STAT5a/b and c-Jun) in early processes associated with cell motility and invasiveness which can be modulated by gefitinib despite tumor progression. The active role of Src, STAT5a/b and p38α in modulating the migratory and invasive properties of HCC827 GR5 cells in response to gefitinib deprivation was also confirmed by siRNA-mediated silencing experiments. Some evidences showed the association of STAT5a/b with increased migration and invasion in prostate cancer cells[98]. In our studies we reported that in gefitinib-deprived HCC827 GR5 cells STAT5

was further phosphorylated at the phosphorylation site Tyr^{694} residue, which is known to be associated with EGFR-dependent Src activation[99], whereas the JAK phosphorylation site Tyr^{699} was not modified. We demonstrated also a significant modulation of other STAT family members, in particular STAT2 and STAT6[100]. Data from literature showed the involvement of p38 in the modulation of cell motility and invasiveness through the regulation of MMPs[101]. In particular, members of the S100 family of calcium-binding proteins promoted cell migration and invasion through p38 MAPK-dependent NF-κB activation, which increased MMP-2 and MMP-12 expression in gastric cells[102]. Moreover, baicalin suppressed cell migration and invasiveness in breast cancer MDA-MB-231 cells by down-regulating p38 MAPK pathway and consequently MMP-2 and MMP-9 expression[103]. In agreement with these and other previous studies, our results showed that gefitinib-treated NSCLC cells with MET amplification display a significant reduction in both MMP-2 and MMP-9 proteolytic activity associated with reduced phosphorylation of p38 MAPK. This modulation was detected by both phospho-kinase array and Western blot, and might be attributed to the direct effect of gefitinib. Some recent data suggested the active role of EMT in the promotion of tumor cell invasion and metastasis[104]. During EMT cells lose E-Cadherin, an adherens junction protein that maintains cell-cell adhesion and epithelial tissue integrity and acquire a mesenchymal fibroblastoid phenotype (increased expression of N-cadherin and vimentin) enhancing cell motility and invasion capability. Src activation is a potent trigger for EMT induction, causing dissociation of the E-cadherin/β-catenin complex and degradation of E-cadherin by promoting its phosphorylation, ubiquitination, endocytosis and lysosomal degradation[105]. Importantly, we demonstrated that gefitinib maintenance after acquisition of resistance is essential to inhibit phenotypic changes associated with EMT. Moreover, gefitinib can prevent the EMT mediated by TGF-β1 and this might also control resistance to apoptosis and the emergence of stem cell like properties as described in previous studies on EMT[104]. Some evidence showed that continuing erlotinib with chemotherapy improves the response rate with acceptable side effects and it is therefore a reasonable treatment option for patients with *EGFR*-mutant lung cancer acquired resistance to EGFR TKIs[91,92,93]. Our preliminary results suggested that maintaining gefitinib after acquired resistance could sensitize the cells to chemotherapy. Indeed, the percent of cell death after 48 and 72h of cisplatin/pemetrexed treatment is significantly higher in HCC827 GR5 cells than in HCC827 GR5-G cells deprived of gefitinib for 10 days.

In conclusion, our data demonstrated that, despite tumor progression after treatment with EGFR-TKIs (in particular gefitinib), NSCLCs with *MET* amplification are still dependent on EGFR signaling. In these tumors EGFR plays an important role in cell motility and invasiveness and prompts the EMT process possibly via Src signaling. For all these reasons, the maintenance of gefitinib after tumor progression emerges as an important new therapeutic strategy to inhibit EGFR-mediated aggressive behavior in NSCLC with MET amplification. Taken together these results contribute to a more comprehensive definition of the molecular mechanisms underlying gefitinib action.

Sorafenib in breast cancer: an example of targeted therapy.

Effects of sorafenib on energy metabolism in breast cancer cells: role of AMPK–mTORC1 signaling (Fumarola C, Caffarra C, La Monica S, Galetti M, Alfieri R, Cavazzoni A, Galvani E, Generali D, Petronini P.G., Bonelli M.; *Effects of sorafenib on energy metabolism in breast cancer cells: role of AMPK–mTORC1 signaling*. Breast Cancer Res Treat (2013) 141:67–78)

Background

Patients with ER- or HER2-positive tumors are treated with hormonal therapy or with drugs directed against HER2/neu. Recently, in patients with advanced-stage and HER2 negative breast cancer, it has been shown that treatment with the multikinase inhibitor sorafenib with anti-proliferative, antiangiogenic and pro-apoptotic activity (already approved for the treatment of HCC and metastatic renal cell carcinoma) has given satisfactory results in terms of PFS[55,57,58]. However, the molecular mechanisms by which sorafenib acts are not completely known. In addition to the direct inhibition of VEGFR, PDGFR-β, c-Kit, Flt-3 and Raf, sorafenib pro-apoptotic action has been also associated with the activation of the mitochondrial pathway or with the direct inhibition of oxidative phosphorylation (OXPHOS) in HCC cells[53] and with the direct target of mitochondrial electron transport chain complex I in neuroblastoma cells, impairing mitochondrial energy production[54]. Thus, sorafenib action may also be associated with perturbation of cell respiration and cell metabolism.

AMPK is a master energy stress sensor that, in response to increased cellular AMP:ATP ratio, switches on the catabolic pathways (generating ATP) and switches off the anabolic pathways in order to restore the energy balance of the energy status of the cells; further, it plays a crucial role in metabolic stress conditions. In particular, when ATP level decreases, both AMP and ADP levels rise activating AMPK; on the contrary, ATP competes with AMP and ADP for binding to the regulatory sites on the enzyme, thus preventing its activation, therefore AMPK activation depends on ADP:ATP and AMP:ATP ratios[106]. A condition of energetic stress promotes the activation of AMPK that shift the cells to an oxidative metabolic phenotype and inhibits cell proliferation. AMPK has two regulatory subunits, β and γ, along with its catalytic α subunit that is activated by phosphorylation from a complex of three subunits LKB1, STRAD, MO25[107]. AMPK activation inhibits the synthesis of most cellular macromolecules, including fatty acids, triglycerides, cholesterol, glycogen, ribosomal RNA and proteins, thus inhibiting cell growth[108].

In particular, AMPK inhibits mTORC1 by phosphorylating its upstream regulator TSC2 and its regulatory subunit Raptor[109], thus inhibiting translation of many proteins required for rapid cell growth. Although AMPK activation can acutely increase glucose uptake (either by promoting the translocation of GLUTs to the plasma membrane, or by enhancing the transcription of genes encoding for these transporters) and glycolysis (by activating 6-PFK II) in certain cells, in the longer term it promotes the more energy-efficient oxidative metabolism by upregulating mitochondrial biogenesis and expression of oxidative enzymes[110]; by downregulating the glycolytic pathway and by inhibiting mTORC1. It is noteworthy that cancer cell metabolism is unequivocally altered. In particular, compared to normal cells, malignant cells show an increased glucose uptake, a higher rate of glycolysis associated with reduced pyruvate oxidation and increased lactic acid production. Glucose utilization by cancer cells is therefore greatly enhanced when compared to normal or benign tissues. Glucose is taken up by cells and then phosphorylated to glucose-6-phosphate. Facilitative glucose uptake is achieved by 14 transmembrane transporters, termed GLUT 1–14. GLUTs are proteins of about 500 amino acids and possess 12 transmembrane-spanning alpha helices and a single N-linked oligosaccharide. The GLUT transporters differ in their kinetics and are tailored to the requirements of the cell type they serve[111]. Although more than one GLUT may be expressed by a particular cell type, tumors frequently overexpress GLUT-1, which is a high affinity glucose transporter. Glucose uptake and glycolysis are regulated by many pathways and proteins such as AKT1, c-Myc, Ras and AMPK.

In the last part of my thesis I investigated the effects underneath the molecular mechanisms of the multi-kinase inhibitor sorafenib in a panel of breast cancer cell lines with particular attention on the effects on intracellular signaling pathways that control either cell proliferation/survival or energy metabolism.

Results

Effect of sorafenib on cell proliferation, growth signaling pathways and cell survival.

Various BC cell lines of different subtypes (divided in ERα-positive and ERα-negative) were treated with increasing concentrations of sorafenib (from 0.1μM to 10μM) and submitted to

crystal violet assay. Sorafenib inhibited cell proliferation in a dose-dependent manner, with IC_{50} values ranging from 2.1μM for T47D cells to 5.9μM for MDA-MB-231 cells **(Figure 27)**.

Cell line	Sorafenib IC_{50} (μM)
MCF-7	2.9 ± 0.3
T47D	2.1 ± 0.1
BT474	2.3 ± 0.2
MDA-MB-231	5.9 ± 0.1
MDA-MB-468	5.0 ± 0.5
SKBR3	3.2 ± 0.4

Figure 27. Effect of sorafenib on cell proliferation. 3–5 x 10^3 cells, seeded in 96-multiwell plates, were treated with or without increasing concentrations of sorafenib (0.1–10μM). After 72h, cell proliferation was assessed using crystal violet staining. The IC_{50} values, expressed as mean ± SD of three independent experiments, were calculated by fitting the experimental data with a hyperbolic function and constraining Ymax to 100 (GraphPad Prism 4.00).

Concurrently, BC cells were treated with or without various concentrations of sorafenib and then the phosphorylation/expression of proteins related to MAPK and AKT signaling pathways were analyzed by Western blotting. As shown in **Figure 28,** phospho-ERK1/2 and phospho-AKT levels decreased in the ERα-negative MDA-MB-231 and SKBR3 cells, and increased or remained unchanged in the ERα-positive cell models as well as in MDA-MB-468 ERα-negative cells, suggesting that sorafenib-mediated effects are neither correlated with modulation of MAPK and AKT pathways nor dependent on the ERα status. Instead, the phosphorylation of mTORC1 and its targets p70S6K and 4E-BP1 significantly decreased in all the cell lines, thus pointing to the inhibition of mTORC1 signaling as a general, central mechanism of sorafenib action in BC.

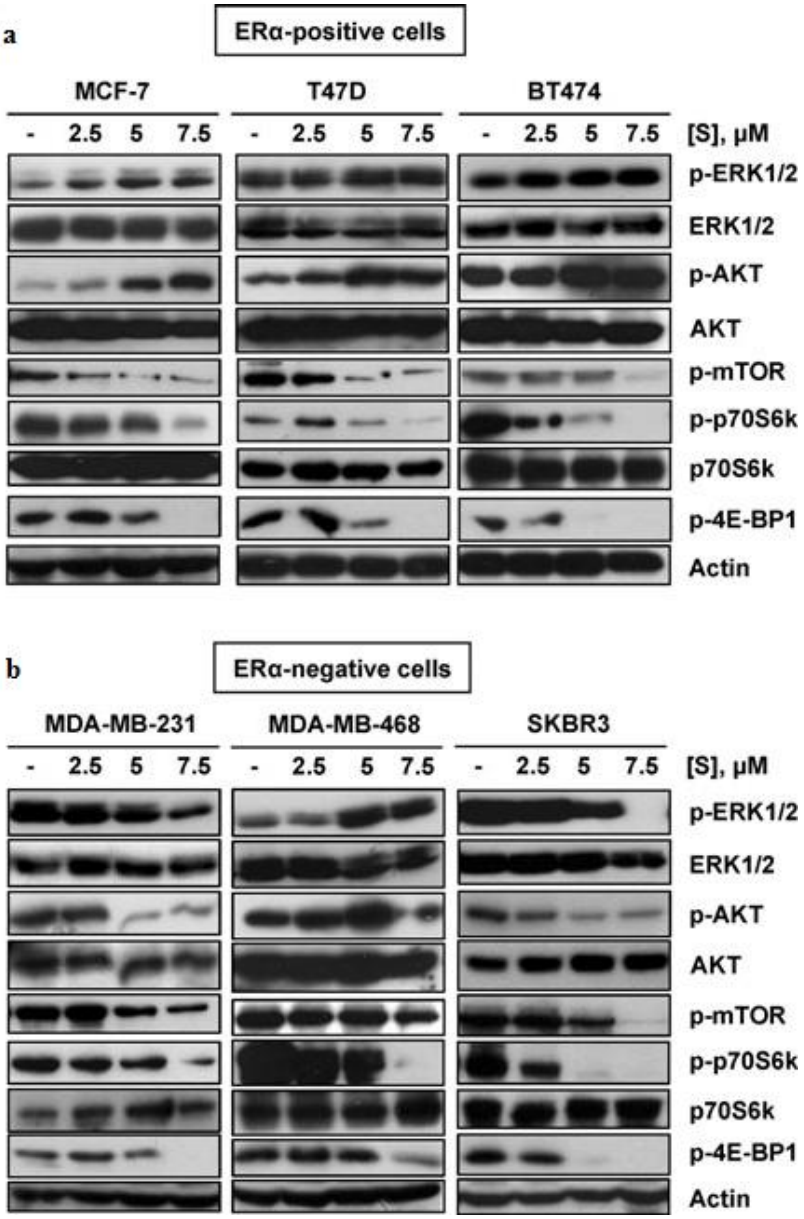

Figure 28. Effect of sorafenib on growth signaling pathways. ERα-positive (a) and ERα-negative (b) BC cells were treated with or without various concentrations of sorafenib (S). After 24h, expression of the indicated proteins was analyzed by Western blotting. Results are representative of three independent experiments.

Moreover, 5-7.5μM sorafenib induced cell death in all the cell lines through the apoptotic intrinsic pathway, as indicated by cleavage of the caspase substrate PARP-1 and activation of caspase-9 and caspase-7 **(Figure 29a,b)**. In addition, the anti-apoptotic protein Mcl-1 was down-regulated, presumably as a consequence of STAT3 inhibition **(Figure 29c)**. However, p-src down-regulation occurred in MCF-7 and SKBR3, but not in MDA-MB-231 cells, indicating that

in this model a different mechanism is implicated in p-STAT3 inhibition **(Figure 29c)**. Treatment with the pan-caspase inhibitor z-VAD-fmk failed to inhibit cell death completely in SKBR3 cells, suggesting that caspase-independent pathways might also be involved in the cytotoxic action of sorafenib **(Figure 29d)**.

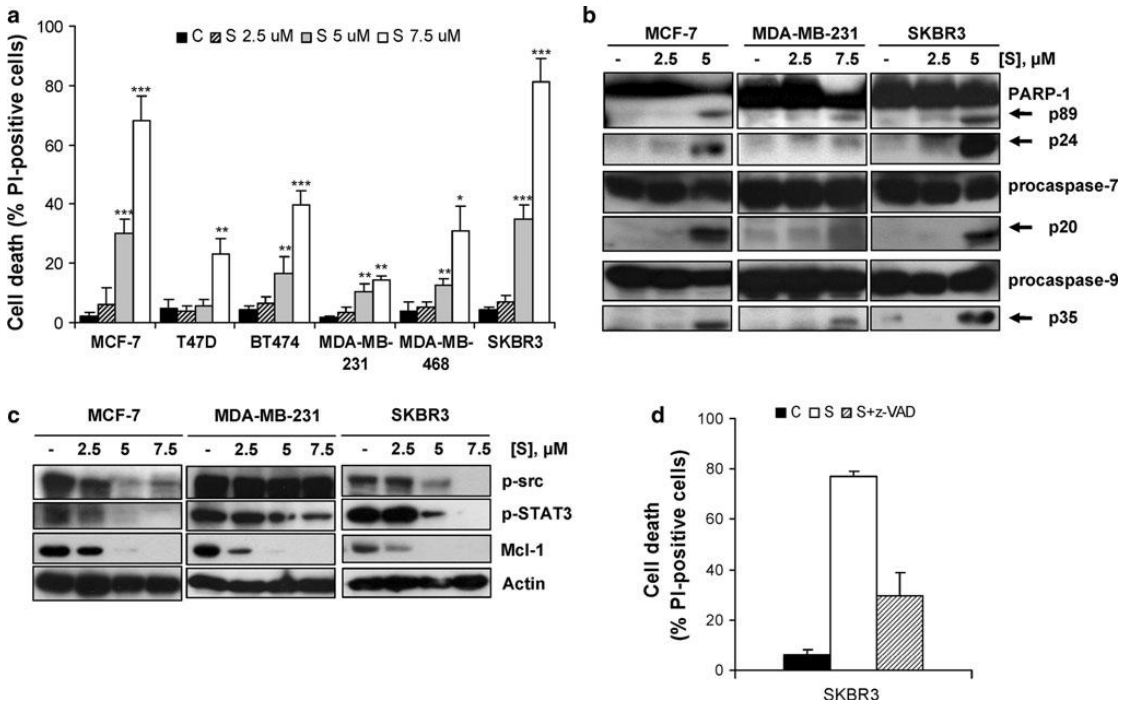

Figure 29. Effect of sorafenib on cell survival. Cells were treated in the absence (C) or presence of the indicated concentrations of sorafenib (S). (a) Cell death was quantitated after 72h on Hoechst 33342/PI stained cells. Columns mean of three independent experiments; bars, SD. (b) PARP-1, procaspase-7, and procaspase-9 cleavage were assessed by Western blotting after 72h. (c) p-src, p-STAT3, Mcl-1, and actin protein expression were evaluated by Western blotting after 48h. Results in b, and c are representative of three independent experiments. (d) SKBR3 cells were untreated (C) or treated with sorafenib 7.5µM in the absence (S) or presence of the pan-caspase inhibitor z-VAD-fmk 50µM (S + z-VAD). After 72h, cell death was quantitated as described in (a). Columns mean of three independent experiments, bars, SD. *Statistical significance versus C. ***P<0.001, **P<0.01, *P<0.05.

Sorafenib induces the activation of AMPK as a consequence of mitochondrial ATP depletion.

In order to investigate the effects underlying the molecular mechanisms of sorafenib, we evaluated whether the emergence of an energy stress might have a role in the antitumoral activity

of sorafenib in BC cells. All the cell lines were incubated with or without sorafenib at various concentrations, and then p-AMPKα1 expression was analyzed by Western blotting. As shown in **Figure 30a,** the master energy stressor AMPKα1 was activated in all the cell lines after 2h of treatment with sorafenib. We investigated the ATP levels in three cell lines MCF-7, MDA-MB-231, and SKBR3, selected as models representative of each BC subtype. These three cell lines were also selected because they show a different metabolic behavior; indeed, data from literature indicate that MCF-7 cells are mainly dependent on mitochondrial respiration, the more aggressive MDA-MB-231 cells display a glycolytic phenotype, whereas SKBR3 cells have an intermediate bioenergetic organization. MCF-7, MDA-MB-231, and SKBR3 cell lines were incubated with or without sorafenib (7.5μM) and then ATP levels were measured after 2h: as shown in **Figure 30b** sorafenib treatment reduced ATP intracellular levels in all the three cell lines.

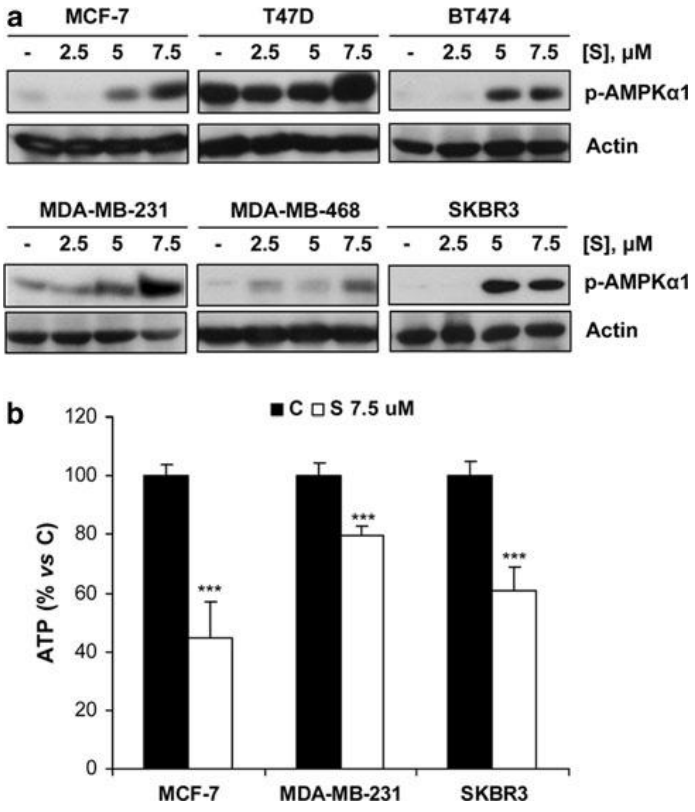

Figure 30. Sorafenib early induces AMPK activation and ATP depletion. (a) Cells were incubated in the absence (C) or presence of sorafenib (S) at the indicated concentrations. p-AMPKα1 expression was analyzed after 2h by Western blotting. Results are representative of three independent experiments. (b) Cells were incubated in the absence (C) or presence of sorafenib (S 7.5μM). After 2h, ATP levels were measured by a luminescence assay. Columns, mean of three independent experiments, bars, SD. *Statistical significance versus C. ***P<0.001.

In order to establish whether the ATP levels decrease associated with sorafenib treatment was due to a perturbation of mitochondrial respiration, MCF-7, MDA-MB-231, and SKBR3 cells were incubated with or without 7.5μM sorafenib, 10mM 2DG (a non-metabolizable glucose analog that blocks glycolysis), and oligomycin 20μg/ml (a mitochondrial ATPase inhibitor) either alone or in combination. As shown in **Figure 31a**, MCF-7 cells were the most sensitive to either sorafenib- or oligomycin-mediated effects on ATP levels. In addition, when sorafenib was combined with oligomycin, intracellular ATP decreased to levels comparable to those observed with each agent alone, both in MCF-7 cells as well as in MDA-MB-231, and SKBR3 cells. In contrast, ATP levels were further lowered by the combination of sorafenib with 2DG as compared with single agents, mimicking the effect of oligomycin-2DG combination. These data suggest that sorafenib, as oligomycin, led to ATP decrease and energy stress by affecting mitochondrial respiration in BC cell lines. These results were also confirmed by the observation that sorafenib induced MMD **(Figure 31b)**, associated with an increase of ROS generation up to 24h **(Figure 31c)**. Both effects were evident as early as 1h after sorafenib exposure, when also AMPK appeared significantly induced **(Figure 31d)**. The accumulation of ROS might contribute to AMPK activation that persisted during prolonged incubations with sorafenib (**Figure 31d**). Moreover, to unravel the role of ROS generation in the mechanisms of sorafenib action, we incubated MCF-7 with NAC, a precursor of reduced glutathione (GSH) which acts as a H_2O_2 scavenger. As shown in **Figure 31e,f**, NAC is not able to protect cells from death although it reduced sorafenib-mediated production of H_2O_2. In addition, sorafenib increased also the production of O_2^- **(Figure 31e),** on which NAC had no relevant effect. Recently, Coriat et al.[112] demonstrated the active role of NADPH oxidase-dependent production of O_2^- in sorafenib effectiveness in HCC. Thus, we pre-treated MCF-7 cells with the NADPH oxidase inhibitor DPI before exposure to sorafenib. Surprisingly, DPI promoted instead of inhibiting ROS production, and further enhanced both H_2O_2 and O_2^- induced by sorafenib **(Fifure 31e)**. In accordance, DPI potentiated the cytotoxic action of sorafenib **(Figure 31f)**.

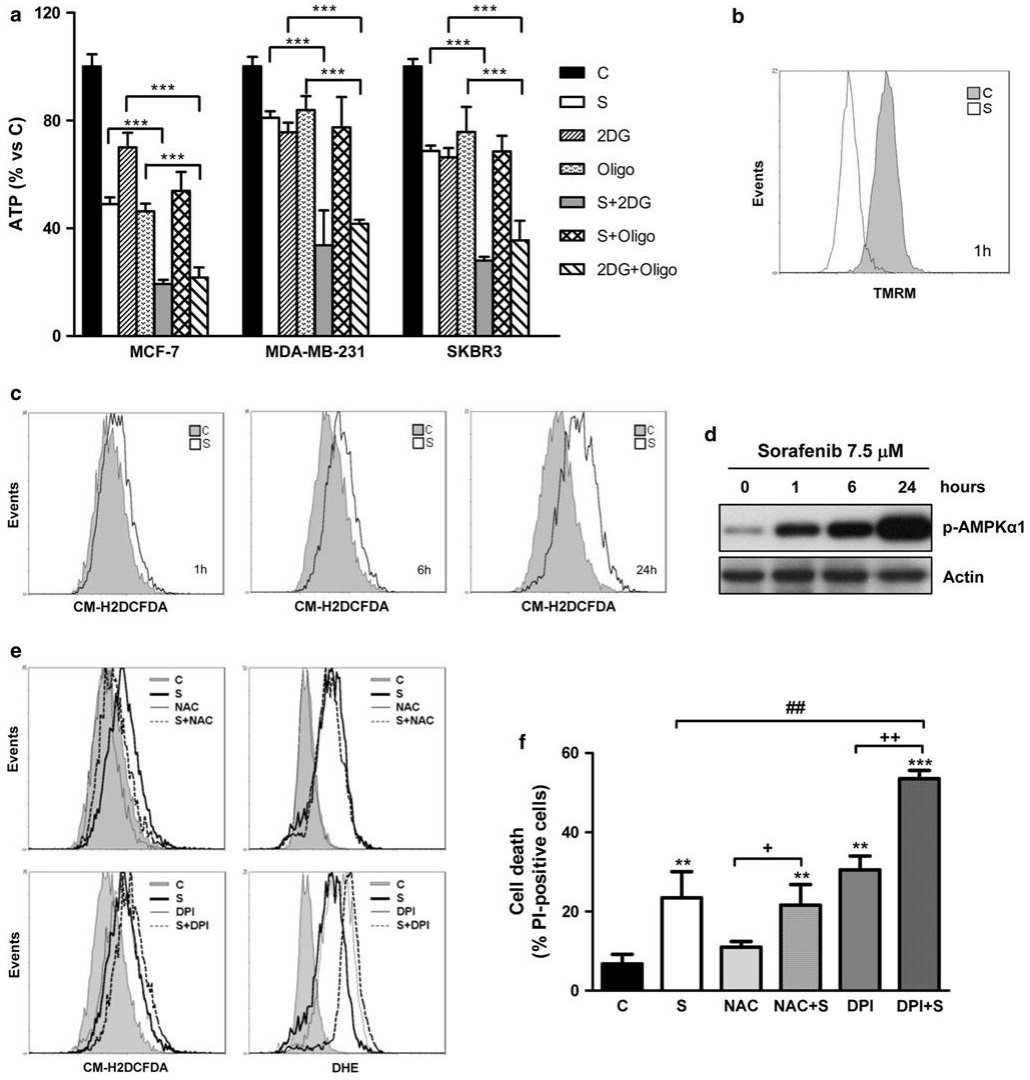

Figure 31. Sorafenib impairs mitochondrial function, causing MMD and increasing ROS production. Cells were untreated (C) or treated with sorafenib 7.5μM (S), 2DG 10mM, and oligomycin 20μg/ml (Oligo) either alone or in combination (S + 2DG, S + Oligo, 2DG + Oligo). After 2h, ATP levels were measured by a luminescence assay. Columns, mean of three independent experiments; bars, SD. MCF-7 cells were incubated in the absence (C) or presence of sorafenib 7.5μM (S). MMD (b), ROS (more specifically H_2O_2) (c), p-AMPKa1 and actin expression (d) were analyzed at the time points indicated. *Statistical significance versus C.***P<0.001. MCF-7 cells were incubated in the absence (C) or presence of sorafenib 7.5μM (S), NAC 5mM, DPI 10μM either alone or in combination (S + NAC, S + DPI). After 6 h, production of H2O2 and O_2^- was measured by using CM-H2DCFDA and DHE probes, respectively (e). Results are representative of three independent experiments. After 24h, cell death was quantitated on Hoechst 33342/PI-stained cells (f). *Statistical significance versus C. ++P<0.01, +P<0.05, ##P<0.01.

Sorafenib produces opposite early and long-term effects on glucose metabolism.

To get insight into the molecular mechanisms underlying the inhibitory action of sorafenib, we evaluated whether sorafenib-mediated impairment of oxidative phosphorylation affected cell glucose metabolism.

As shown in **Figure 32,** in MCF-7 and SKBR3 cells, a 6h treatment with sorafenib increased glucose uptake by up-regulating the expression of GLUT-1, stimulated aerobic glycolysis to compensate for the loss of mitochondrial ATP, and increased lactate production. After 24h of treatment these effects were still maintained in SKBR3 cells, whereas in MCF-7 cells both glucose transport and glucose consumption were decreased **(Figure 32a,c)**. However, a more prolonged exposure to sorafenib ultimately hindered glucose utilization also in SKBR3 cells, as suggested by inhibition of GLUT-1 expression after 48h of treatment **(Figure 32b)**. Furthermore our data showed that in the highly glycolytic MDA-MB-231 cells, sorafenib induced mitochondrial perturbation slightly affected glucose metabolism after 6h; however a significant down-regulation of GLUT-1 expression, glucose transport, and glycolysis was observed after 24h and persisted after 48h, as suggested by inhibition of GLUT-1 expression **(Figure 32a,b,c)**.

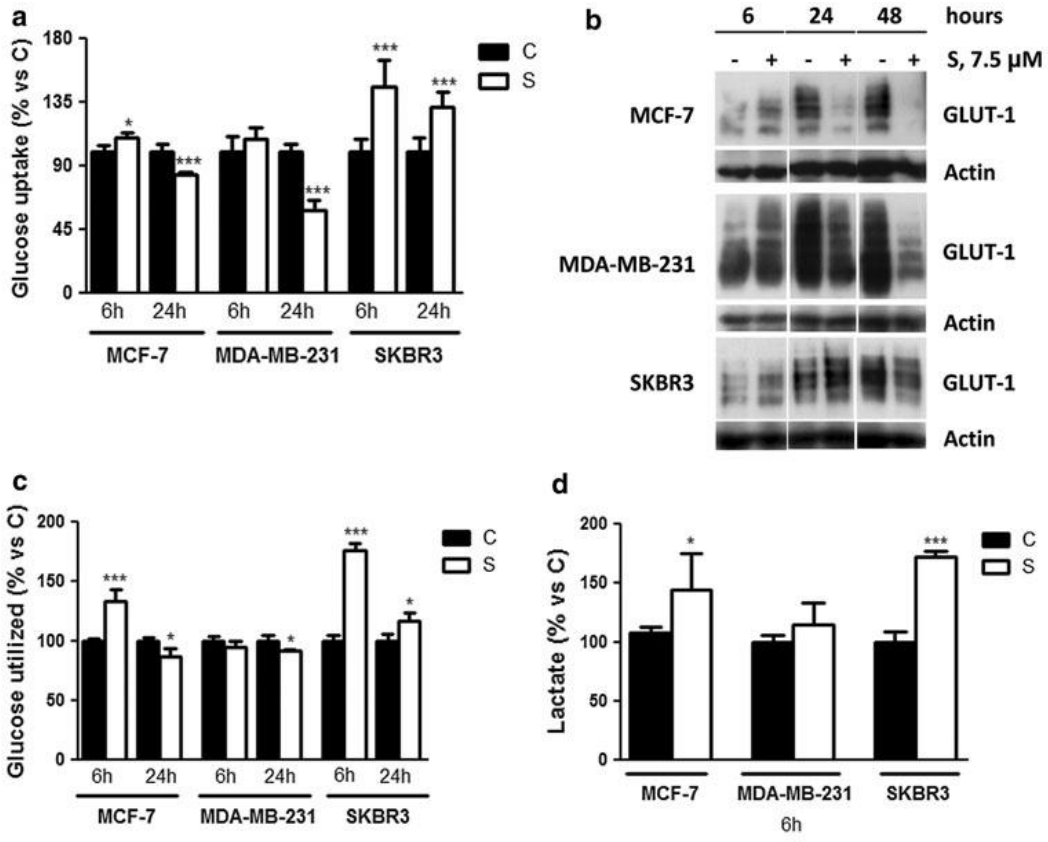

Figure 32. Sorafenib affects glucose metabolism. Cells were incubated in the absence (C) or presence of sorafenib 7.5µM (S). Glucose uptake (a), GLUT-1 and Actin protein expression (b), glycolysis (c), and lactate production (d) were analyzed at the time points indicated. Columns in a, c, d mean of three independent experiments, bars, SD. *Statistical significance versus C. ***P<0.001, *P<0.01. Results in (b) are representative of three independent experiments.

In order to confirm whether GLUT-1 is actually the glucose transporter involved in sorafenib-mediated effects on glucose metabolism, we incubated SKBR3 cells with fasentin, a specific GLUT-1 inhibitor. Unexpectedly, incubation of SKBR3 cells with fasentin down-regulated the basal uptake of glucose and inhibited the uptake induced by sorafenib **(Figure 33a)**. In addition, fasentin, by inhibiting glucose utilization, rendered SKBR3 cells unable to compensate for sorafenib-induced impairment of OXPHOS, thus potentiating sorafenib cytotoxic action **(Figure 33b)**. All together these results indicate that, despite the initial attempt to adapt to the energy stress through AMPK activation and GLUT-1 induction, BC cells exposed to sorafenib ultimately experienced a significant impairment of glucose metabolism, which might contribute to sorafenib cytotoxic activity.

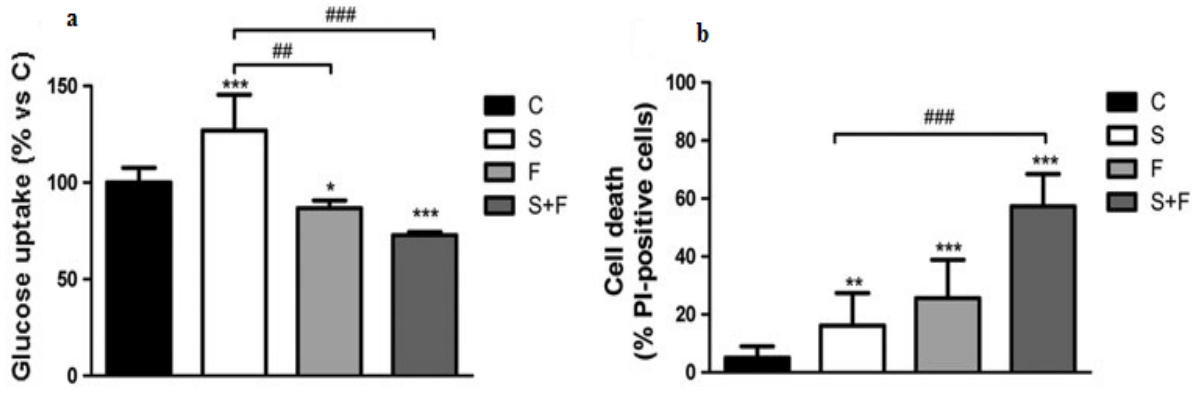

Figure 33. GLUT-1 is the glucose transporter involved in sorafenib mediated-effects on glucose metabolism. SKBR3 cells were untreated (C) or treated with sorafenib 7.5μM (S) and fasentin 200μM (F) either alone or in combination (S+F). Glucose uptake (a) and cell death on Hoechst 33342/PI-stained cells (b) were analyzed after 6 and 24h, respectively. Columns in (a,b) mean of three independent experiments, bars, SD. *Statistical significance versus C. ***P<0.001, **P<0.01, *P<0.05, ###P<0.001, ##P<0.01

Sorafenib-mediated down-regulation of glucose metabolism involves inhibition of mTORC1 signaling.

Although AMPK might be responsible for the enhancement of glycolysis at early time points after sorafenib exposure, its persistent activation may produce the opposite effect on glucose metabolism through down-regulation of mTORC1 signaling. To evaluate whether this mechanism could be sufficient to hamper glucose utilization during sorafenib treatment, MCF-7 cells were treated for 24h with sorafenib, the mTORC1 inhibitor rapamycin, the dual PI3K/ mTORC1-C2 inhibitor NVP-BEZ-235, or the MEK1/2 inhibitor U0126. As indicated in **Figure 34**, U0126 had no effect, while rapamycin and sorafenib down-regulated both GLUT-1 expression and glucose uptake to similar extents. A deeper effect was produced by NVP-BEZ-235, due to the simultaneous inhibition of AKT and mTORC1. These results suggest that sorafenib-mediated inhibition of mTORC1 signaling, possibly consequent to persistent AMPK activation, was sufficient to alter glucose metabolism in BC cells.

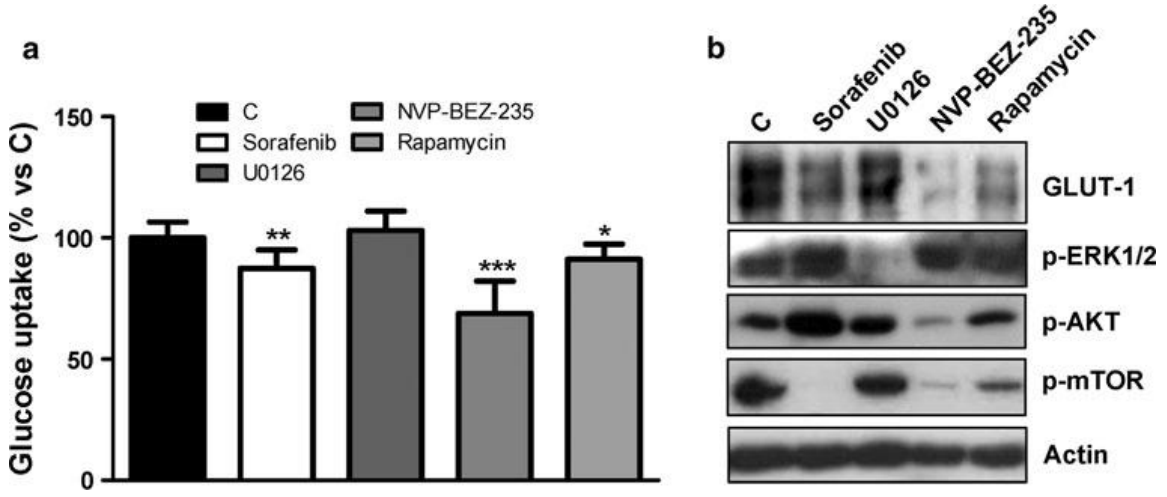

Figure 34. Inhibitors of proliferation/survival signaling pathways differently affect glucose utilization in MCF-7 cells. MCF-7 cells were incubated in the absence (C) or presence of sorafenib 7.5μM, U0126 3μM, NVP-BEZ-235 0.1μM, or Rapamycin 0.1μM. Glucose uptake (a) and Western blotting (b) were performed after 24h. Columns in (a) mean of two independent experiments, bars, SD. Results in (b) are representative of two independent experiments. *Statistical significance versus C. ***P<0.001, **P<0.01, *P<0.05.

AMPKα1 silencing has a significant impact on sorafenib-mediated effects.

In order to assess the role of AMPK activation in the early effects mediated by sorafenib and to further validate the relevance of AMPK-dependent inhibition of mTORC1 in sorafenib long-term action, we down-regulated AMPKα1 expression by RNA interference. As shown in **Figure 35a,b,** AMPKα1 silencing did not prevent sorafenib mediated induction of MMD and ROS production, implying that both these events preceded AMPK activation. In addition, AMPKα1 knockdown blocked the increase of GLUT-1 protein expression induced by a 6h treatment with sorafenib **(Figure 35c)**, and prevented the down-regulation of mTORC1 signaling observed after 24h **(Figure 35d)**. These results indicate that AMPK activation is required to stimulate glucose metabolism as an early adaptation to sorafenib-mediated energy stress and definitely demonstrate that long-term exposure to sorafenib inhibits the mTORC1 pathway through an AMPK-dependent mechanism in BC cells. Importantly, restoration of mTORC1 signaling by AMPKα1 silencing reduced the cytotoxic effects of sorafenib **(Figure 35e)**.

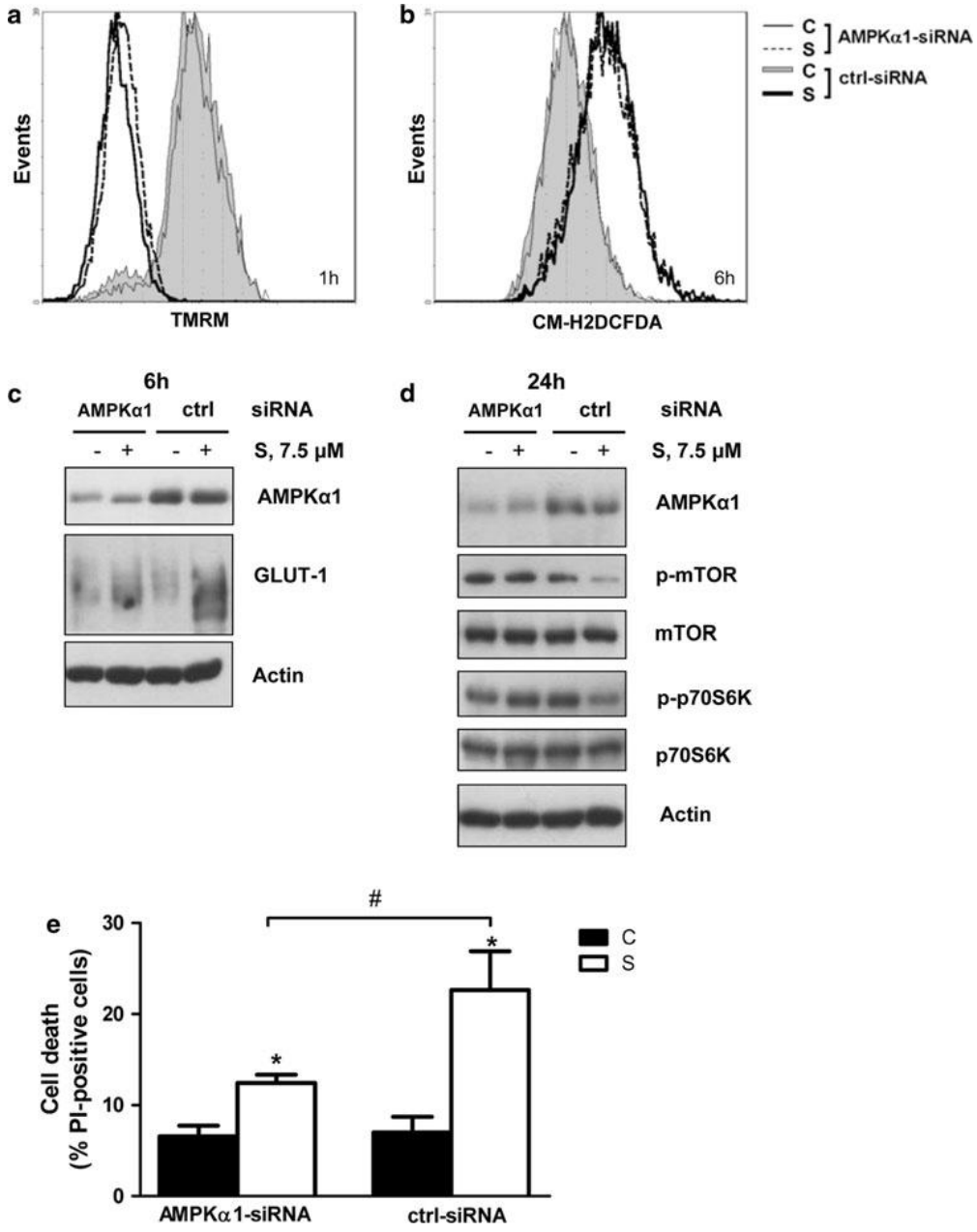

Figure 35. AMPKα1 silencing alters sorafenib-mediated effects. MCF-7 cells were transfected with AMPKα1 or control siRNA. After 48h, the medium was replaced with fresh medium with or without sorafenib 7.5μM. At the time points indicated the following analyses were performed: MMD (a), H_2O_2 assessment (b), western blotting (c, d), cell death on Hoechst 33342/PI stained cells (e). Results in a–d are representative of three independent experiments. Columns in (e) mean of three independent experiments, bars SD. *Statistical significance versus C. *P<0.05, #P<0.05.

Discussion and conclusions

In the last part of my thesis we demonstrated that sorafenib anti-tumor activity in BC cells is mediated by a Raf/MEK/ERK-independent, AMPK/mTORC1-dependent mechanism that involves the induction of energy stress. In particular, we showed that sorafenib-mediated inhibition of cell proliferation was associated with downregulation of mTORC1 signaling in all the cell lines selected.

Although the multi-kinase inhibitor sorafenib is approved by FDA for the treatment of HCC and metastatic renal cell carcinoma, and it has also shown efficacy against a wide variety of tumors in preclinical studies[47,48], the molecular mechanisms by which sorafenib acts are not completely known. A previous study showed that sorafenib inhibited the MAPK pathway in MDA-MB-231 cells containing activating mutations in both K-Ras and B-Raf proto-oncogenes, suggesting this as a general mechanism for sorafenib activity in BC[49, 113], instead our results demonstrated that upon sorafenib treatment ERK1/2 phosphorylation/activation decreased only in MDA-MB-231 and SKBR3 cells, while it increased in the other cell models. The increase was presumably due to Ras-dependent C-Raf homo/heterodimerization and activation[114] or to the release of mTOR-dependent feedback inhibition of RTK/IRS-1/Ras/MAPK signaling[115]. By relieving the negative feedback on IRS-1, sorafenib-mediated down-regulation of mTORC1 signaling may be also responsible for the phosphorylation/activation of AKT observed in MCF-7, T47D, and BT474 ERα-positive cells as well as in MDA-MB-468 triple negative cells. This phenomenon may be explained considering that these cells are characterized by an aberrant activation of the PI3K signaling pathway, due to PIK3CA mutations in the ERα-positive cell lines and to PTEN mutations in MDA-MB-468 cells. Indeed, a recent study on cancer cell sensitivity to mTOR inhibitors demonstrated that rapamycin-mediated activation of AKT signaling is greater in rapamycin-sensitive cells and that these cells are more likely to have PIK3CA and/or PTEN mutations[116]. Taken together, our results suggest that the observed differences in sorafenib-mediated effects on MAPK and AKT signaling are correlated with genetic features other than the ERα status that defines BC standard classification. We demonstrated that sorafenib at 5–7.5μM induced apoptosis through the intrinsic pathway, although activation of caspase-independent pathways cannot be ruled out. It is noteworthy that MDA-MB-231 cells appeared less prone to undergo apoptosis as compared with the other cell lines, showing a significant lower percentage

of cell death after 72h of treatment. This result reinforces the suggestion that inhibition of MAPK pathway cannot be considered as a predictive factor of sorafenib sensitivity in BC. These data agree with previous works delineating different MAPK-independent mechanisms to explain sorafenib action in a variety of cancer cell types[117,118,119,120]. It is becoming clear that sorafenib acts through mechanisms that involve multiple targets, including novel unexpected molecules[121]. Among these, the mitochondrial electron transport chain complex I has been recently identified in neuroblastoma cells as an early sorafenib's target, whose down-regulation, through protein destabilization, causes a rapid caspase-independent MMD[122]. Inhibition of complex I enzyme activity may account for both MMD and impairment of OXPHOS that we observed in BC cells as early effects of sorafenib treatment. As a consequence of these events, ATP levels decreased in all the cell lines analyzed, although this reduction was more pronounced in MCF-7 cells, whose energy metabolism is mainly based on mitochondrial activity. ATP depletion, in turn, rapidly induced the phosphorylation/activation of the energy sensor AMPK. Upon activation, AMPK has been shown to stimulate glucose uptake, either by promoting the translocation of GLUTs to the plasma membrane, or by enhancing the transcription of genes encoding for these transporters[123]. In addition, AMPK may favor glycolysis by phosphorylating and activating 6-PFK II[124,125]. Here we demonstrate that sorafenib-mediated activation of AMPK initially stimulated glucose uptake by increasing GLUT-1 protein expression in MCF-7 and SKBR3 cells. GLUT-1 induction was prevented by AMPKα1 silencing; moreover, the GLUT-1 inhibitor fasentin inhibited the glucose uptake induced by sorafenib, thus indicating that GLUT-1 is the glucose transporter actually involved in sorafenib-mediated effects on glucose metabolism. Sorafenib enhanced also glycolysis in MCF-7 and SKBR3 cells, consequently increasing lactate production. All these effects were observed after 6h of sorafenib treatment. In contrast, no significant change in glucose metabolism was detected at this time point in MDA-MB-231 cells, which display a highly glycolytic phenotype and experienced a moderate decrease of ATP levels. Our data showed that the activation of AMPK persisted all along sorafenib treatment. Since previous data reported the involvement of AMPK in the cell response to oxidative stress[126] the prolonged activation of AMPK during all the treatment with sorafenib might be due to the ability of the drug to increase ROS production. Intracellular ROS in BC cells increased early upon sorafenib exposure and further accumulated during the treatment. In a recent paper by Coriat et al.[112], sorafenib effectiveness in HCC was associated with NADPH oxidase-dependent production of

O_2^-. In accordance with this study, we demonstrated that the H_2O_2 scavenger NAC, being unable to reduced O_2^- production, did not reduce the growth-inhibitory effects of sorafenib in MCF-7 cells. In contrast, the NADPH oxidase inhibitor DPI, that was shown to hinder both the generation of ROS and the induction of apoptosis in HCC cells, acted in the opposite manner in MCF-7 cells, increasing ROS and potentiating sorafenib activity. This result finds support in previous studies showing that DPI, instead of protecting, may augment oxidative stress and exert cytotoxic effects in some cellular systems[127]. Persistence of the energy stress during sorafenib treatment in BC cells resulted in a previously unrecognized inhibitory effect on glucose metabolism. Indeed, either GLUT-1 protein expression and hence glucose uptake or glycolysis were down-regulated after a prolonged exposure to the drug. We suggest that these long-term effects, despite being opposite to the acute stress response induced by AMPK, are still dependent on AMPK. Indeed, persistent activation of AMPK by sorafenib resulted in the inhibition of mTORC1 signaling, whose role in the regulation of glucose metabolism is well established[128]. mTORC1 is recognized as a master metabolic sensor that integrates nutrient and mitogen signals to regulate cell growth/division, by promoting protein synthesis and activating bioenergetic and anabolic processes, such as glycolysis. AMPK provides the link with the energy status of the cell, to allow proliferation only under conditions of sufficient energy supply. Therefore, AMPK activation by energy stress may lead to suppression of mTORC1 signaling even in the presence of growth factors and active AKT and ERK signaling[129]. Here we demonstrate that inhibition of mTORC1 is sufficient to hinder glucose utilization in BC cells, as indicated by the ability of the mTORC1 inhibitor rapamycin to down-regulate both GLUT-1 protein expression and glucose uptake in MCF-7 cells, effect enforced by NVP-BEZ-235, a dual PI3K/mTORC1-C2 inhibitor. The importance of AMPK-dependent inhibition of mTORC1 in sorafenib mechanisms of action was clearly demonstrated by using AMPKα1 RNA interference; indeed, APMK depletion in MCF-7 cells restored mTORC1 activity at 24h, conferring a significant protection from cell death. Sorafenib, as also indicated by our study, has a broad spectrum of activity often independent of its canonical targets. Therefore, it is difficult to define a predictive biomarker of sensitivity for this drug. In a recent work performed on HCC cell lines and xenografts, sorafenib resistance has been correlated with the bioenergetic propensity to use glycolysis[130]. However, caution should be used in extending this conclusion to BC cells. Indeed, the highly glycolytic MDA-MB-231 cells cannot be considered resistant to sorafenib, despite being less sensitive than

other cell models that mainly rely on mitochondrial ATP production for their energy demands. Our results suggest that sorafenib, being effective in all the BC cell subtypes, may be proposed as a valid support to the current established therapy for ERα-positive or HER-positive BC. In triple negative BC subtype, its use in clinical practice warrants further validations.

GENERAL CONCLUSIONS

In the last decade, a new concept was raised in medicine: translation medicine. Often described as an effort to carry scientific knowledge "from bench to bedside," translational medicine builds on basic research advances and uses them to develop new therapies or medical procedures in order to personalize the treatment. Translation medicine can be defined as the constellation of activities which seek to translate the science of gene discovery, gene transfer, and functional genomics into gene-targeted therapies. Identification of different driver mutations that define new molecular subsets of cancer has been critical in defining novel targeted therapeutic approaches. Targeted therapy lays the basis onto the concept that some cancers for their survival and proliferation depend on a single oncogene activated by somatic mutation. As a consequence targeted cancer therapies are based on the use of drugs that block the growth and spread of cancer by interfering with specific molecules involved in tumor growth and progression. Indeed, targeted therapies focus on proteins involved in cell signaling pathways which form a complex communication system that drives pivotal cellular functions and activities (such as cell division, cell metabolism, cell movement etc); TKs are an especially important target because they play an important role in the modulation of growth factor signaling. Progress in understanding cancer biology and mechanisms of oncogenesis has allowed the development of treatment against specific molecular targets such as EGFR (one of the most deregulated and overexpressed molecular target in many malignencies) in NSCLC and the MAP kinases pathway, PI3K/AKT/mTOR pathway and Jak-STAT pathway in BC. In particular, here I studied the molecular mechanisms underneath three targeted drugs: erlotinib and gefitinib (both against EGFR) in NSCLC, and sorafenib (an oral multikinase inhibitor with anti-proliferative and antiangiogenic activity) in BC. The findings of our studies highlight the importance of targeted therapy as a strategy to treat cancer. At the same time, they underline the necessity to understand better the mechanisms of action of targeted drugs with the ultimate purpose to defeat cancer. Regarding NSCLC, this investigation shows that FDG-PET (a non invasive, simple and efficacy technique) assessment after 2 days of erlotinib treatment could be useful to identify early resistant patients and to predict survival in unselected NSCLC pretreated population. Moreover, we have shown that, despite tumor progression after treatment with gefitinib, NSCLCs with *MET* amplification are still dependent on EGFR signaling. In particular, the maintenance of gefitinib after tumor progression emerges as an important new therapeutic strategy to inhibit EGFR-mediated aggressive behavior in NSCLC with MET amplification. Concerning breast cancer, our results indicate that sorafenib may be

proposed as a valid support to the current established therapy for ERα-positive or HER2-positive BC; moreover, sorafenib could be also proposed in triple negative BC subtype.

In conclusion, targeted therapy (here we give three examples of targeted drugs in NSCLC and breast cancer) could be a promising strategy in order to defeat cancer. The development of targeted drugs against specific biological molecules (altered in cancer) potentially increases antitumor efficacy while minimizing the toxicity to the patient that is seen with conventional therapeutics, such as chemotherapy.

BIBLIOGRAPHY

1. Siegel R et al. *Cancer Statistics.* Cancer J Clin, 60(5):277-300, 2012.
2. Parums D.V. et al. *Current status of targeted therapy in non-small cell lung cancer.* Drugs of today, (62): 10- 29, 2012.
3. Hecht SS, et al. *Lung carcinogenesis by tobacco smoke.* Int J Cancer, 131(12): 2724-32, 2012.
4. Wei S, et al. *Genome-wide gene-environment interaction analysis for asbestos exposure in lung cancer susceptibility.* Carcinogenesis, 33(8):1531-7, 2012.
5. Roengvoraphoj M. et al. *Epidermal growth factor receptor tyrosine kinase inhibitors as initial therapy for non-small cell lung cancer: focus on epidermal growth factor receptor mutation testing and mutation-positive patients.* Cancer Treatment Reviews, (39) 839–850, 2013.
6. Mirsadraee S, et al. *The 7th lung cancer TNM classification and staging system: Review of the changes and implications.* World J Radiol, 4(4): 128-134, 2012.
7. Grzegorz J. Korpanty G. J. et al, *Biomarkers that currently affect clinical practice in lung cancer: EGFR, ALK, MET, ROS-1, and KRAS.* Front. In oncology vol 4:204, 2014.
8. Sheng-Xiang L. Et al., *Molecular therapy of breast cancer: progress and future directions*. Nat. Rev. Endocrinol. 6, 485–493, 2010.
9. Jemal A. et al. *Cancer statistics, 2010*. CA Cancer J. Clin. 60, 277–300, 2010.
10. Sorlie T. et al. *Gene expression patterns of breast carcinomas distinguish tumor subclasses with clinical implications.* Proc Natl Acad Sci U S A. 98(19):10869–10874, 2001.
11. Perou CM. et al. *Molecular portraits of human breast tumours.* Nature 406(6797):747–752, 2000.
12. Lin S. X. et al. *Molecular therapy of breast cancer: progress and future directions*. Nat. Rev. Endocrinol. (6):485–493, 2010.
13. Desantis C. E. et al. *Cancer Treatment and Survivorship Statistics, 2014.* CA CANCER J CLIN 64:252–271, 2014.
14. R. Shah et al. *Pathogenesis, prevention, diagnosis and treatment of breast cancer* World J Clin Oncol 5(3): 283-298, 2014.
15. Vuong D. et al. *Molecular classification of breast cancer.* Virchows Arch 465:1–14, 2014.

16. Bertos N. R. Et al. *Breast cancer one term, many entities?* J Clin Invest. 121(10):3789–3796, 2011.
17. Polyak K. Et al. *Heterogeneity in breast cancer*. J Clin Invest. 121(10):3786–3788, 2011.
18. ASCO meeting, San Francisco 2014.
19. Cao Y. Et al. *Cancer research: past, present and future.* Nature Reviews Cancer **11**, 749-754, 2011.
20. Korpanty G. J. et al. *Biomarkers that currently affect clinical practice in lung cancer: EGFR, ALK, MET, ROS1, andr KRAS.* Frontier in oncology. Aug 2014,vol4, 204, 2014.
21. Arora A. et al. *Role of Tyrosine Kinase Inhibitors in Cancer Therapy*. The Journal of Pharmacology and Experimental Therapeutics Vol. 315, No. 3, 2005.
22. Joo W.D. et al. *Targeted cancer therapy – Are the days of systemic chemotherapy numbered?* Maturitas 76(4):308-14, 2014.
23. Kumar R et al. *Targeted cancer therapies: the future of cancer treatment.* Acta Biomed. 83(3):220-33, 2012.
24. Semrad T. J. Et al. *Fibroblast Growth Factor Signaling in Non-Small-Cell Lung Cancer* Clinical Lung Cancer. 13:90–95, 2012.
25. Di Cosimo S. Et al. *Management of breast cancer with targeted agents: importance of heterogenicity.* J. Nat. Rev. Clin. Oncol. 7, 139–147, 2010.
26. Pengyu H., et al. MAPK signaling in inflammation-associated cancer development. Protein Cell. 1(3):218-26, 2010.
27. Cargnello M. et al. Activation and function of the MAPKs and their substrates, the MAPK-activated protein kinases. Microbiol. Mol.Biol.Rev. 75(1): 50–83, 2011.
28. Boutros T. et al. Mitogen-activated protein (MAP) kinase/MAP kinase phosphatase regulation: roles in cell growth, death, and cancer. Pharmacol. Rev. 60(3): 261–310, 2008.
29. Raman M., et al. Differential regulation and properties of MAPKs. Oncogene 26(22), 3100–12, 2007.
30. Dhillon A.S. et al. MAP kinase signalling pathways in cancer. Oncogene (26): 3279–3290, 2007.

31. Tan Li. Et al. Targeting of the PI3K/Akt/mTOR Pathway: Toxicity Reduction and Therapeutic Opportunities. Int. J. Mol. Sci. (15):18856-18891, 2014.
32. Martelli A.M. et al. Phosphoinositide 3-kinase/Akt signaling pathway and its therapeutical implications for human acute myeloid leukemia. Leukemia 20:911-928, 2006.
33. Robey RB et al. Is Akt the "Warburg kinase"?-Akt-energy metabolism interactions and oncogenesis. Semin.Cancer Biol. 19(1), 25–31, 2009.
34. Cairns R.A. et al. Regulation of cancer cell metabolism. Nature Reviews Cancer. (11); 85-95, 2011.
35. Laplante M., et al. mTOR signaling at a glance. J. Cell. Sci. (122); 3589–94, 2009.
36. Kisseleva T. et al. *Signaling through the JAK/STAT pathway, recent advances and future challenges.* Gene 20;285(1-2):1-24, 2002.
37. Quintás-Cardama A. Et al. *Molecular Pathways: JAK/STAT Pathway: Mutations, Inhibitors, and Resistance.* Clin Cancer Res. 15;19(8):1933-40, 2013.
38. Parsons S. J. Et al. *Src family kinases, key regulators of signal transduction.* Oncogene 23, 7906–7909, 2004.
39. Roskoski R Jr et al. *Src kinase regulation by phosphorylation and dephosphorylation.* Biophys Res Commun. (27);331(1):1-14, 2005.
40. Vansteenkiste J. et al. *Early and locally advanced non-small-cell lung cancer (NSCLC): ESMO Clinical Practice Guidelines for diagnosis, treatment and follow-up.* Annals of Oncology 24: vi89–vi98, 2013.
41. Zhao C. et al., *Non-small-cell lung cancers: a heterogeneous set of diseases*. Nature review. Vol 14, 2014.
42. Korpanty G.J. et al. *Biomarkers that currently affect clinical practice in lung cancer: EGFR, ALK, MET, ROS1 and RAS.* Front Oncol. (4): 204, 2014.
43. Peters S. et al. *Success and limitations of targeted cancer therapy.* Prog. tumor research. Basel. Karger, vol 41: 62-77, 2014.
44. Remon J. et al. *Beyond EGFR TKI in EGFR-mutant Non-Small Cell Lung Cancer patients: Main challenges still to be overcome.* Cancer Treatment Reviews (40):723–729, 2014.

45. Siegelin M.D. et al. *Epidermal growth factor receptor mutations in lung adenocarcinoma* Laboratory Investigation, 94: 129-137, 2014.
46. De Abreu F.B. et al. *Personalized therapy for breast cancer*. Clin Genet 86: 62–67, 2014.
47. Kane RC, et al. *Sorafenib for the treatment of advanced renal cell carcinoma*. Clin Cancer Res 12(24):7271–7278, 2013.
48. Kane RC, et al. *Sorafenib for the treatment of unresectable hepatocellular carcinoma.* Oncologist 14(1):95–100, 2009.
49. Wilhelm SM et al. *BAY 43-9006 exhibits broad spectrum oral antitumor activity and targets the RAF/MEK/ERK pathway and receptor tyrosine kinases involved in tumor progression and angiogenesis*. Cancer Res 64(19):7099–7109, 2004.
50. Plaza-Menacho I et al., *Sorafenib functions to potently suppress RET tyrosine kinase activity by direct enzymatic inhibition and promoting RET lysosomal degradation independent of proteasomal targeting.* J Biol Chem 282(40):29230–29240, 2007.
51. Yu C et al., *The role of Mcl-1 downregulation in the proapoptotic activity of the multikinase inhibitor BAY 43-9006.* Oncogene 24(46):6861–6869, 2005.
52. Ding Q et al., *Downregulation of myeloid cell leukemia-1 through inhibiting Erk/Pin1 pathway by sorafenib facilitates chemosensitization in breast cancer.* Cancer Res 68(15):6109–6117, 2008.
53. Fiume L et al., *Effect of sorafenib on the energy metabolism of hepatocellular carcinoma cells.* Eur J Pharmacol 670(1):39–43, 2011.
54. Bull VH et. al, *Sorafenib-induced mitochondrial complex I inactivation and cell death in human neuroblastoma cells.* J Proteome Res 11(3):1609–1620, 2012.
55. Baselga J et al., *Sorafenib in combination with capecitabine: an oral regimen for patients with HER2-negative locally advanced or metastatic breast cancer.* J Clin Oncol 30(13):1484–1491, 2012.
56. Hudis C et al., *Sorafenib (SOR) plus chemotherapy (CRx) for patients (pts) with advanced (adv) breast cancer (BC) previously treated with bevacizumab (BEV)*. J Clin Oncol 29(suppl; abstr 1009), 2011.

57. Gradishar WJ et al., *A double-blind, randomised, placebo-controlled, phase 2b study evaluating sorafenib in combination with paclitaxel as a first-line therapy in patients with HER2-negative advanced breast cancer*. Eur J Cancer 49(2):312–322, 2013.
58. Isaacs C et al., *Phase I/II study of sorafenib with anastrozole in patients with hormone receptor positive aromatase inhibitor resistant metastatic breast cancer.* Breast Cancer Res Treat 125(1):137–143, 2011.
59. Shepherd FA et al. *A prospective randomized trial of docetaxel versus best supportive care in patients with non-small-cell lung cancer previously treated with platinum-based chemotherapy.* J Clin Oncol (18);2095-103, 2000.
60. Therasse P. Et al. *New guidelines to evaluate the response to treatment in solid tumors.* J Natl Cancer Inst 92:205–216, 2000.
61. Mok TS et al. *Gefitinib or carboplatin-paclitaxel in pulmonary adenocarcinoma.* N Engl J Med 361:947–957, 2009.
62. Gogvadze V. et al. *The Warburg effect and mitochondrial stability* Mol. Aspect Med (31); 60-74,2010.
63. Winehouse S. et al. *Glycolysis, respiration and anomalous gene in expression in experimental hepatomas* Cancer Res. (32); 2007-2016, 1972.
64. Dakubo G.D. et al. *The Warburg phenomenom and other metabolic alterations of cancer cells.* Springer-Verlag Berlin Heidelberg, 2010.
65. Tuma R. et al. *Sometimes size doesn't matter: re-evaluating RECIST and tumor response rate endpoints.* J Natl Cancer Inst (98):1272–1274, 2006.
66. Lee DH et al. *Early prediction of response to first-line therapy using integrated 18F-FDG PET/CT for patients with advanced/metastatic non-small cell lung cancer.* J Thorac Oncol 4:816–821, 2009.
67. Walter MA et al. *Metabolic imaging allows early prediction of response to vandetinib.* J Nucl Med (52):231–240, 2011.
68. Herrmann K et al. *(18)F-FDG-PET/CT in evaluating response to therapy in solid tumors: where we are and where we can go.* Q J Nucl Med Mol Imaging 55:620–632, 2011.

69. Everitt S et al., *The impact of time between staging PET/CT and definitive chemo-radiation on target volumes and survival in patients with non-small cell lung cancer.* Radiother Oncol 106:288–291, 2013.
70. Carey KD et al., *Kinetic analysis of epidermal growth factor receptor somatic mutant proteins shows increased sensitivity to the epidermal growth factor receptor tyrosine kinase inhibitor, erlotinib.* Cancer Res 66: 8163-8171, 2006.
71. Yun CH et al., *Structures of lung cancer-derived EGFR mutants and inhibitor complexes: mechanism of activation and insights into differential inhibitor sensitivity.* Cancer Cell 11: 217-227, 2007.
72. Kobayashi S et al., *EGFR mutation and resistance of non-small-cell lung cancer to gefitinib.* N Engl J Med 352: 786-792, 2005.
73. Pao W et al., *Acquired resistance of lung adenocarcinomas to gefitinib or erlotinib is associated with a second mutation in the EGFR kinase domain.* PLOS Med 2: e73, 2005.
74. Engelman JA et al., *MET amplification leads to gefitinib resistance in lung cancer by activating ERBB3 signaling.* Science 316: 1039-1043, 2007.
75. Yu H et al., *Analysis of Mechanisms of Acquired Resistance to EGFR TKI therapy in 155 patients with EGFR-mutant Lung Cancers.* Clin Cancer Res 2013.
76. Sequist LV et al., *Genotypic and histological evolution of lung cancers acquiring resistance to EGFR inhibitors.* Sci Transl Med 3: 75, 2012.
77. Thomson S et al., *Kinase switching in mesenchymal-like non-small cell lung cancer lines contributes to EGFR inhibitor resistance through pathway redundancy.* Clin Exp Metastasis 25: 843-854, 2008.
78. Yauch RL et al., *Epithelial versus mesenchymal phenotype determines in vitro sensitivity and predicts clinical activity of erlotinib in lung cancer patients.* Clin Cancer Res 11: 8686-8698, 2005.
79. Kalluri R et al. *The basics of epithelial-mesenchymal transition* The Journal of clinical investigation. Vol 119, number 6, 2009.
80. Steinestel K. et al. *Clinical significance of epithelial-mesenchymal transition.* Clinical and Translational Medicine (3);17, 2014.

81. Masin M. et al. *GLUT3 is induced during epithelial-mesenchymal transition and promotes tumor cell proliferation in non-small cell lung cancer* Cancer metabolism. (2);11, 2014.
82. Sato M et al. *Emerging evidence of epithelial-to-mesenchymal transition in lung carcinogenesis.* Respirology (17); 1048–1059, 2012.
83. Asami Ket al., *Continued treatment with gefitinib beyond progressive disease benefit patients with activating EGFR mutations.* Lung Cancer 79: 276-282, 2013.
84. Faehling M et al., *EGFRtyrosine kinase inhibitor treatment beyond progression in long-term Caucasian responders to erlotinib in advanced non-small cell lung cancer: A case-control study of overall survival.* Lung Cancer 80: 306-312, 2013.
85. Nishie K et al., *Epidermal growth factor receptor tyrosine kinase inhibitors beyond progressive disease: a retrospective analysis for Japanese patients with activating EGFR mutations*. J Thorac Oncol 7: 1722-1727, 2012.
86. Nishino M et al., *Radiographic assessment and therapeutic decisions at RECIST progression in EGFR-mutant NSCLC treated with EGFR tyrosine kinase inhibitors.* Lung Cancer 79: 283-288, 2013.
87. Watanabe S et al., *Clinical responses to EGFR-tyrosine kinase inhibitor retreatment in non-small cell lung cancer patients who benefited from prior effective gefitinib therapy: a retrospective analysis.* BMC Cancer 11: 1, 2011.
88. Riely GJ et al., *Prospective assessment of discontinuation and reinitiation of erlotinib or gefitinib in patients with acquired resistance to erlotinib or gefitinib followed by the addition of everolimus.* Clin Cancer Res 13: 5150-5155, 2007.
89. Hata A et al., *Does T790M disappear? Successful gefitinib rechallenge after T790M disappearance in a patient with EGFR-mutant non-small-cell lung cancer.* J Thorac Oncol 8: e27-e29, 2013.
90. Suh Y et al., *Claudin-1 induces epithelial-mesenchymal transition through activation of the c-Abl-ERK signaling pathway in human liver cells.* Oncogene, 2013.
91. Goldberg SB et al., *Chemotherapy with erlotinib or chemotherapy alone in advanced non-small-cell lung cancer with acquired resistance to EGFR tyrosine kinase inhibitors."* J Clin Oncol 30:15s, 2012.

92. Song G et al., *Efficacy of chemotherapy plus gefitinib treatment in advanced non-small-cell lung cancer patients following acquired resistance to gefitinib.* Molecular and Clinical Oncology, 1:875-878, 2013.
93. Pirker R et al., *Integrating Epidermal Growth Factor Receptor–Targeted Therapies into Platinum-Based Chemotherapy Regimens for Newly Diagnosed Non–Small-Cell Lung Cancer.* Clinical Lung Cancer Volume 9, Supplement 3:109–115, 2008.
94. Jo M et al. *Cross-talk between epidermal growth factor receptor and c-Met signal pathways in transformed cells*. J Biol Chem 275, 2000.
95. Peghini PL et. al *Overexpression of epidermal growth factor and hepatocyte growth factor receptors in a proportion of gastrinomas correlates with aggressive growth and lower curability*. Clin Cancer Res (8): 2273-2285, 2002.
96. Guo A. et al., *Signaling networks assembled by oncogenic EGFR and c-Met.* Proc Natl Acad Sci U S A 105: 692-697, 2008.
97. Guarino M et al. *Src signaling in cancer invasion.* J Cell Physiol 223:14-26, 2010.
98. Gu L et al., *Stat5 promotes metastatic behavior of human prostate cancer cells in vitro and in vivo.* Endocr Relat Cancer 17: 481-493, 2010.
99. Quesnelle KM et al. *STAT-mediated EGFR signaling in cancer.* J Cell Biochem 102: 311-319, 2007.
100. Das S et al. *Signal transducer and activator of transcription-6 (STAT6) is a constitutively expressed survival factor in human prostate cancer.* Prostate 67: 1550-1564, 2007.
101. Cuenda A et al., *p38 MAP-kinases pathway regulation, function and role in human diseases*. Biochim Biophys Acta 1773: 1358-1375, 2007.
102. Kwon CH et al., *S100A8 and S100A9 promotes invasion and migration through p38 mitogenactivated protein kinase-dependent NF-kappaB activation in gastric cancer cells.* Mol Cells (35); 226-234, 2013.
103. Wang XF et al., *Baicalin Suppresses Migration, Invasion and Metastasis of Breast Cancer via p38MAPK Signaling Pathway.* Anti Cancer Agents Med Chem (13); 923-931, 2013.
104. Nurwidya F et al., *Epithelial mesenchymal transition in drug resistance and metastasis of lung cancer*. Cancer Res Treat (44): 151-156, 2012.

105. Palacios F et al., *Lysosomal targeting of E-cadherin: a unique mechanism for the down-regulation of cell-cell adhesion during epithelial to mesenchymal transitions.* Mol Cell Biol (25): 389-402, 2005.

106. Cairns R et al., *Regulation of cancer cell metabolism*. *Nature* Reviews Cancer (11); 85-95, 2011.

107. Baas AF. et al, *Activation of the tumor suppressor kinase LKB1 by the STE20-like pseudokinase STRAD*. Embo J 22(19);5102-5114, 2003.

108. Hardie DG et al, AMPK *a nutrient and energy sensor that maintans energy homeostasis.* Mol Cell Biol (13);251-262, 2012.

109. Gwinn DM et al, *AMPK phosphorylation of raptor mediates a metabolic checkpoint*. Mol Cell 30(2);214-26, 2008.

110. Winder WW et al, Activation of *AMPK-activated protein kinase increases mitochondrial enzymes in skeletal muscle*. J App Physiol (88);2219-2226, 2000.

111. Mueckler M et al., *The SLC2 (GLUT) family of membrane transporters.* Mol Aspects Med; 34(2-3):121-38, 2013.

112. Coriat R et al., *Sorafenib- induced hepatocellular carcinoma cell death depends on reactive oxygen species production in vitro and in vivo.* Mol Cancer Ther 11(10):2284–2293, 2012.

113. Wilhelm SM et al., *Preclinical overview of sorafenib, a multikinase inhibitor that targets both Raf and VEGF and PDGF receptor tyrosine kinase signaling.* Mol Cancer Ther 7(10):3129–3140, 2008.

114. Hatzivassiliou G et al., *RAF inhibitors prime wild-type RAF to activate the MAPK pathway and enhance growth.* Nature 464(7287):431–435, 2010.

115. O'Reilly KE et al., *mTOR inhibition induces upstream receptor tyrosine kinase signaling and activates Akt.* Cancer Res 66(3):1500–1508, 2006.

116. Meric-Bernstam F et. al, *PIK3CA/ PTEN mutations and Akt activation as markers of sensitivity to allosteric mTOR inhibitors.* Clin Cancer Res 18(6):1777–1789, 2012.

117. Rahmani M et al., *The kinase inhibitor sorafenib induces cell death through a process involving induction of endoplasmic reticulum stress.* Mol Cell Biol 27(15):5499–5513, 2007.

118. Sanchez-Hernandez I et al., *Dual inhibition of (V600E)BRAF and the PI3K/AKT/mTOR pathway cooperates to induce apoptosis in melanoma cells through a MEK-independent mechanism.* Cancer Lett 314(2):244–255, 2012.

119. Ulivi P et al., *Role of RAF/MEK/ERK pathway, p-STAT-3 and Mcl-1 in sorafenib activity in human pancreatic cancer cell lines.* J Cell Physiol 220(1):214–221, 2009.

120. Llobet D et al., *The multikinase inhibitor Sorafenib induces apoptosis and sensitises endometrial cancer cells to TRAIL by different mechanisms.* Eur J Cancer 46(4):836–850, 2010.

121. Cervello M et al., *Molecular mechanisms of sorafenib action in liver cancer cells.* Cell Cycle 11(15):2843–2855, 2012.

122. Bull VH et al., *Sorafenib-induced mitochondrial complex I inactivation and cell death in human neuroblastoma cells.* J Proteome Res 11(3):1609–1620, 2012.

123. Cardaci S et al., *Redox implications of AMPK-mediated signal transduction beyond energetic clues.* J Cell Sci 125(Pt 9):2115–2125, 2012.

124. Marsin AS et al., *Phosphorylation and activation of heart PFK-2 by AMPK has a role in the stimulation of glycolysis during ischaemia.* Curr Biol 10(20):1247–1255, 2000.

125. Almeida A et al., *Nitric oxide switches on glycolysis through the AMP protein kinase and 6-phosphofructo- 2-kinase pathway.* Nat Cell Biol 6(1):45–51, 2004.

126. Wu SB et al., *AMPK-mediated increase of glycolysis as an adaptive response to oxidative stress in human cells: implication of the cell survival in mitochondrial diseases.* Biochim Biophys Acta 1822(2):233–247, 2012.

127. Riganti C et al., *Diphenyleneiodonium inhibits the cell redox metabolism and induces oxidative stress.* J Biol Chem 279(46):47726–47731, 2004.

128. Duvel K et al., *Activation of a metabolic gene regulatory network downstream of mTOR complex 1.* Mol Cell 39(2):171–183, 2010.

129. Shaw RJ et al. *Glucose metabolism and cancer.* Curr Opin Cell Biol 18(6):598–60, 2006.

130. Shen YC et al., *Activating oxidative phosphorylation by a pyruvate dehydrogenase kinase inhibitor overcomes sorafenib resistance of hepatocellular carcinoma.* Br J Cancer 108(1):72–81, 2013.

Thanks...

Eccoci giunti alle battute finali. Le ultime pagine di questo indimenticabile romanzo di avventura stanno per essere scritte. Soddisfatta ed entusiasta di chiudere un'altra piccola, grande tappa di un lungo percorso. Triste per dovere lasciare il *mio* lab.

Un grazie di cuore a tutta la squadra capitanata dal Prof. Petronini e dalla Prof.ssa Alfieri. Grazie per i vostri consigli e suggerimenti. Grazie per avermi permesso di fare parte del vostro team e di essermi stati sempre vicini, anche ora che sono lontana. Questi anni sono volati. Grazie perchè mi avete arricchita, scientificamente e umanamente. Grazie perché non avrei potuto domandare amici(colleghi*)* migliori. Grazie per avermi fatto sentire sempre a casa. Ognuno di voi, con la propria storia, le proprie avventure e i propri consigli mi ha lasciato un suo pezzettino da aggiungere al mio "puzzle". Grazie Lab. Vi voglio davvero bene. (vi ringrazierò poi uno ad uno… non temete ☺). Un grazie particolare lo rivolgo ad una persona speciale. Una persona senza la quale questi tre anni non sarebbero stati così pieni di risate, allegria, feste, "pasticci", cene, gite fuori bordo, chiacchiere, film, "caldi abbracci", "bido bidooo" e chi più ne ha più ne metta. Grazie Dani. Sono stata davvero fortunata ad averti trovato sul mio cammino. Sei una persona unica. Grazie per aver reso questi tre anni indimenticabili.

Grazie a tutti i ragazzi che sono passati dal lab. Ognuno di voi mi ha lasciato un bellissimo ricordo. Con alcuni di voi ho stretto un'amicizia rara. Un legame che so continuerà nel tempo vincendo ogni distanza. Grazie a chi mi ha accompagnata con messaggi, skypecall, abbracci virtuali e che mi ha lasciato un dolce orsetto. Grazie a chi mi ha lasciato una pietra amuleto da stringere in caso di bisogno. Grazie a due sorelle tecnologizzate e molto speciali :-*. Grazie a chi mi ha lasciato una cuffia, tanti messaggi, tante mail, tante chiamate e tanti bigliettini. Grazie ai pochi uomini passati nel lab. Come si dice: "pochi ma buoni" ;-).

Grazie a "Ho piu' p..... che t...." senza la vostra pazzia non saprei come avrei fatto e come farei. Grazie per le serate danzanti (anche di quelle alternative nelle balere :-)). Grazie dei tatuaggi della non estate, delle risate, delle gite fuori bordo e delle serate alternative. Grazie per avermi trasmesso un po' della vostra pazzia. La nostra amicizia non teme alcun fuso e alcuna distanza. Dolce ex compagna di liceo grazie di tutto. Della tua amicizia. Del tuo supporto. Della tua forza. Hai una famiglia fantastica. Grazie ai baci e alle coccole delle mie patatine. Senza di voi le giornate sarebbero in bianco e nero. Non sapete quanto ogni singolo abbraccio, bacino, disegno, videomessaggio, CRIIIIs, (Z)IA mi abbiano strappato un tenero sorriso :-). Vi voglio davvero bene.

Grazie a due amiche molto speciali conosciute sui banchi dell'universita' che ormai sono lontane da qualche annetto. Una a Vienna e una a Losanna. Grazie per il vostro supporto e sostegno. La lontananza non ci ha mai divise. Anzi. Sono davvero orgogliosa di voi. Grazie a tutti gli amici di una vita con i quali ho condiviso tante esperienze e che so ci saranno sempre. Grazie a chi ho conosciuto nella grigia e solare Milano. Grazie per le risate, le ciacere, i gelati. Grazie per i nostri indimenticabili (e pazzi) viaggi intorno al mondo. Grazie agli amici "giovani e meno giovani" ;-) della montagna dai quali mi sono rifugiata per ricaricare le batterie. Grazie alla mia famiglia americana. Senza di voi questi mesi non sarebbero stati la stessa cosa. Mi avete dimostrato che è possibile sentirsi a casa anche a migliaia di km di distanza. Un abbraccio.

Ringrazio i miei genitori e mio fratuz, una guida, un punto fermo nella mia vita. Grazie per avermi insegnato ad essere quella che sono. Grazie per avermi insegnato che per arrivare in cima al Seceda bisogna prendere un sentiero lungo, tortuoso ed erto e non servirsi dell'ovovia. Grazie perche' mi avete insegnato a voler bene, a tendere non una ma tutte e due le mani a chi ha bisogno. Grazie perché mi avete insegnato ad essere sempre ottimista e a guardare il bicchiere mezzo pieno. Grazie perchè il mio essere allegra e solare lo devo molto a voi. Sono orgogliosa di avere una famiglia come voi. Spero di rendervi orgoliosi anche solo una briciola di quanto lo sono io di voi. Grazie perchè su di voi ho potuto, posso e potro' sempre contare, qualsiasi cosa accada. Non vi ringrazierò mai abbastanza. Vi voglio bene.
Un grazie infinito va alla mia famiglia adottiva. Siete entrati tanti anni fa a fare parte della mia vita e so che non ne uscirete mai. Grazie. Vi ringrazio del vostro affetto sincero. Grazie per rendermi parte attiva della vostra quotidianità. Grazie perchè casa vostra la sento come casa mia. Grazie perché su di voi so che posso sempre contare. Vi voglio davvero bene. Cati. Sorellona. La nostra amicizia è un legame unico. Più siamo lontane e più siamo vicine. Più passano gli anni e più siamo unite. La nostra amicizia non teme davvero nulla. Non ho parole per esprimere la mia gratitudine, la gioia, la felicità ad averti come sorella. Ti voglio un bene infinito, inquantificabile. Ci siamo sempre state l'una per l'altra. Ci siamo tutt'ora e ci saremo sempre. Grazie di avermi scelto come miglior amica. Grazie per esserci sempre. Ti voglio bene.
Grazie a due persone molto speciali che non ci sono più. Grazie perché la vostra instancabile danza mi ha insegnato tantissimo. Mi avete insegnato a sorridere, sempre. Mi avete lasciato la vostra forza. La vostra allegria. Grazie perché la vostra danza mi ha insegnato a donare. A voler

veramente bene. Ad amare. Grazie infinite di cuore. Non scorderò mai quei giorni. Non dimenticherò mai la vostra mano.

Grazie a tutti voi, amici miei. Questa tesi è anche un po' vostra. Senza il vostro aiuto, supporto e allegria questa avventura non sarebbe stata la stessa.
Grazie.